Luís Filipe Moreira Simões de Oliveira Negrão

Silver-based Stretchable Electronic Systems: Materials and Fabrication Methods

Thesis submitted to the University of Coimbra for the degree of Master in Physics Engineering under the scientific supervision of PhD Mahmoud Tavakoli (UC).

Setembro de 2018

FCTUC FACULDADE DE CIÊNCIAS
E TECNOLOGIA
UNIVERSIDADE DE COIMBRA

LUÍS FILIPE MOREIRA SIMÕES DE OLIVEIRA NEGRÃO

Silver-based stretchable electronic systems: Materials and fabrication methods

Thesis submitted to the
University of Coimbra for the degree of
Master in Physics Engineering

Supervisors:
Prof. Dr. Mahmoud Tavakoli (Electrical and Computers Engineering Department,
University of Coimbra)

Coimbra, 2018

Dedication

Now that my dissertation work is coming to an end, and the clock marks 00:46 the night before I'm expected to submit the final document, I am deeply regretting having thought that writing a decent dedication on such short notice would be a good idea. Nonetheless, I will try my best.

First of all, I would like to thank my thesis supervisor, Mahmoud Tavakoli, for his guidance and for having given me the opportunity to carry out my dissertation work at ISR, in the emerging and exciting research field of stretchable electronics. While working on such a practical, hands-on topic presented a different challenge for someone with a Physics Engineering background, I feel like it added a new dimension to the skills I have acquired during my university years. Second, I would like to thank Pedro Lopes and João Lourenço, respectively a PhD student and a former researcher at ISR, for having always been willing to share their expertise with me. I would also like to thank the rest of the ISR team, namely researchers Hugo Paisana, Davide Vaz, Daniel Fernandes and Daniel Marques, as well as fellow Masters students Cristina Leal and Joana Pastor, for having created a great work environment in which we could help each other out with opinions and ideas, and also share relaxing moments. Finally, I would like to thank my family and friends for all the help and support they gave me in the times I needed most. To name them all would make quite an extensive list but I know every one of them will know they are included.

Acknowledgments

This work was conducted at the Insitute of Systems and Robotics' facilities at University of Coimbra, with the institute's funding.

Furthermore, this work was partially supported by the Foundation for Science and Technology through the CMU-Portugal Stretchtronics project (Nr. CMUP-ERI/TIC70021/2014) ,the Portuguese Additive Manufacturing Initiative (Nr. CENTRO-01-0145-FEDER-022158), the 'Portugal2020' and 'Compete2020' programmes, and the 'European Structural and Investment Funds' programme.

European Union

European Structural
and Investment Funds

Resumo

Este trabalho incide sobre sistemas eletrónicos extensíveis (*Stretchable*) fabricados com compostos condutores constituídos por micropartículas/microflocos de prata dispersos numa matriz de Polidimetilsiloxano. Num primeiro passo, vários tipos de compostos baseados em prata serão testados e comparados. Isto inclui partículas com diferentes geometrias, nomeadamente micropartículas e microflocos de prata, bem como micropartículas de níquel e ferrite revestidas com prata. Do composto resultante, designado AgPDMS, espera-se que seja um bom condutor e, mais, que mantenha esta característica mesmo quando elongado. O limiar de percolação para cada um destes tipos de partículas será obtido experimentalmente, e a estabilidade das propriedades elétricas do tipo de partícula selecionado será avaliada. De seguida, três métodos de padronização serão avaliados, nomeadamente impressão por *stencil*, serigrafia e moldagem. O objetivo seguinte será reduzir a área dos circuitos desenvolvidos, quer reduzindo a dimensão dos elementos do circuito quer fabricando circuitos com várias camadas. Para fabricar circuitos de várias camadas será usado um método baseado em ablação com laser para criar vias que ligam electricamente camadas adjacentes. Em seguida, métodos para integrar componentes rígidas em circuitos extensíveis serão testados. Será ainda realizada caracterização eletromecânica de amostras fabricadas usando os materias e métodos selecionados no decorrer deste trabalho. Para terminar, serão apresentados dois sistemas electrónicos extensíveis fabricados no ISR, como prova de conceito. O primeiro é um *touchpad* capacitivo extensível, e o segundo um sensor ECG sem fios extensível.

Abstract

This work focuses on stretchable electronics systems, composed of silver-based conductive composites as the conductive material and Polydimethylsiloxane (PDMS) as the stretchable substrate material. First, as a filler for PDMS-based conductive composites, various types of silver particles will be evaluated. This includes silver particles and silver flakes with different geometries, as well as silver-coated nickel/ferrite particles. The resulting composite, called AgPDMS, should be conductive and also tolerate strain without losing conductivity. The percolation threshold for each of these particle types is obtained experimentally, and the stability over time of conductivity for the selected particle type is evaluated. After this, three patterning methods are evaluated, namely stencil printing, screen printing and moulding. The second goal of this work is to reduce the circuit footprint by both reducing feature dimensions and fabricating multilayer AgPDMS stretchable circuits. To fabricate multilayer circuits, a method based on laser ablation is used for creating vias between layers. After this, methods for integrating flexible and rigid components into soft circuits will be assessed. Thorough electromechanical characterisation of samples fabricated using the selected materials and methods will be performed. To conclude, two stretchable electronics systems fabricated at ISR will be presented as proof-of-concept. This includes a multilayer capacitive stretchable touchpad and an ECG sensor.

Keywords

- Stretchable electronics
- AgPDMS
- Multilayer circuits
- Laser-ablated vias
- Soft-rigid Interfaces

Acronyms

AgNW Silver Nanowire.
AgPDMS Silver Polydimethilsiloxane.

ECG Electrocardiography.
EMG Electromiography.

Flex PCB Flexible Printed Circuit Board.

LM Liquid Metal.

PDMS Polydimethilsiloxane.
PET Polyethylene Terephtalate.

SBS Styrene-Butadiene-Styrene.

zPDMS Anisotropic z-axis conductive PDMS.

List of Figures

1.1 Number of published scientific papers on flexible and stretchable electronics per year [1]. . . . 2
1.2 Development stage of different soft electronics technologies, from [2]. . 2
1.3 a) Stretchable wearable heater made with a styrene-butadiene-styrene (SBS)-silver nanowire (AgNW) composite and SBS substrate, [3]. b) Heater working under 60% applied strain [3]. c) AgNW/PDMS wireless strain-sensitive antenna. [4]. d) Variation of the antenna's resonance frequency with strain [4]. . . . 3
1.4 a)3D view of electroluminescent phosphor microparticle layer sandwiched between AgNW electrodes [5]. b) Electroluminescent display working unstrained and at 30% and 50% strain, respectively [5]. c) Stretchable array of LEDs on PDMS substrate [6]. . . . 4
1.5 a) Suit with embedded Liquid Metal elastomeric strain sensors for measuring hip, knee and ankle angles [7]. b) ISR robotic hand with carbon PDMS (cPDMS) strain sensors on fingertips [8]. c) Soft sensing skin for gesture recognition [9]. . . . 4
1.6 a) Working stretchable transistor made with Single Wall Carbon Nanotube (SWCNT) semiconductor and electrodes [10]. b) Scheme of memristor based on electrochemical removal of oxide skin from Liquid Metal (LM) surface [11]. . . . 5
1.7 a) Scheme of wearable pulse oximeter device [9]. b) Pulse oximeter device [9]. c) Biker wearing pulse oximeter to track oxigen levels during physical activity [9]. . . . 5
1.8 Sinusoidal copper tracks as stretchable electrical interconnects.[12] . . 7
1.9 a) Out of plane Ti:Au serpentine bridges connecting CMOS inverters [13]. b) Out-of-plane interconnections under 140% applied strain [13]. c) Simple out of plane bridges connecting CMOS inverters [13]. . . . 7
1.10 a) Schematic representation of stencil printing of liquid metal track on a substrate [14]. b) Syringe filling of microchannels with liquid metal [14]. . . . 8
1.11 a) Selective wetting of prepatterned substrate with Gallinstan [15]. b) Memristor based on electrochemical removal of oxide skin from Liquid Metal surface [11]. . . . 9

1.12 a) Formation of conductive paths according to Percolation Theory [1]. b) Typical curve of conductivity as function of conductive filler percentage. 10
1.13 a) Patterned AgPDMS two-layer circuit on PDMS substrate [16]. b) Stretchable heater with SBS substrate and AgNW-SBS conductive composite [3]. 11
1.14 a) Carbon Black conductive traces on PDMS substrate [8]. b) cPDMS strain sensor on robotic fingertip [8]. 11
1.15 a) 3-D view of aligned columns of particles in zPDMS. [17]. b) 3-D view of rigid component interfacing Liquid Metal pads by surface mounting on intermediate zPDMS layer [17]. 12
1.16 Maximum conductivity vs Strain at break for several conductive composites (and also LM); PUA - Polyurethane Acrylate, PU - Polyurethane, PA- PolyAcrylate,BS-Styrene-Butadiene-Styrene, PEDOT:PSS - poly(3,4-ethylenedioxythiophene):poly(styrenesulfonate), poly(TBA-co-AA) - copolymer of tert-butyl acrylate (TBA) and acrylic acid (AA). 1-[18], 2-[19] 3-[3], 4-[5], 5-[20], 6-[21], 7-[22], 8-[23], 9-[24], 10-[25], 11-[26], 12-[16], 14-[27]. 13
1.17 Reference values of normalized resistance vs strain.1-[18], 2-[19] 3-[3], 4-[5], 5-[20], 6-[21], 7-[22], 8-[23], 9-[24], 10-[25], 11-[26], 12-[16], 13-[27]. 14
1.18 a) Scheme of stencil printing procedure [18]. b)150 μm wide AgPDMS lines spaced by 100 μm [16]. 15
1.19 Dry transfer stamping procedure [28]. 15
1.20 a) Diagram of filtration procedure [16]. b) 10 micrometer wide AgNW lines with 10 micrometer separarion achieved through filtration procedure [16]. 16
1.21 Laser ablation procedure [14]. 16
1.22 Array of EGaIn nanoparticle strain gauges patterned on glove with inkjet printing technique [29]. 17
1.23 Steps in photolithographic procedure for creating interlayer electrical connection vias [30]. 18
1.24 a) Scheme illustrating integration of rigid components through immersion of functional islands in soft substrate. [31]. b) Functional rigid islands encapsulated by elastomeric substrate [12]. c) Matrix of organic transistors, interconnected by SWCNT's dispersed in polymer, on a PDMS substrate [32]. 18
1.25 Functional rigid islands enclosed in liquid-filled cavity inside elastomeric substrate [33]. 19

2.1 a) Chemical structure of PDMS. b) PDMS sample. 22
2.2 a) Uncured zPDMS layer (brown). b) Microscope image of vertically aligned conductive columns of Silver-coated Nickel particles embedded in PDMS matrix.[34] 23
2.3 SEM images of silver flakes (type 1, see Table 2.1) and microparticles (type 2), provided by Technic Inc. 24
2.4 Universal Laser Systems VLS3.50 laser cutter. 25

2.5 a)Thinky ARE-250 Mixer used for fabricating conductive composites.. b) Thin film applicator for fabricating thin circuit layers from Zehntner. 25
2.6 a) Oven from Pol-eko. b) Oven from Puhui. 26
2.7 Kern PCB laboratory weighting scale. 26
2.8 a) Fluke 45 multimeter. b) HP 34401A multimeter 27
2.9 a) Hakko FX888D soldering station. b) Soldering flux. 27
2.10 Ease release agent from Mann. 27
2.11 a) T490A microscope from AMscope. b) MU900 digital camera from AMscope. 28
2.12 a) Instron 5943 universal testing system used to perform tensile tests. b) 1kN pneumatic gripper used for tensile tests. 28
2.13 a) Scheme of circuit for measuring the resistance of AgPDMS samples during tensile tests. b) Circuit board used for measuring the resistance of AgPDMS samples during tensile tests. 29
2.14 Schematic of ideal moulding process. 30
2.15 a) Scheme of stencil printing procedure. b) Adhesive paper stencil. . . 31
2.16 Screen (left); Coating through (top right); Photoemulsion (bottom center left); Emulsion remover (bottom center right); UV lamp (Bottom right). 32
2.17 a) Laser ablated vias connecting two AgPDMS layers. b) Schematic representation of via opening procedure. 33
2.18 a) Flex PCB integration with zPDMS layer. b)Schematic representation of flex PCB integration procedure with zPDMS. 34
2.19 a) Direct flex PCB integration. b) Schematic representation of direct flex PCB integration procedure. 34
2.20 a) Crimping tool. b) Metal 'claws' crimped with AgPDMS lines. c) Crimp connector. 35

3.1 a) Setup for measurement of resistances in percolation tests. b) Scheme of the setup for resistance measurements in percolation tests. 38
3.2 Average conductivity as a function of particle type and weight percentage of silver particles in PDMS matrix. 39
3.3 Conductivity as a function of time elapsed since fabrication of the test sample. 40
3.4 AgPDMS with particles type I cured at a) 50°C, b) 150°C for 3h. . . 41
3.5 a) Scheme of imperfect moulding process, with AgPDMS paste leftover in mould. b) Damaged electrodes mould, with AgPDMS leftover paste. 42
3.6 a) Stencil for 1st layer of circuit. b) Patterned 1st layer of AgPDMS circuit. c) Stencil for 2nd layer of circuit. d) Patterned 2nd layer of AgPDMS circuit. 43
3.7 a) Adhesive stencil paper with lines from 1 millimeter down to 200 micrometers. b) AgPDMS lines from 1 millimeter width down to 200 μm width. 44

3.8 a) 900 μm wide line. b) 500 μm wide line. c) 400μm wide line. d) 300μm wide line. All images were obtained under the same optical microscope with a 4x magnification lens. Cracks are already visibly forming in the 400μm and 300μm wide lines 45
3.9 Stencil-patterned AgPDMS line with expected width of 500μm and real width of 300μm. 46
3.10 a) Stencil line after laser patterning. b) Stencil line after application of AgPDMS paste and lifting from the substrate. 46
3.11 Stencil used for minimum feature separation test. 47
3.12 a) 500μm spacing between lines; on the right there are several lines blended together, as can be seen by the much bigger thickness compared to the line on the left. b) 900 μm spacing between lines. 47
3.13 a)Screen with emulsion applied and photomasks on top. b) Screen exposure setup. 49
3.14 a) AgPDMS paste application after exposure. b) Circuit produced with screen printing procedure. 49
3.15 a) 500μm diameter, 500μm thick via after removal of burnt debris. b) 500μm diameter, 500μm thick via with burnt debris. 51
3.16 Experimental setup for characterisation of the vias, with eight 3cm long, 1mm wide lines per layer and two control lines (one in each layer) which are not connected. 52
3.17 a)Average conductivity of 1mm diameter vias with 1mm, 750μm and 500μm thickness, and success rate of the via fabrication process. b) Average conductivity of 750μm vias with 1mm, 750μm and 500μm thickness, and success rate of the process. c) Average conductivity of 750μm vias with 1mm, 750μm and 500μm thickness, and success rate of the process. 53
3.18 Flex pcb connected to AgPDMS lines. 54
3.19 Outcome of resistance measurements for flex PCB interfaced with AgPDMS tracks 54
3.20 a) Interface between AgPDMS lines and flex PCB copper tracks. b) AgPDMS line on top of copper track. 55
3.21 a) Flex PCB's interfaced with AgPDMS lines through a zPDMS layer. b) Scheme of zPDMS interface between flex PCB and AgPDMS lines. 55
3.22 Resistance values of AgPDMS-zPDMS interface-flex PCB system. . . 56
3.23 a) AgPDMS sample line used for electromechanical characterisation b) Experimental setup for electromechanical characterisation. 57
3.24 a) Resistance as function of uniaxial strain for sample lines with 83% filler particle concentration by weight. b) Uniaxial strain as function of normalised resistance (R/R_0 = 2, 5 and 10) for sample lines with 83% filler particle concentration by weight. 58
3.25 a) Resistance as function of uniaxial strain for sample lines with 85% filler particle concentration by weight. b) Uniaxial strain as function of normalised resistance (R/R_0 = 2, 5 and 10) for sample lines with 85% filler particle concentration by weight. 59

3.26 a) Resistance as function of uniaxial strain for sample lines with 90% filler particle concentration by weight. 60
3.27 a) Resistance as function of strain for 85%wt concentration lines with vias at the middle. b) Uniaxial strain as function of normalised resistance for $R/R_0 = 2$, 5 and 10. 61
3.28 a) Resistance as function of uniaxial strain for rectangular two-layer samples. b) Uniaxial strain as function of normalised resistance for $R/R_0 = 2$, 5 and 10. 62
3.29 Resistance vs Time for 600 cycles of 20% applied strain. 62
3.30 Resistance vs Time for 600 cycles of 20% applied strain of a single sample. 63
3.31 a) Resistance vs Time for 1000 cycles of 20% applied strain with 10 seconds pause between cycles. b) Resistance vs Time for 500 cycles of 20% applied strain with 10 seconds pause between cycles, repeated on the same sample with an interval of 5 hours. 64
3.32 Flowchart for rapid, inexpensive prototyping of soft single/multilayer systems using stencil printing. 66
3.33 Flowchart for batch fabrication of soft systems using screen printing. 67

4.1 a) Top view scheme of the structure of the stretchable touchpad. b) Side view scheme of the structure of the stretchable touchpad. 70
4.2 a) Assembled stretchable touchpad. b) Stretchable touchpad with two halves separated. 70
4.3 a) Direct AgPDMS to flex PCB interfacing method. b) Metal crimps used to interface flex PCB and rigid connector. c) Flex PCB inserted into rigid connector. d) Wires soldered to connector pins. 71
4.4 a)Cypress' development board used for stretchable touchpad application. b) Stretchable touchpad connected to development board. The black layer under the sensor columns serves as the dielectric between columns and rows, the latter being under the black layer. 72
4.5 Software response to finger pressing sensor at the a) top left corner, b)top right corner, c) center. d) Software response to full hand on top of sensor. 72
4.6 a) Sample ECG circuit with two layers. b) Scheme of ECG module with top layer in red and bottom layer in blue. 73
4.7 a) MAX30003CTI+ biopotential Analog Front End used for cardiac signal processing. b) TXB0108PWR Voltage Level Translator. c) CYBLE 022001-00 Bluetooth Low Energy communication module. . . 73
4.8 Procedure for interfacing rigid islands with soft circuit. 74
4.9 a) Full ECG circuit fabricated with zPDMS interface method. b) Full ECG circuit fabricated direct contact method. 74

List of Tables

2.1 Types of conductive composites which were tested, with information relative to size, manufacturer and silver particles percentage. 23

3.1 Conductivity of AgPDMS as function of curing temperature and curing time. 40
3.2 Success rate of line patterning as function of line width. 45
3.3 Properties of different materials tested as substrate. 50

Contents

Acronyms xi

List of Figures xiii

List of Tables xix

1 State of the Art 1
1.1 Stretchable electronics in academia and industry . . . 1
1.2 Proof-of-concept devices . . . 3
1.3 Materials . . . 6
1.3.1 Conductive materials . . . 6
1.4 Fabrication techniques . . . 13
1.4.1 Patterning techniques . . . 13
1.4.2 Multilayer circuits . . . 17
1.4.3 Rigid component integration . . . 17
1.5 Objectives . . . 19
1.6 Conclusion . . . 20

2 Materials, Equipment and Methods 21
2.1 Materials . . . 21
2.1.1 Stretchable silicone: PDMS . . . 21
2.1.2 Anisotropic z-axis conductor: zPDMS . . . 22
2.1.3 Conductive Composites . . . 22
2.1.4 Equipment . . . 24
2.2 Methods . . . 29
2.2.1 Moulding . . . 29
2.2.2 Stencil Printing . . . 30
2.2.3 Screen Printing . . . 31
2.2.4 Multilayer fabrication . . . 32
2.2.5 Rigid-soft interfaces . . . 32
2.3 Conclusion . . . 35

3 Results 37
3.1 Choice of conductive composite . . . 37
3.1.1 Percolation Behavior . . . 37
3.1.2 Electrical stability of AgPDMS over time . . . 39

3.2 Fabrication procedure 40
3.2.1 Curing procedure 40
3.2.2 Patterning Methods 41
3.2.2.1 Moulding 41
3.2.2.2 Stencil Printing 42
3.2.2.3 Screen Printing 48
3.2.3 Curing substrate 48
3.2.4 Vias Characterisation 50
3.2.5 Interface Characterisation 52
3.2.6 Electromechanical characterisation 56
3.2.7 Conclusion 63

4 Case Studies **69**
4.1 Stretchable Touchpad 69
4.2 Wireless ECG module 71

5 Conclusions **77**

Bibliography **79**

1

State of the Art

1.1 Stretchable electronics in academia and industry

Research into the field of Stretchable Electronics has been steadily building over the past decade, driven by a desire to bridge the existing gap between the mechanical properties of current electronic systems, which are rigid, and biological systems, which are soft. The evolution of yearly research output in both flexible and stretchable electronics can be seen in Figure 1.1, taken from[1]. The authors of this paper predict that the yearly research output in the stretchable electronics field will reach 5600 papers by 2020. The endgame is to make commercial, novel, unconventional applications such as conformable and stretchable displays, stretchable sensors (e.g. pressure and proximity) which can be integrated into electronic skin-like devices, stretchable batteries, stretchable radio frequency antennas, etc. These novel devices are expected to have a significant impact in fields as diverse as robotics, consumer electronics, biomedical monitoring or the sports and clothing industries.

IDTechEx forecasts, in their extensive report on soft electronics technologies in the upcoming decade (2018-2028), that the size of this market will outgrow 800 million dollars per year by 2028. Elements such as strain gauges, stretchable electroluminescent displays, stretchable PCB's or resistive and inductive sensors are reported to be either arriving at, already at or already past full market launch, while other stretchable electronics-enabling technologies are expected to remain in earlier stages of development by 2028. This can be seen in Figure 1.2, taken from this report [2].

In this chapter, an overview of the most relevant work done so far in the field of stretchable electronics will be given, with emphasis on some remarkable applications, followed by a summary of the wide range of elastomeric materials that have been used as the substrate for stretchable electronics. After this, the main topic of

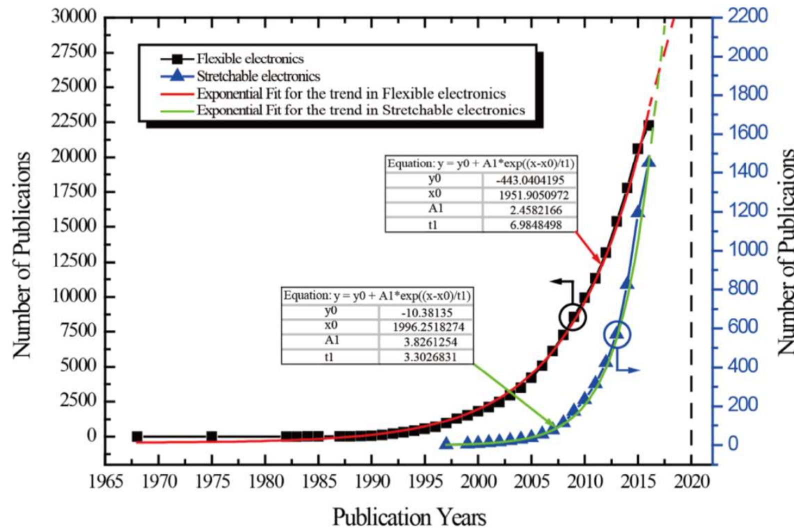

Figure 1.1: Number of published scientific papers on flexible and stretchable electronics per year [1].

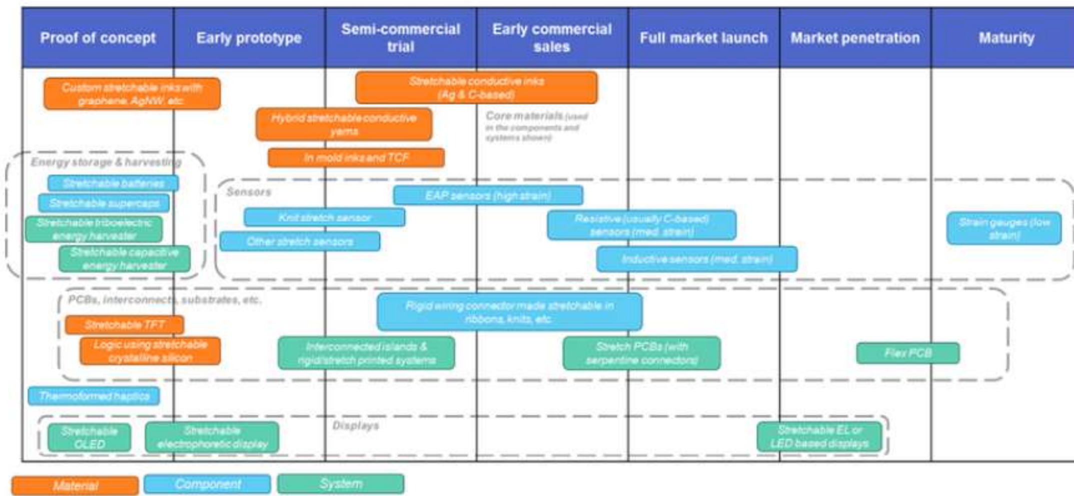

Figure 1.2: Development stage of different soft electronics technologies, from [2].

the chapter, namely the conductive materials used for establishing electrical interconnections in stretchable electronic devices, will be addressed, with focus on conductive composites. The main strengths and shortcomings of the different available conductive material options will be addressed. After this, the fabrication methods employed in the manufacturing of such devices will be explored.

1.2 Proof-of-concept devices

Research work in the field of Stretchable Electronics has seen considerable growth over the past decade. In this time period, proof-of-concept of several stretchable counterparts to devices traditionally built in a rigid fashion, from circuits powering a blinking LED to electroluminescent displays, were put forth by different research groups. In this section, examples of functional prototypes with potential application in diverse areas, such as clothing or biomonitoring, will be presented.

One such example is the stretchable wearable wrist heater developed by Choi and colleagues [3], exhibited in Figures 1.3a and 1.3b. This device proved capable of heating up to 40ºC. Song and colleagues, in turn, developed a wireless strain sensor based on an Silver Nanowire (AgNW)/ Polydimethilsiloxane (PDMS) antenna, the resonant frequency of which varies with applied strain [4], as can be seen in Figures 1.3c and 1.3d.

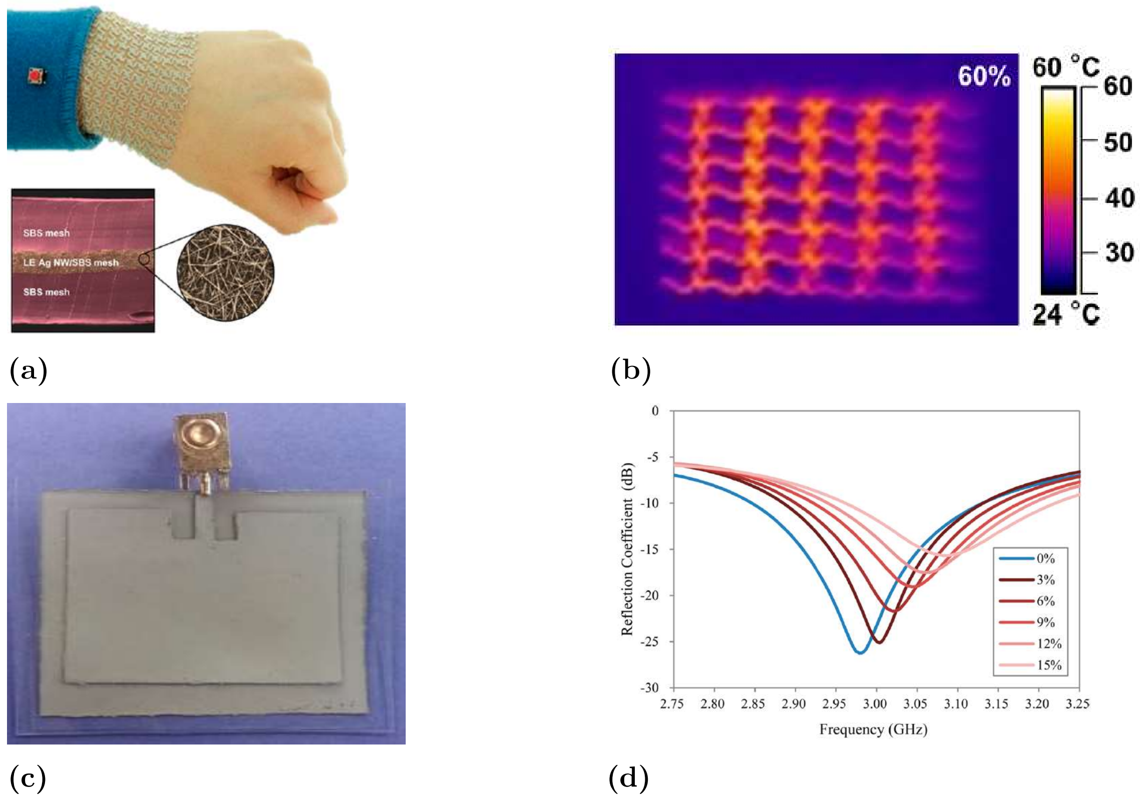

(a) (b) (c) (d)

Figure 1.3: a) Stretchable wearable heater made with a styrene-butadiene-styrene (SBS)-silver nanowire (AgNW) composite and SBS substrate, [3]. b) Heater working under 60% applied strain [3]. c) AgNW/PDMS wireless strain-sensitive antenna. [4]. d) Variation of the antenna's resonance frequency with strain [4].

More complex devices have also been demonstrated, such as displays. In particu-

lar, Tybrandt and colleagues fabricated a matrix display by sandwiching phosphor microparticles dispersed in PDMS between two grids of AgNW tracks, displayed in Figures 1.4a and 1.4b [5], while the group of Park made a stretchable array of interconnected LEDs on a PDMS substrate, shown in Figure 1.4c [6].

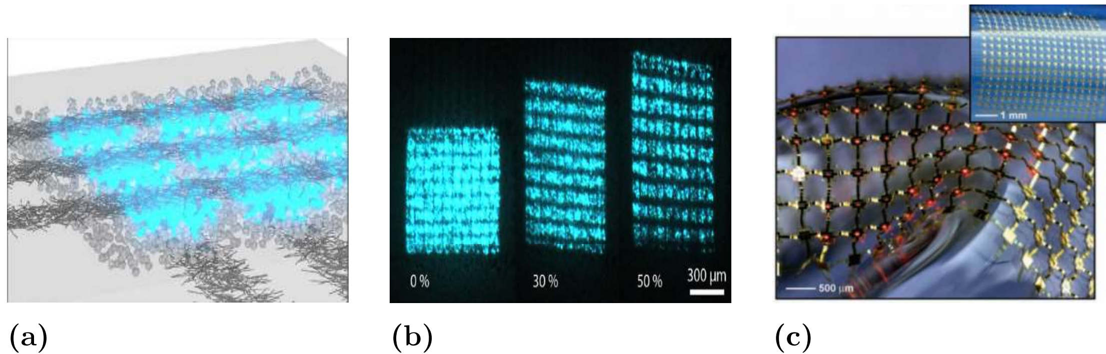

(a) (b) (c)

Figure 1.4: a)3D view of electroluminescent phosphor microparticle layer sandwiched between AgNW electrodes [5]. b) Electroluminescent display working unstrained and at 30% and 50% strain, respectively [5]. c) Stretchable array of LEDs on PDMS substrate [6].

Stretchable electronics has also been integrated into robots, clothing, and directly on the human skin, to enable measurement of proximity, pressure, strain, etc. Examples of applications of this kind are, for instance, the 'Soft Hand' developed at ISR by Tavakoli et al. [8], Figure 1.5b, the sensing suit developed by Menguc et al., Figure 1.5a [7], or the soft sensing skin fabricated by Majidi et al., Figure 1.5c [9].

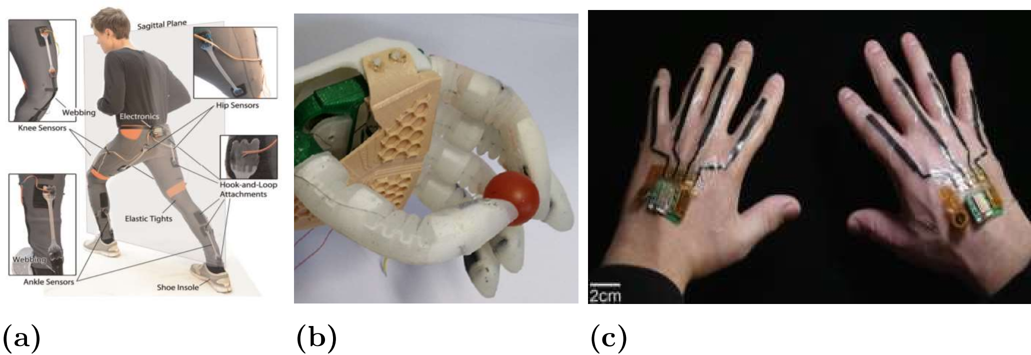

(a) (b) (c)

Figure 1.5: a) Suit with embedded Liquid Metal elastomeric strain sensors for measuring hip, knee and ankle angles [7]. b) ISR robotic hand with carbon PDMS (cPDMS) strain sensors on fingertips [8]. c) Soft sensing skin for gesture recognition [9].

Most of the devices mentioned so far must still rely on conventional rigid electronics modules for logic or memory functions. For now, active electronic components such as memory cells or transistors cannot be made intrinsically stretchable in a

practical and efficient way. Still, proof-of-concept transistors (Figure 1.6a) and memory components (such as the one in Figure 1.6b) have been fabricated using soft components only [10], [11]. These devices, however, remain impractical in terms of speed, size, reliability and fabrication processes.

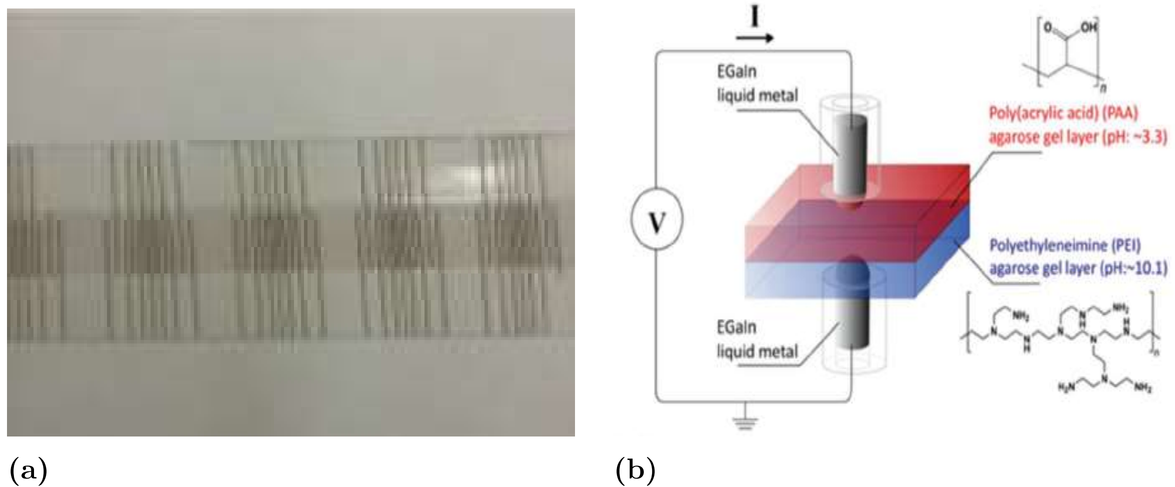

(a) **(b)**

Figure 1.6: a) Working stretchable transistor made with Single Wall Carbon Nanotube (SWCNT) semiconductor and electrodes [10]. b) Scheme of memristor based on electrochemical removal of oxide skin from Liquid Metal (LM) surface [11].

To end this section, an application of soft electronics to biomedical monitoring is presented. Namely, a wearable pulse oximeter built by Majidi and colleagues [9]. Many other applications of soft electronics to biomonitoring, such as Electrocardiography (ECG) or Electromiography (EMG) have also been demonstrated.

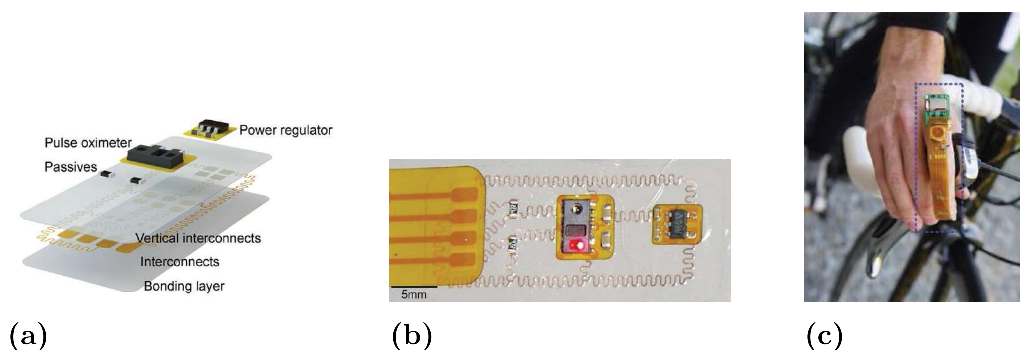

(a) **(b)** **(c)**

Figure 1.7: a) Scheme of wearable pulse oximeter device [9]. b) Pulse oximeter device [9]. c) Biker wearing pulse oximeter to track oxigen levels during physical activity [9].

1.3 Materials

A stretchable electronics module typically consists of two components, namely a stretchable, insulating polymeric substrate – PDMS, Polyurethane (PU), among others, have been used – and a patterned conductive material. Polymers are the material of choice for serving as the substrate because of their intrinsically low stiffness, resembling that of biological systems.

PDMS, Ecoflex, Polyethylene Terephtalate (PET) [18], Styrene-Butadiene-Styrene (SBS) [3], PU [19], Polyacrylate (PA) [25], among other polymers, have reportedly been used as the stretchable substrate material for stretchable electronic devices. The choice of the substrate material is relevant in defining the curing procedure, for instance its duration and temperature, and also for the properties of the final device, such as stretchability, transparency or quality of adhesion of the conductive material to the substrate. Although a few studies based on other substrate materials are mentioned in this section, the focus will be on PDMS-based stretchable electronic devices.

While an adequate choice of substrate material is relevant for adhesion, stretchability and other properties of the final device, as mentioned previously, the true challenge of soft electronics lies in the choice of conductive material, which is why the rest of this chapter will mostly focus on the latter.

1.3.1 Conductive materials

Several approaches to tackle the conductive material issue, using different materials, geometries and fabrication procedures, have been and still are under investigation by different groups. The conductive materials utilised are of the utmost importance since it is with them that electrical interconnections will be established. These must show excellent conductivity and, what is more, maintain useful conductivity values under applied strains that can range from a few percent to 100% or more, depending on the application requirements. While several different approaches have been explored to deal with this issue, these generally can be categorised into three classes.

The first consists in using conventional rigid conductive materials such as copper in deterministic geometries that enable stretchability. One example of such an approach is the work of Bossuyt and colleagues [12], in which thin wires of a conven-

tional intrinsically rigid electrically conductive material, namely copper, were used for interconnections in an in-plane sinusoidal shape. In this work, stretchability of up to 20% was demonstrated. Furthermore, conductivity remained practically unaltered after 89000 5% strain cycles, after which fracture suddenly occurred. In cyclic strain tests of 10% and 20%, 3400 and 400 cycles were completed before rupture, respectively. The copper interconnects can be seen in figure 1.8.

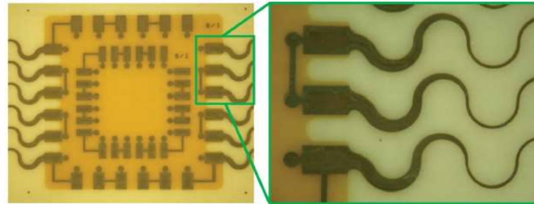

Figure 1.8: Sinusoidal copper tracks as stretchable electrical interconnects.[12]

Alternatively, the research group of Kim and colleagues reported the fabrication of a grid of rigid islands (CMOS inverters) connected by out-of-plane interconnection Ti:Au bridges, in both simple (Figure 1.9c) and serpentine (Figures 1.9a and 1.9b) shapes, in a PDMS substrate. This was accomplished by patterning sufficiently thin interconnection lines on a pre-strained substrate. Upon release of the applied strain, compressive forces deformed the interconnections and made them partially detach from the substrate[13]. When fabricated with a 90% prestrain applied to the PDMS substrate, the device withstood 140% stretching in both x and y directions while maintaining stable electrical properties (Figure 1.9b).

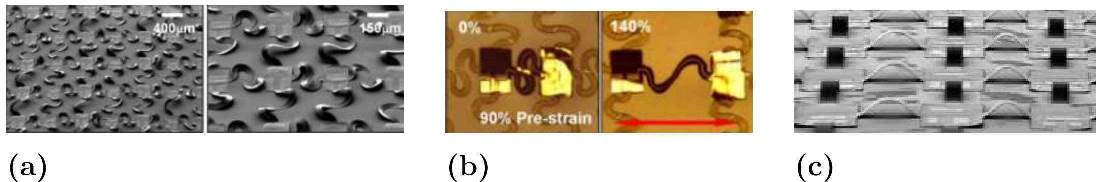

(a) **(b)** **(c)**

Figure 1.9: a) Out of plane Ti:Au serpentine bridges connecting CMOS inverters [13]. b) Out-of-plane interconnections under 140% applied strain [13]. c) Simple out of plane bridges connecting CMOS inverters [13].

The deterministic structure approach has, as its main advantage, the bulk-like conductivity values of the interconnections. Also, it allows soldering of components. However, stretchability of devices with this approach is often limited, and the fabrication requirements are cumbersome, requiring clean room environments and lithographic processes.

The second category consists in using Liquid Metal (LM) (metals which are liquid at room temperature), such as eutectic gallium indium (EGaIn, melting temperature

15.7°C) and gallium indium tin (Gallinstan, melting temperature -19°C), to establish electrical interconnections. This is done by forming microchannels in an elastomeric substrate which can be filled with LM. The way in which one fills these microchannels with LM can be varied. More specifically, one can inject LM into the microchannels with a syringe, as in figure 1.10b, or selectively cover the surface with LM by stencil printing, as illustrated in Figure 1.10a. A very comprehensive report on the work already done based on the LM approach can be found in [14].

The limit on the stretchability of LM devices is mostly imposed by the elastomer which surrounds the LM wiring since the LM will just conform to changes in the shape of the encapsulating microchannels without conductivity loss. M. D. Dickey reports, in his survey of LM usage in stretchable electronics research, strains as high as 600% before rupture of the elastomeric substrate, which in this case is a thermoplastic elastomer gel (TPEG), and stability of electrical properties over 600000 100% strain cycles. [14][35]

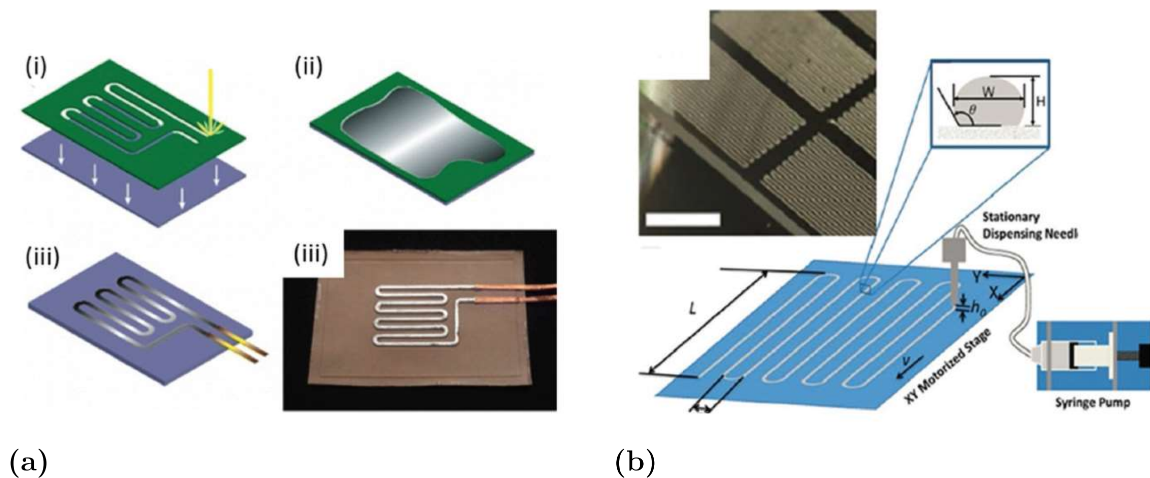

(a) (b)

Figure 1.10: a) Schematic representation of stencil printing of liquid metal track on a substrate [14]. b) Syringe filling of microchannels with liquid metal [14].

Yet another way to do this is through selective wetting of the substrate, done by simultaneously taking advantage of well established photolithographic techniques and different adhesion properties of LM's to different materials. This approach was explored, for example, by Krammer and colleagues [15], as schematically shown in figure 1.11a.

It is interesting to mention that one group took one step further by making an electronic component, a memristor, with LM [11]. They used the fact that, in contact with oxygen, a thin oxide skin quickly forms on the LM surface, which can be electrochemically manipulated, to create a memristor, which has been previously

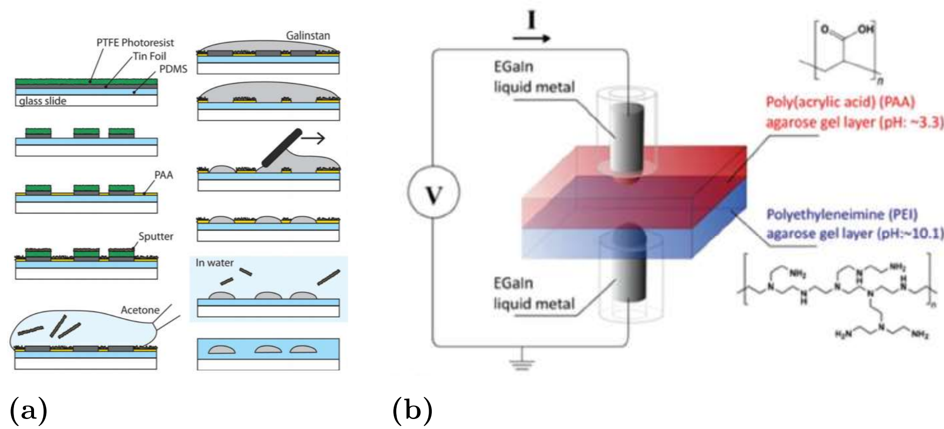

(a) (b)

Figure 1.11: a) Selective wetting of prepatterned substrate with Gallinstan [15]. b) Memristor based on electrochemical removal of oxide skin from Liquid Metal surface [11].

shown in Figure 1.6b. Referring to this figure, the oxide skin of one of the LM tips is constantly removed, while the other can be present (a logic '0') or removed (a logic '1') depending on the applied voltage.

The LM approach has obvious advantages, but also disadvantages. On one hand, the combination of the mechanical properties of a liquid, conforming to the shape of the containing volume, with the electrical attributes of a metal, mean excellent conductivity and high stretchability. On the other hand, the fact that LM's are liquid makes them difficult to pattern. Furthermore, in case of rupture of the encapsulating material, LM may leak.

Last, but not least, the third category of materials for establishing electrical interconnections in soft electronics comprises conductive composites, which are mixtures of conductive filler micro/nanoparticles, flakes or wires and polymers, and share properties of both components, namely high conductivity and stretchability. The approach taken by Tybrandt and colleagues [5], for instance, falls into this category. Although particles/wires of several different elements (e.g. silver, gold, copper, carbon) have all been the focus of studies, silver has, so far, shown to be the most promising material, which is why it features much more prominently in current research.

Upon dispersing conductive filler particles, such as silver flakes or carbon black powder (CB), in a polymer, such as PDMS, one gets a paste that, after proper treatment (e.g. oven baking), is simultaneously conductive, albeit less than the bulk material, and stretchable, although not as much as the polymer itself.

The onset of conductivity in these composites only comes about at a certain percentage of conductive filler concentration, coined percolation threshold from percolation theory, which may vary widely depending on both the type of conductive filler and polymer used. To better illustrate this point, it is worthwhile mentioning that, whereas for typical silver flakes dispersed in PDMS, the percolation threshold is roughly 12.6% by volume or approximately 80% by weight[1], for AgNW dispersed in SBS very high values of conductivity (12000 S/cm) have been reported at a filling ratio of 9% by volume [1], and for AgNW dispersed in PUA conductivity values of 45000S/cm at only 0,83% by volume have been observed [1]. This is slightly higher than the conductivity of the previously mentioned liquid metals, and only one order of magnitude lower than the bulk conductivity of silver. As yet another example, the percolation threshold of CB powder dispersed in PDMS (cPDMS) was reported to be approximately 12% by weight [8], though its conductivity is low, making it less attractive for stretchable circuit production. Figures 1.12a and 1.12b are illustrative of the process by which these composites start conducting. Figures 1.13a, 1.13b and 1.14a show circuits using electrical interconnects made of silver microparticles dispersed in PDMS, AgNW dispersed in SBS and conductive traces of cPDMS, respectively. Figure 1.14b shows the application of a cPDMS based strain sensor on the tip of a finger of a robotic hand, by Tavakoli and colleagues [8].

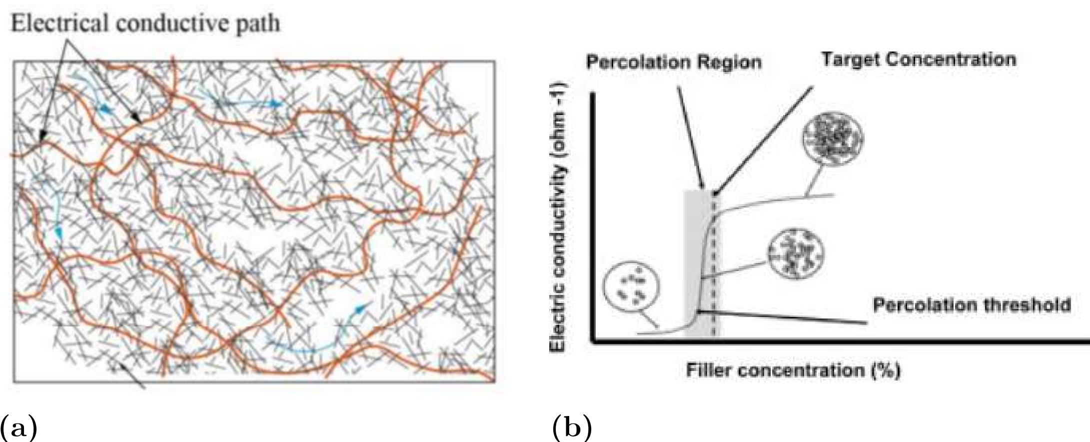

(a) (b)

Figure 1.12: a) Formation of conductive paths according to Percolation Theory [1]. b) Typical curve of conductivity as function of conductive filler percentage.

Since in conductive composites conductivity comes at the cost of stretchability - the more one loads the mixture with conductive filler particles, the bigger the mismatch between the elastic properties of the composite and those of the polymer becomes - one wants to operate as close to the percolation threshold as possible without significant conductivity losses, as Figure 1.12b neatly shows. Furthermore, an excessively high concentration of filler particles in the mixture might make the composite too

viscous for typical processing procedures such as inkjet printing.

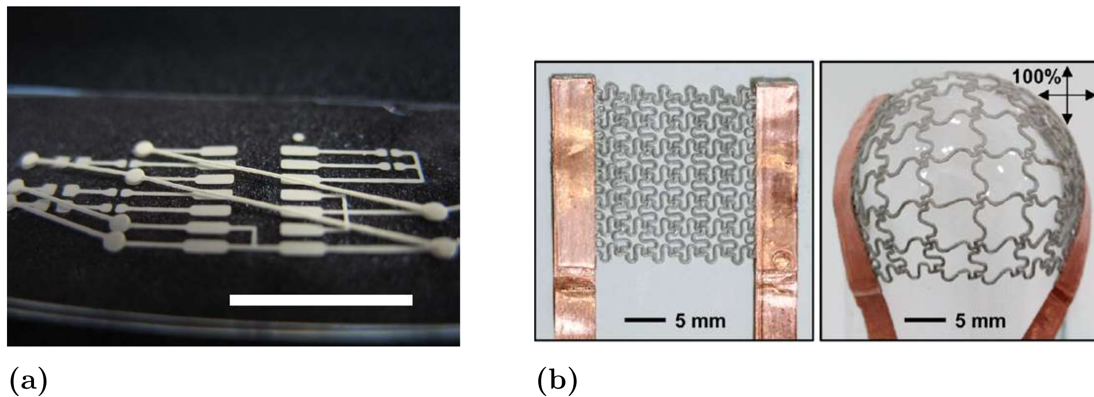

Figure 1.13: a) Patterned AgPDMS two-layer circuit on PDMS substrate [16]. b) Stretchable heater with SBS substrate and AgNW-SBS conductive composite [3].

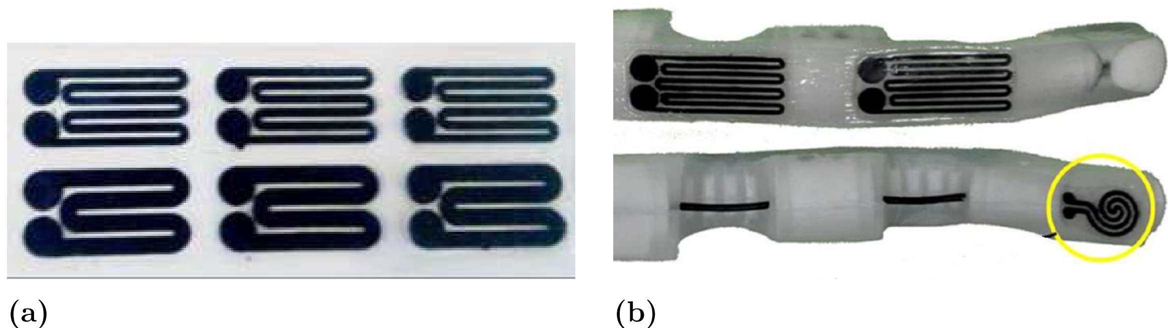

Figure 1.14: a) Carbon Black conductive traces on PDMS substrate [8]. b) cPDMS strain sensor on robotic fingertip [8].

One interesting twist to the concept of conductive composites is Anisotropic z-axis conductive PDMS (zPDMS), in which silver coated nickel microparticles are dispersed in PDMS and placed on top of a flat magnet, the magnetic field of which forms columns of aligned microparticles, as illustrated in Figure 1.15a. This alignment procedure is done while simultaneously baking the sample at approximately 100°C. The final result is a layer of zPDMS that conducts only in the vertical direction and which can be used as a 'stretchable solder'. This fact can be taken advantage of to establish electrically conductive paths between a patterned circuit layer and a surface-mounted rigid chip, just as illustrated in Figure 1.15b. C. Majidi and colleagues report, in their work, resistance values of 0.2 ohms for a zPDMS layer roughly 70 micrometers thick with 40% silver coated nickel by weight, considerably lower than the filling percentage required for Silver Polydimethilsiloxane (AgPDMS) for instance [17].

While the conductivity of most conductive composites may not be as high as that of

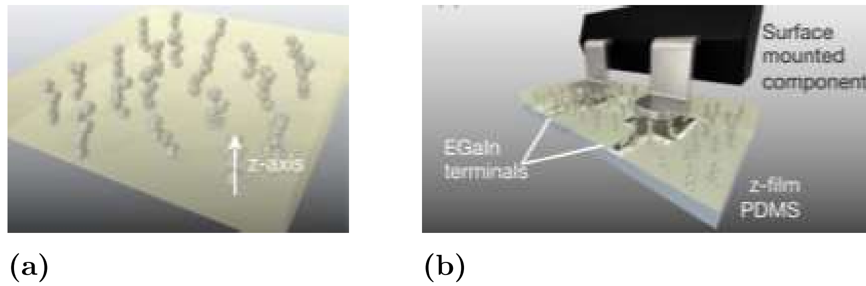

(a) (b)

Figure 1.15: a) 3-D view of aligned columns of particles in zPDMS. [17]. b) 3-D view of rigid component interfacing Liquid Metal pads by surface mounting on intermediate zPDMS layer [17].

liquid metals, and their stretchability more limited, conductive composites are easier to pattern than liquid metals and do not leak out in case of rupture. Additionally, the electrical and mechanical properties of composites can be tuned by varying the filler particle concentration. Furthermore, composites with conductivities very close to that of liquid metals have been produced, most of which based on silver fillers, and used together with different substrate materials to make devices which endured strain levels more than sufficient for most applications. For these reasons, AgPDMS conductive composites were chosen as the main topic of this dissertation.

Ideally, one would like to have a material which simultaneously matched the conductivity of bulk metal and the stretchability of the flexible substrate itself. In reality, better conductivity often comes at the cost of stretchability, and vice-versa. For this reason, it would be useful to gather in one graph the conductivity and stretchability of different composites, as well as how the former varies with stretching. Thus, to facilitate quick comparison of characteristic electrical and elastic properties of different combinations of composites and substrates, after scanning some of the related works during the last decade, two Ashby graphs were prepared, the first of which conveys information on the maximum conductivity (the conductivity with 0% strain) and strain at break for each composite (Figure 1.16). The second graph shows the strain at which the normalised resistance (R/R_0) exceeds a certain threshold value, which one may take for instance as (R/R_0) = 10 (Figure 1.17). This threshold value differs for each composite included in the graphic because not all authors report the strain at the same threshold value of normalised resistance. Research for the elaboration of these graphs drew strongly on Dang's survey of works based on conductive composites.[1]

Silver composites feature predominantly in Figures 1.16 and 1.17 because silver shows the most promise as a metal filler for conductive composites. One composite with a mixture of Copper and Zirconium also features in the graphs as an example

of other metals that have shown promising results. Finally, a study of Multiwalled Carbon Nanotubes features in the graphics as well and evidences the much lower values of conductivity normally attained with carbon-based composites. Liquid metals EGaIn and Gallistan were also included in Figure 1.16 to highlight its potential for higher strain limits, ultimately imposed by strain limit of the encapsulating elastomer. This is the reason why LM is highlighted in red.

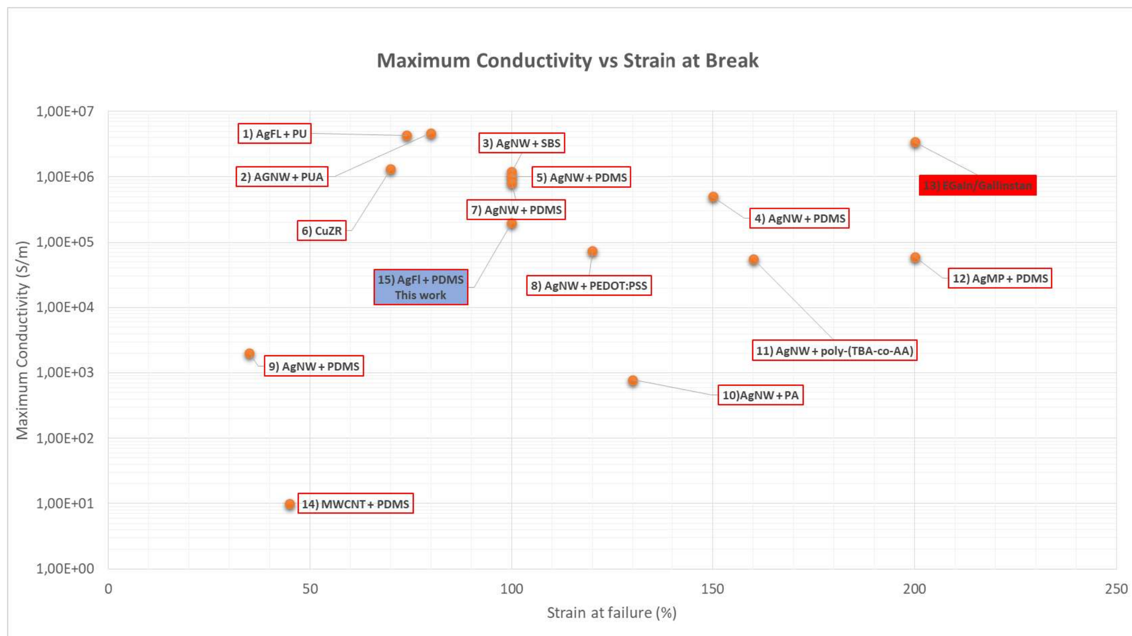

Figure 1.16: Maximum conductivity vs Strain at break for several conductive composites (and also LM); PUA - Polyurethane Acrylate, PU - Polyurethane, PA- PolyAcrylate,BS-Styrene-Butadiene-Styrene, PEDOT:PSS - poly(3,4-ethylenedioxythiophene):poly(styrenesulfonate), poly(TBA-co-AA) - copolymer of tert-butyl acrylate (TBA) and acrylic acid (AA). 1-[18], 2-[19] 3-[3], 4-[5], 5-[20], 6-[21], 7-[22], 8-[23], 9-[24], 10-[25], 11-[26], 12-[16], 14-[27].

1.4 Fabrication techniques

In this section, a summary of the most relevant techinques for fabrication of stretchable circuits is presented.

1.4.1 Patterning techniques

Stretchable circuit fabrication makes use of a wide range of techniques for patterning and material deposition. Some of these are already mature techniques, developed in

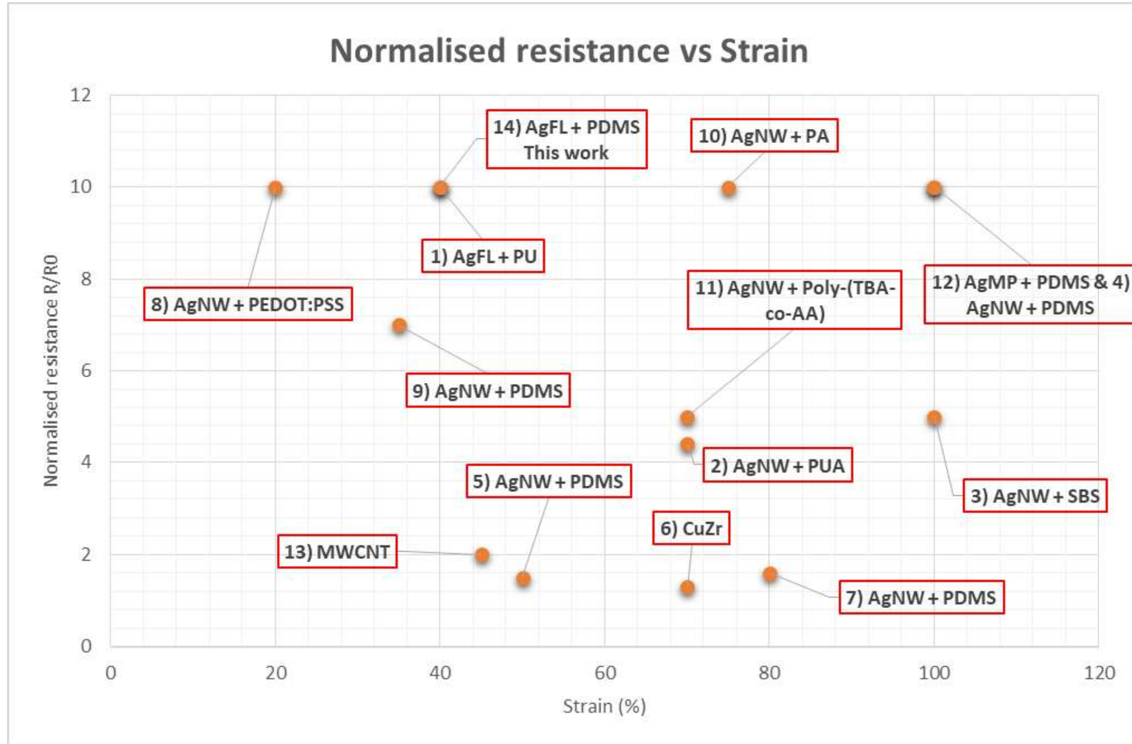

Figure 1.17: Reference values of normalized resistance vs strain.1-[18], 2-[19] 3-[3], 4-[5], 5-[20], 6-[21], 7-[22], 8-[23], 9-[24], 10-[25], 11-[26], 12-[16], 13-[27].

the context of IC fabrication, and can be applied to stretchable circuit fabrication as well. Others needed to be developed specifically for stretchable circuit fabrication, and are currently less developed and thus less reliable.

One of the main techniques utilised in this field is stencil printing, in which a patterned stencil selectively protects the substrate from being wetted with a conductive paste or ink. Wetting might be done with a range of techniques, for instance pressing the paste/ink against the stencil with a squeegee as illustrated in Figure 1.18a, spraying the stencil with an airbrush, effectively transferring the stencil pattern to the substrate, or also by drop-casting. So far, stencil printing allows resolutions down to, at best, approximately 50 μm . Larmagnac and colleagues, for instance, report 150 μm wide lines with 100 μm spacing [16], as shown in Figure 1.18b.

Alternatively, dry transfer procedures such as the one realised by Madaria and colleagues to transfer 1 millimeter pixels from PDMS stamp to a PET substrate [28], as illustrated in Figure 1.19, are also an option for soft circuit patterning.

Photolithographic techniques, paramount to IC fabrication technology, are also of use in soft circuit fabrication. Even though it might be difficult to use photolithography to pattern materials such as liquid metals, it is still sometimes used for this

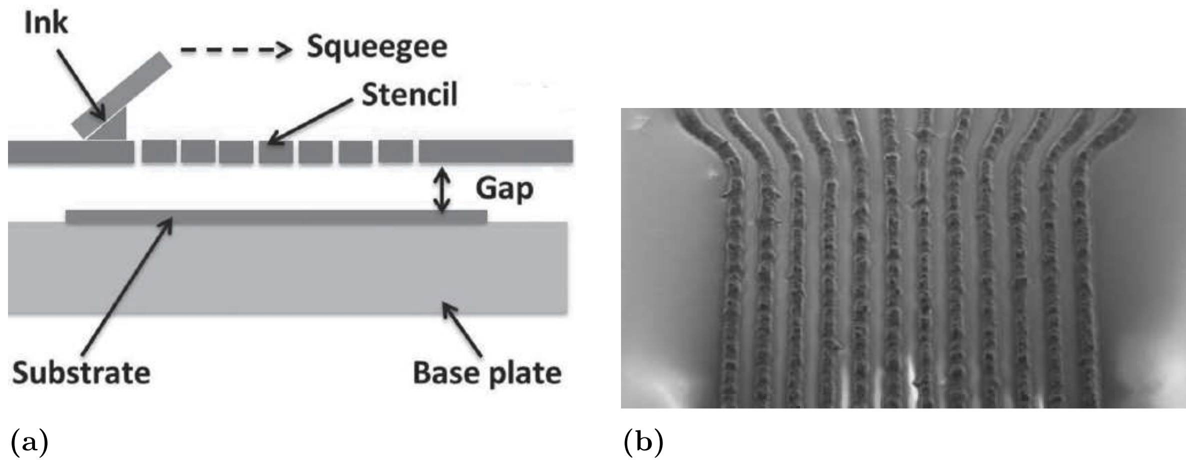

(a) **(b)**

Figure 1.18: a) Scheme of stencil printing procedure [18]. b)150 μm wide AgPDMS lines spaced by 100 μm [16].

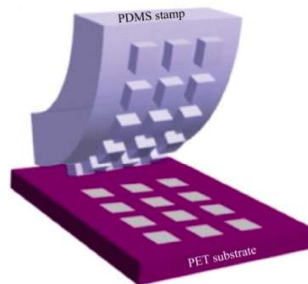

Figure 1.19: Dry transfer stamping procedure [28].

purpose when other conductive materials are used, as was done by Martinez and colleagues to pattern an AgNW layer [20], as well as in the production of stencils or in the patterning of rigid components of soft circuits, as mentioned for instance in [12].

Filtration can also be used to transfer a pattern from a mask to a substrate, as reported by [5]. In his work, a photoresist layer placed on top of a PDMS wafer was exposed to UV light according to the desired patterned. After this, the wafer was put in an diluted aqueous AgNW solution which was subsequently sucked by vacuum, in turn leading to deposition of the nanowires in the openings of the photoresist. The authors report feature resolution down to 10 micrometers, as shown in Figure 1.20b

Yet another method to pattern stretchable electronic circuits, used in the specific context of Liquid Metals, is syringe filling of microchannels in the bulk of the elastomeric substrate, as was already illustrated in Figure 1.10b. The syringe must be able to apply sufficient pressure for the oxide skin of the Liquid Metal to yield.

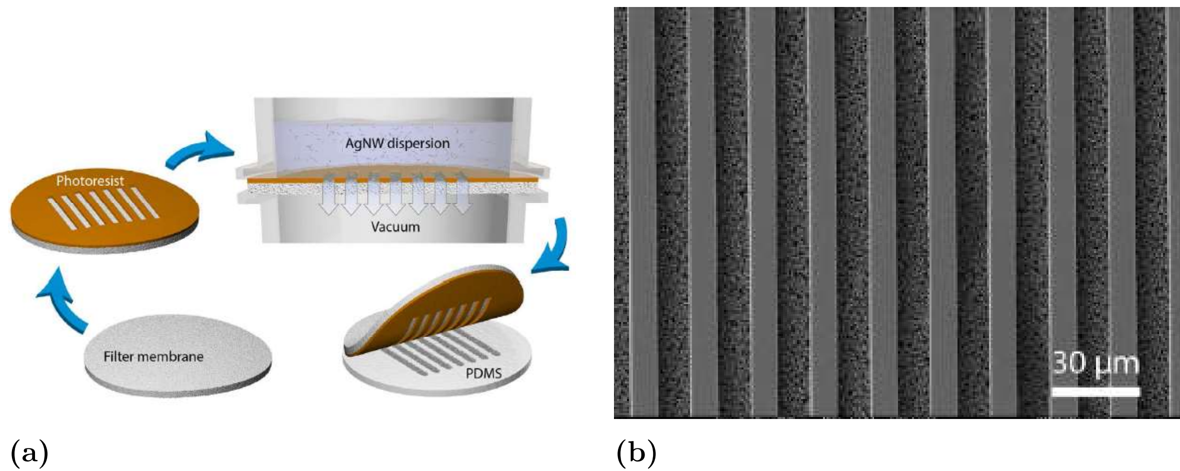

(a) **(b)**

Figure 1.20: a) Diagram of filtration procedure [16]. b) 10 micrometer wide AgNW lines with 10 micrometer separarion achieved through filtration procedure [16].

Laser ablation is another option for patterning soft circuits. Indeed, by first sandwiching a layer of the conductive element, be it Liquid Metal or a conductive composite, between two layers of elastomer, and then pointing a sufficiently powerful and narrow laser beam at the surface, one can remove material from it and create any desired pattern. This is neatly illustrated in Figure 1.21.

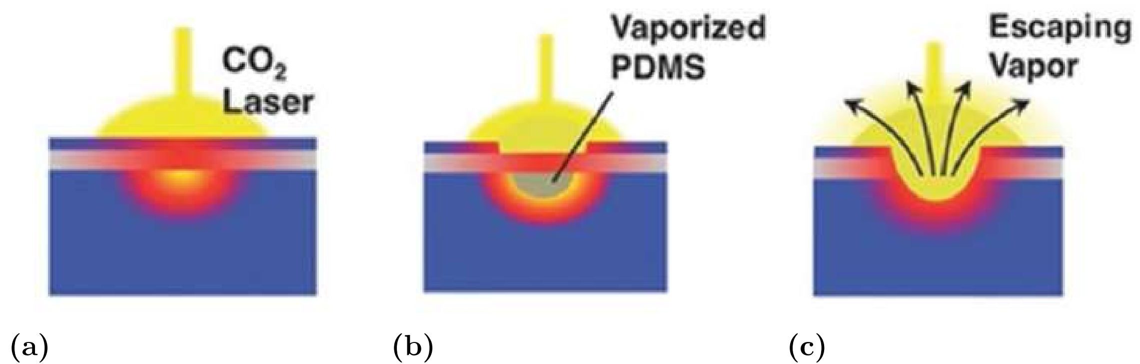

(a) **(b)** **(c)**

Figure 1.21: Laser ablation procedure [14].

Inkjet Printing, a mature technology that has widespread use ranging from home to industrial environments, has also found application in the patterning of soft circuits, given that the conductive inks/pastes have sufficiently low viscosity to be ejected. This has been done, for example, by Boley and colleagues, namely to print EGaIn nanoparticle strain gauge arrays in a glove, as shown in Figure 1.22.

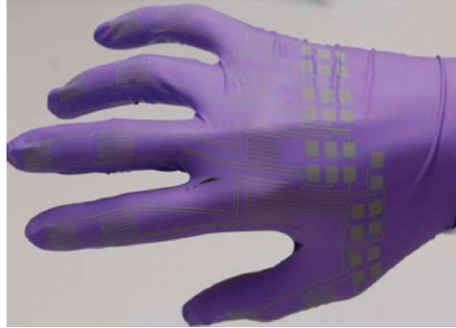

Figure 1.22: Array of EGaIn nanoparticle strain gauges patterned on glove with inkjet printing technique [29].

1.4.2 Multilayer circuits

Inevitably, as the complexity of the desired circuit increases, so will its feature density and surface area. At some point, this becomes impractical, and the need for multilayer circuits to reduce feature density while maintaining reasonable device footprint becomes apparent. This raises the issue of how to electrically interconnect different layers of a soft device in a reliable way.

Guo and Deweerth [30], for instance, tackled this issue with a photolithographic technique, illustrated in Figure 1.23. Here, a photoresist layer on top of a substrate was partially exposed to UV light in a way such that, after removing the part of the photoresist which had been exposed to light, an inverted trapezoidal portion of unexposed photoresist was left on the substrate. Covering the exposed substrate with PDMS and removing the photoresist remainder left an open inclined via in the PDMS layer, on which a gold layer was deposited, effectively establishing a contact point to the next layer. It is worthwhile noticing the importance of the via being inclined. A straight via would prevent the gold layer from depositing on the via's walls, undermining the goal of establishing an interlayer connection.

1.4.3 Rigid component integration

As mentioned in the introduction section, realising functional components such as memory cells or transistors in an intrinsically stretchable fashion in a practical and efficient way is still not feasible, although some transistor and memory component concepts have been proposed and realised (Figures 1.6a and 1.6b). These devices, however, are still far from competitive in terms of speed, size, reliability, or fabrication processes.

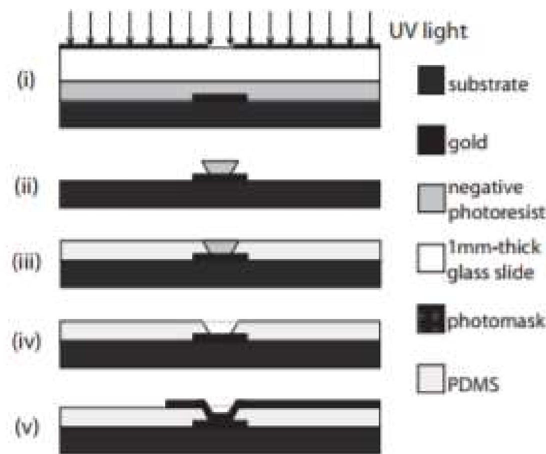

Figure 1.23: Steps in photolithographic procedure for creating interlayer electrical connection vias [30].

Because of this, it becomes necessary to integrate functional rigid components with soft interconnection circuits. The most common way to do this is to encapsulate conventional rigid components as islands inside an elastomeric substrate, as shown in the scheme in Figure 1.24a. Two practical examples of this are shown in both Figure 1.24b and Figure 1.24c. Alternatively, if the soft interconnection circuit is sealed with a layer that is conductive along its thickness, e.g. a zPDMS layer, rigid components can be mounted directly on the surface and sealed. This has been shown earlier in Figure 1.15b. In this way, though the overall system is partially composed of rigid components, it maintains its flexibility.

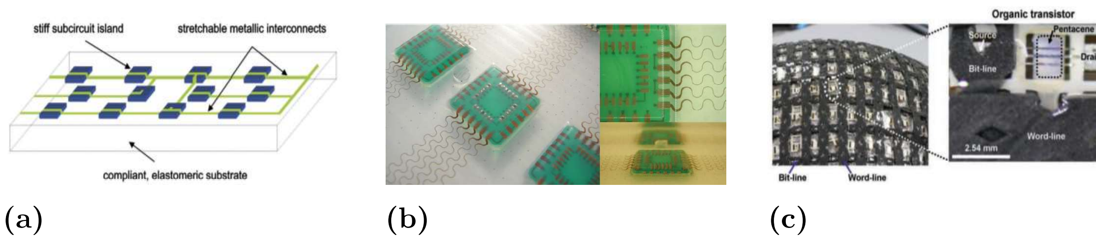

(a) **(b)** **(c)**

Figure 1.24: a) Scheme illustrating integration of rigid components through immersion of functional islands in soft substrate. [31]. b) Functional rigid islands encapsulated by elastomeric substrate [12]. c) Matrix of organic transistors, interconnected by SWCNT's dispersed in polymer, on a PDMS substrate [32].

One common issue with these integration methods is that stress tends to accumulate in the edges of rigid components, whether they are immersed in the substrate or mounted on its surface. Fracture often occurs at the soft-rigid interface. In an attempt to circumvent this problem, another clever approach was tried out by Xu and colleagues [33]. These researchers tried to encapsulate functional rigid islands in cavities filled with liquid within the substrate, thus mechanically decoupling the

rigid components from the elastomeric substrate, as can be seen in Figure 1.25. This does introduce, however, the risk of leakage in case of rupture of the encapsulating material.

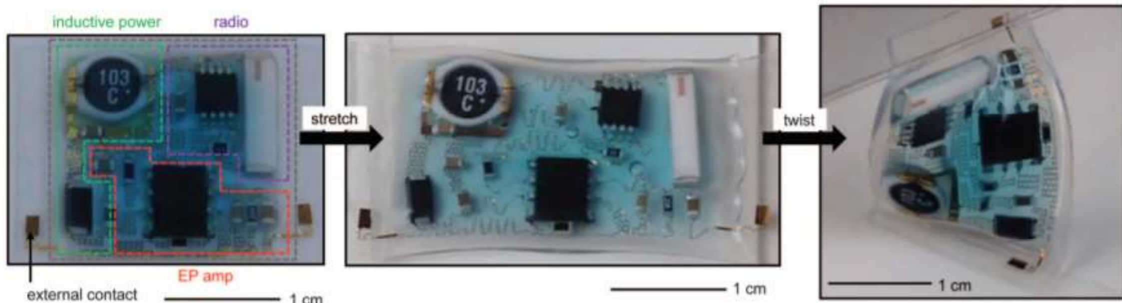

Figure 1.25: Functional rigid islands enclosed in liquid-filled cavity inside elastomeric substrate [33].

1.5 Objectives

The main goals of this dissertation are four-fold:

1) **Materials**: To select the best conductive composite out of several available silver-based options. To do this, the percolation behavior of several different silver conductive particles will be studied in order to select the particle type with the best electrical properties. The electrical stability over time of the selected particle type will also be adressed.

2) **Fabrication Methods**: To select the best fabrication procedure for both single and multilayer stretchable systems. Being able to fabricate multilayer systems will allow reducing circuit footprint and this issue is not extesively adressed in the literature. To do this, the conductivity as a function of curing temperature and time will be studied for the selected conductive particle type. The best substrate material in which to fabricate stretchable systems will be selected. Circuit patterning methods will be tested and characterised and their advatages and disadvantages weighted. A method for making interlayer electrical connections will be tested and characterised. Methods for interfacing flexible and rigid components to our stretchable systems will be adressed.

3) **Characterisation**: To perform thorough electromechanical characterisation of the stretchable electronics systems fabricated with the selected materials and methods. To do so, tensile tests will be performed measuring the reistance of samples as

a function of applied strain until rupture occurrs, as well as cyclic tensile tests to test system longevity.

4) **Case Studies**: To present two functioning AgPDMS-based multilayer stretchable electronics systems fabricated with the chosen materials and methods, a stretchable touchpad and a wireless ECG sensor.

1.6 Conclusion

Despite rapid advances in the fabrication methods of stretchable electronics, their application still requires addressing several challenges, including low-cost fabrication of multilayer circuits populated with silicon chips. These rigid chips will then be electrically interconnected either through rigid interconnection lines laid out in deterministic architectures, liquid metal lines or conductive composite lines. Stretchable electronics based on the last option will be the focus of the rest of this dissertation.

2

Materials, Equipment and Methods

This chapter consists of a thorough overview of all the materials, equipment and methods utilised in the context of this dissertation, albeit without presenting the experimental results which led to the choice of some materials and methods over others. That will be done in the next chapter. Of chief importance among the used materials are the stretchable polymer materials which served as the structure of our soft electronics modules, and the silver-based conductive composites which were used to establish electrically conductive paths. The following section will cover these and other materials. After that, the next section will focus on the equipment which was employed, throughout my work, for soft electronics systems fabrication. Finally, the last section will shine light on the methods which were used for the fabrication of soft electronics systems, as well as each method's advantages and disadvantages.

2.1 Materials

2.1.1 Stretchable silicone: PDMS

PDMS (Polydimethylsiloxane) is a silicon-based organic polymer, the structure of which is illustrated in Figure 2.1a, where the small n indicates the number of monomer blocks in one particular chain. It is optically transparent, non-toxic and inert, characteristics which make it a natural candidate for substrate/encapsulating material in soft electronics applications. It has a Young's Modulus ranging from 1.32 to 2.97 MPa and can typically be stretched to more than 100% its original length.[36]

While a number of companies commercialize PDMS, the PDMS used in the course

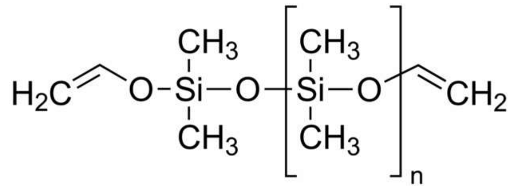

(a)

(b)

Figure 2.1: a) Chemical structure of PDMS. b) PDMS sample.

of this work was part of Sigma Aldrich's Sylgard 184 product, which in turn contains two products - monomer material and curing agent - which must be mixed (often, but not necessarily, at a 10:1 ratio) for polymerization and crosslinking to occur upon appropriate heat treatment, thus forming a solid piece of PDMS, as can be seen in Figure 2.1b.

2.1.2 Anisotropic z-axis conductor: zPDMS

Although zPDMS is actually a mixture of two other materials mentioned in this chapter, it is worthwhile introducing it briefly. zPDMS is a dispersion of magnetic, conducting filler particles (e.g. silver coated nickel microparticles) in PDMS in the right proportion (typically 30-40%). Upon proper heat treatment of this mixture under an applied magnetic field, the outcome is a material that conducts anisotropically, more specifically only in the direction of the magnetic field applied during heating. Figure 2.2a shows a layer of uncured zPDMS on top of a PDMS/AgPDMS layer, and Figure 2.2b shows a microscope image of a zPDMS layer, highliting the vertically aligned conductive columns.[34]

This material is used as a conductive interface between soft and rigid components, a 'stretchable solder paste'.

2.1.3 Conductive Composites

To establish electrically conductive paths, conductive composites were used in this work. Conductive composites are fabricated by mixing electrically conductive filler particles with a polymer material (e.g. PDMS) in a ratio such that the mixture

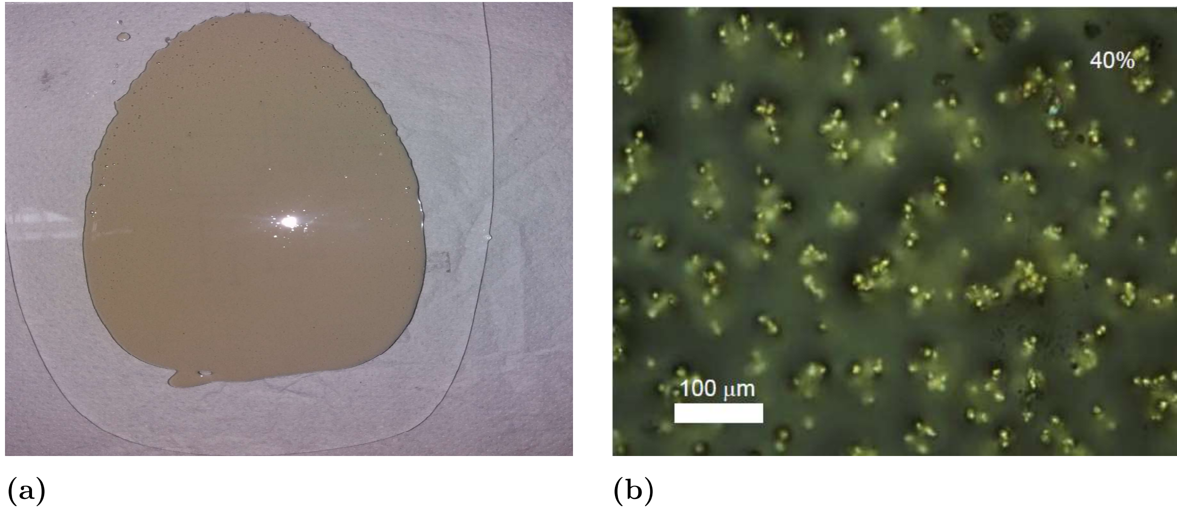

(a) (b)

Figure 2.2: a) Uncured zPDMS layer (brown). b) Microscope image of vertically aligned conductive columns of Silver-coated Nickel particles embedded in PDMS matrix.[34]

preserves the electrical properties of the composite (good conductivity) and the mechanical properties of the polymer (stretchability). The electrical behavior of this mixture as a function of composite percentage is well explained by Percolation Theory (see State of the Art chapter for a brief explanation). In the context of this dissertation, several AgPDMS conductive composites were tested for use in stretchable electronics applications. Table 2.1 contains the names and main properties of each of these candidates. Figures 2.3a and 2.3b contains SEM images of particles type I and II (see Table 2.1) provided by the manufacturer.

Filler Particle	Manufacturer	Average size (μm)	Type	Silver %
Silver Flake 071	Technic Inc.	2.0	I	100
Silver Microparticle 586	Technic Inc.	0.5-2.5	II	100
Silver Flake 105	Technic Inc.	15.0	III	100
Silver Microparticle 304	Technic Inc.	2.0	IV	100
Silver Microparticle	Sigma Aldrich	2.0-3.5	V	100
Silver-coated Nickel	Potters Industries	15.0	VI	30
Silver-coated Nickel	Potters Industries	8.0	VII	40
Silver-coated Ferrite	Potters Industries	25.0	VIII	20

Table 2.1: Types of conductive composites which were tested, with information relative to size, manufacturer and silver particles percentage.

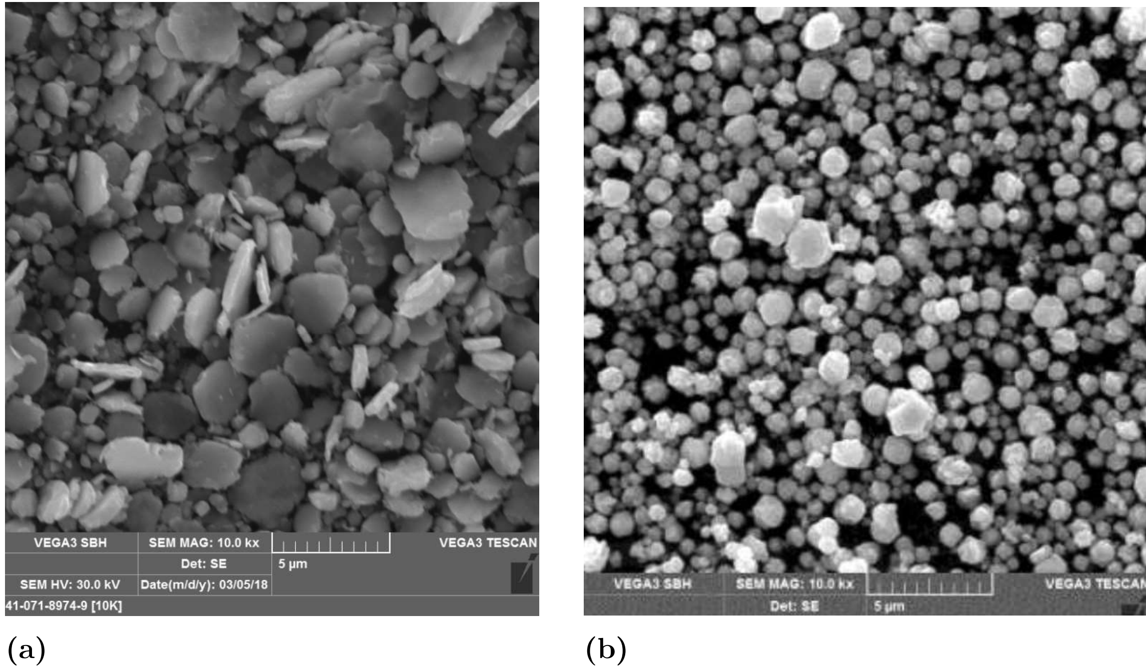

(a) **(b)**

Figure 2.3: SEM images of silver flakes (type 1, see Table 2.1) and microparticles (type 2), provided by Technic Inc.

2.1.4 Equipment

Many pieces of equipment were used for performing paramount steps in the fabrication of soft electronics systems in our lab. This section briefly introduces these pieces of equipment.

The most relevant equipment was the VLS3.50 laser cutter from Universal Laser Systems® was used to pattern stencils, to fabricate moulds and to open vias connecting different circuit layers. This laser cutter consists of a horizontal arm which can move in the x and y directions and a platform that is able to move along the z-direction. Furthermore, the arm is equipped with a 10.6 μm CO_2 50W laser. The speed and effective power output of the laser can be further controlled with device-specific software. The laser cutter can be seen in Figure 2.4.

The fabrication of conductive composites by mixing polymer material and conductive filler particles was achieved with the mixer Thinky ARE-250, which performs mixing through centrifugation, and also degasses mixtures, at a maximum speed of 2000 and 2200 rpm's, respectively. This equipment is shown below in Figure 2.5a.

The application of thin PDMS films to serve as either substrate layer or encapsulating layer was performed using the thin film applicator ZUA 2000 from Zehnter. This thin film applicator allows film thicknesses from 50 μm up to 3000μm. This

Figure 2.4: Universal Laser Systems VLS3.50 laser cutter.

instrument is shown in Figure 2.5b.

(a) **(b)**

Figure 2.5: a)Thinky ARE-250 Mixer used for fabricating conductive composites.. b) Thin film applicator for fabricating thin circuit layers from Zehntner.

The curing of samples was performed in one of two ovens, model SLN 115 from the company 'Pol-eko Aparatura' (Figure 2.6a), and model T962C DGC from 'Puhui' (Figure 2.6b). Both ovens are capable of reaching 300ºC, the former having an accuracy of 0.1°C and the latter an accuracy of 1°C.

The weighting of samples, in turn, was performed with a Kern PCB laboratory scale with milligram precision. This equipment is shown in Figure 2.7.

The measurement of resistance, in general, was performed with either a Fluke 45 dual display multimeter, shown in Figure 2.8a, or an HP34401A multimeter for 4-terminal sensing measurements, shown in Figure 2.8b. These pieces of equipment are accurate to the milliohm. The tensile tests presented in the results section were a notable exception, as the resistance measurements were performed with a setup

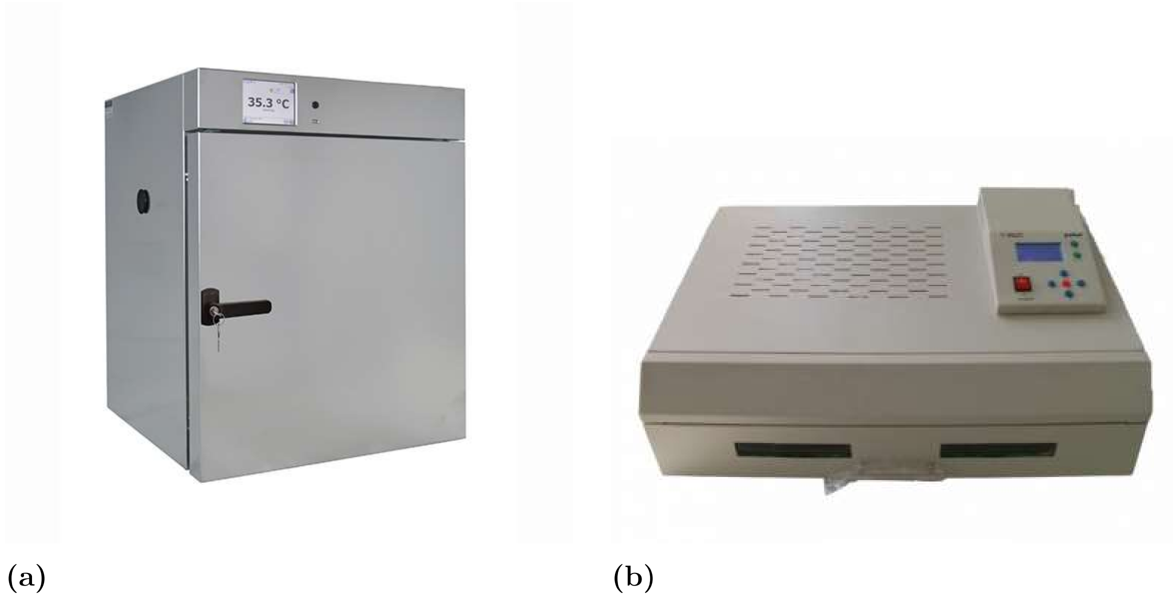

(a) **(b)**

Figure 2.6: a) Oven from Pol-eko. b) Oven from Puhui.

Figure 2.7: Kern PCB laboratory weighting scale.

built in our laboratory.

The soldering of rigid components and alloying of liquid metal droplets to flex PCB copper pads was performed with a Hakko FX88D soldering station, shown in Figure 2.9a. Soldering flux SMD291NL fabricated by Chipquick, shown in Figure 2.9b, was used to facilitate both soldering and alloying.

Ease Release 200 agent from *Mann* was applied to substrates prior to deposition of either PDMS or AgPDMS, to facilitate the lifting process after curing. This prevents cracks, which would irreversibly damage the circuit, from forming in the system.

Detailed observation of small features at the micrometer scale was performed using

(a)

(b)

Figure 2.8: a) Fluke 45 multimeter. b) HP 34401A multimeter

(a)

(b)

Figure 2.9: a) Hakko FX888D soldering station. b) Soldering flux.

Figure 2.10: Ease release agent from Mann.

AMscope's T490A microscope, shown below in Figure 2.11a. A MU900 digital camera from Amscope was connected to the microscope and to a computer for

image capture. This camera can be seen in Figure 2.11b. In general, throughout this work, the 4x magnification lens was used for imaging.

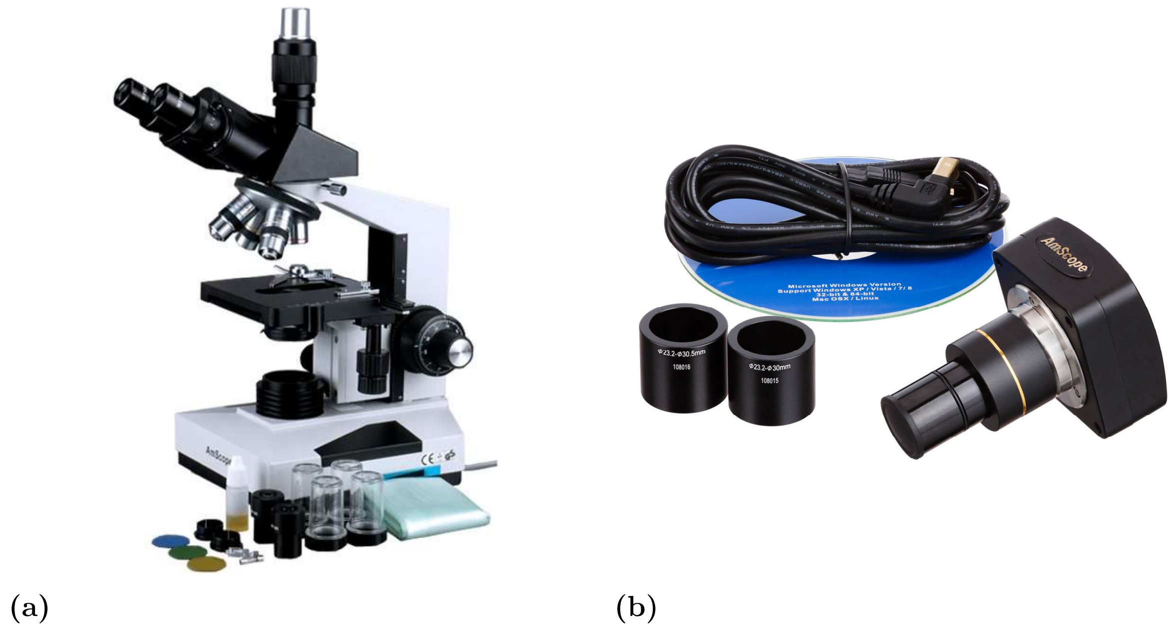

(a) **(b)**

Figure 2.11: a) T490A microscope from AMscope. b) MU900 digital camera from AMscope.

Tensile tests were performed using an Instron 5943 universal testing system, with a load cell capable of achieving 1 kN of tension force and with a vertical testing space of 1123 mm. The equipment is shown in Figures 2.12a and 2.12b.

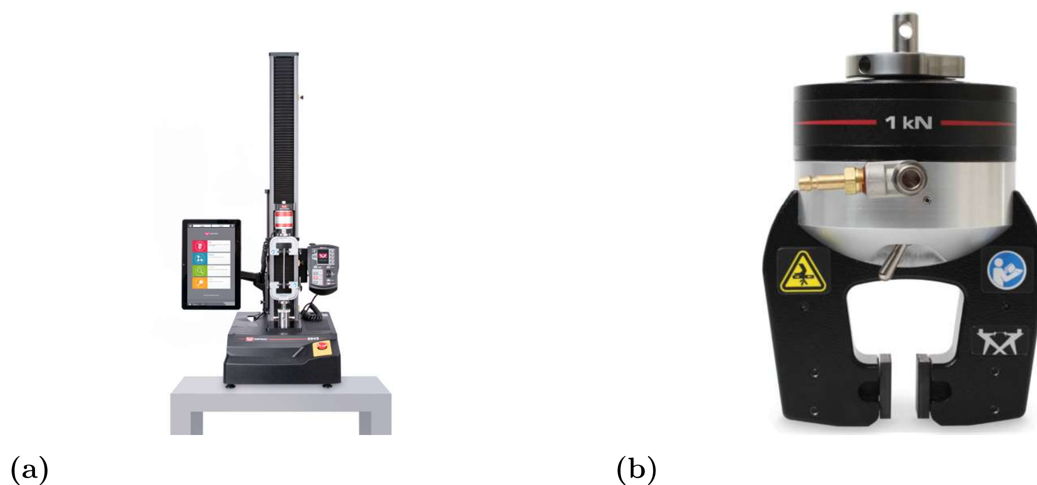

(a) **(b)**

Figure 2.12: a) Instron 5943 universal testing system used to perform tensile tests. b) 1kN pneumatic gripper used for tensile tests.

The tensile tester is not capable of measuring resistances by itself. It is capable, however, of incorporating user-defined measurements into the results of tests per-

formed with it. To measure resistances during the tensile tests, a setup was built at our laboratory, shown in Figures 2.13a and 2.13b.

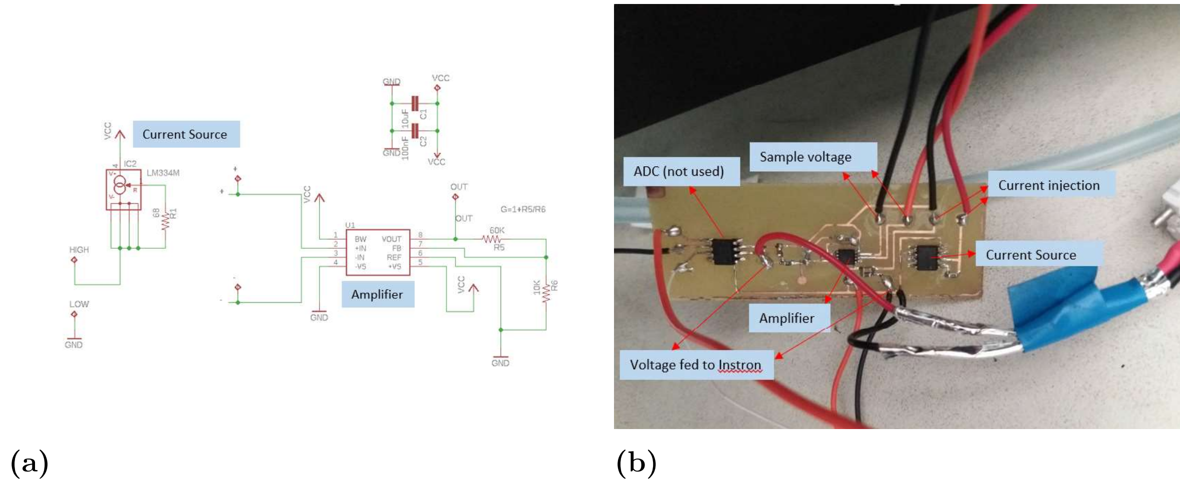

(a) (b)

Figure 2.13: a) Scheme of circuit for measuring the resistance of AgPDMS samples during tensile tests. b) Circuit board used for measuring the resistance of AgPDMS samples during tensile tests.

2.2 Methods

This section serves to introduce all the methods which were utilised in the fabrication of soft electronics modules. This includes patterning methods, multilayer fabrication methods and methods to integrate flexible and rigid components into soft electronics modules. Patterning methods will be introduced first.

2.2.1 Moulding

The PDMS pre-polymer is a viscous liquid. Its mixture with silver filler particles, however, is not. Nonetheless, it can still be processed as a material which fills cavities. For this reason, moulding is an applicable patterning technique. To do this, cavities must first be carved in a block of material (e.g. acrylic) in the shape of the desired circuit. Then, one must press AgPDMS paste into these cavities with a squeegee, cover the mould with PDMS and apply an heat treatment to the mould. After this, the cured PDMS/AgPDMS system should be easily lifted from the mould. In the context of this dissertation, moulds made of different materials - acrylic, Teflon, aluminum - were tested. The main disadvantage of this method is the mechanical damage that often occurs during the lifting steps, with substantial

amounts of AgPDMS breaking apart and being left on the mould. Figure 2.14 illustrates the moulding process in a simplified way.

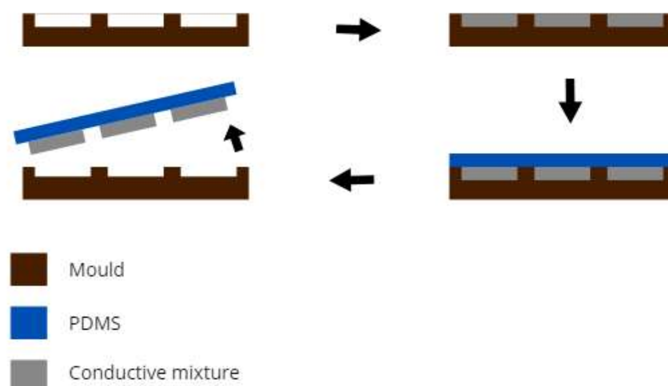

Figure 2.14: Schematic of ideal moulding process.

2.2.2 Stencil Printing

Alternatively, stencil printing was tested as another technique to pattern circuits. To do so, an inexpensive adhesive paper was used as the stencil material which was patterned with a laser printer, shown in Figure 2.4. AgPDMS circuits are then deposited by spreading AgPDMS paste on top of the stencil with a squeegee. Tempered glass was used as the substrate on which the stencil was placed and the conductive pastes deposited. Figure 2.15a illustrates the stencil printing procedure, and Figure 2.15b shows an actual stencil patterned by laser printing. This technique allows for rapid, inexpensive prototyping of stretchable electronics circuit, which makes it an attractive option. Among the disadvantages of this method are the bottom limit on feature dimension imposed by the stencil mechanical fragility and the limitation it imposes on the type of patterns which can be transferred, as splitting the stencil into two or more parts makes the lifting step more difficult.

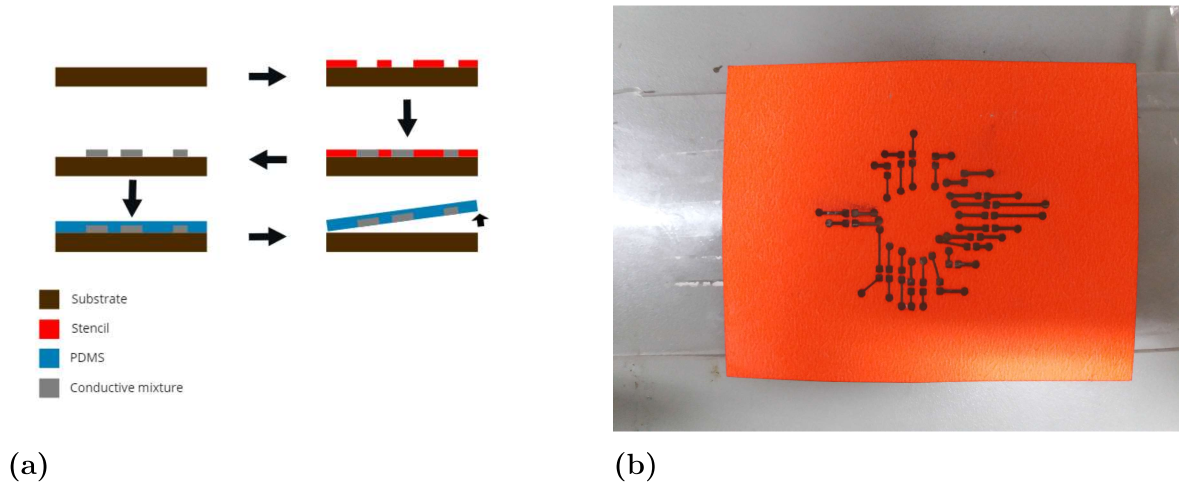

(a) (b)

Figure 2.15: a) Scheme of stencil printing procedure. b) Adhesive paper stencil.

2.2.3 Screen Printing

Another technique which was considered as a means of patterning circuits was screen printing. This consists of a screen with a tightly woven mesh (made of stainless steel). Upon application of a photoresistive product to the mesh and selective exposure to light of the appropriate wavelength (UV in the case of our setup) the desired pattern will be imprinted on the screen in the form of open mesh nodes through which an applied conductive ink such as one of our silver pastes can be squeezed. In our experiments, the screen which was utilised had a mesh count of 140T - 140 openings per centimeter. This screen can be seen in Figure 2.16. The photoresistive material which was used was a 2-part pre-sensitized photo emulsion from the company 'Art2silk', shown in Figure 2.16. This emulsion, in turn, was applied to the screen using a coating through, shown in Figure 2.16. To do this, the coating through was pressed against the screen and tilted, and then passed over the whole length of the screen to soak it with emulsion. After letting the emulsion dry, a mask would be put on top of the screen and the setup would be exposed to UV light (Figure 2.16), to transfer the pattern from the mask to the mesh. After this step, application of the conductive ink would ensue, followed by the final step, screen reclaiming, for which a screen strip product from 'Art2silk', shown in Figure 2.16, was used. While this procedure involves more steps than the stencil printing technique, its main advantage is the possibility of printer higher resolution, higher feature density patterns, due to the mechanical rigidity of the screen.

Figure 2.16: Screen (left); Coating through (top right); Photoemulsion (bottom center left); Emulsion remover (bottom center right); UV lamp (Bottom right).

2.2.4 Multilayer fabrication

Inevitably, as the feature density of our circuit designs increased, successful patterning became harder, with adjacent features blending together, which limited the fabrication of our stretchable electronics systems. Thus, it became necessary to resort to multilayer circuit designs, which allowed reducing the feature density while maintaining the overall circuit estate (area). This was done by using the stencil printing technique for each circuit layer, but using a laser cutter with optimised speed and power parameters to open vias to the previous layer before applying conductive paste for the current circuit layer. For this to work, exact alignment between successive layers is of the utmost importance. This issue has a simple solution, which is placing an alignment piece on the laser cutter table to have a permanent reference point. The laser cutter which was used for this purpose is shown in Figure 2.4. Figure 2.17a shows laser-ablated vias connecting two AgPDMS layers. Figure 2.17b shows schematically the procedure for opening vias.

2.2.5 Rigid-soft interfaces

The interface between rigid and stretchable materials remains the bottleneck of stretchable electronics systems. Indeed, given that functionalities such as memory or processing aren't yet implementable with stretchable materials, they must be provided by rigid components integrated into stretchable modules. The interface

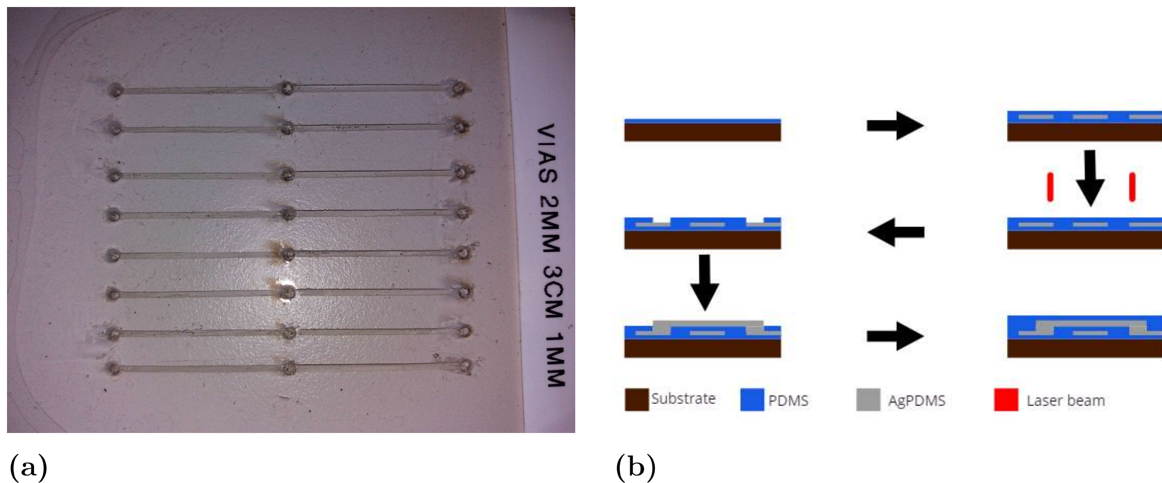

(a) (b)

Figure 2.17: a) Laser ablated vias connecting two AgPDMS layers. b) Schematic representation of via opening procedure.

between these rigid components and the surrounding stretchable module is often where stress builds up the most, and thus where mechanical/electrical failure normally happens first. In this work, a few solutions were explored to interface rigid components with stretchable circuits. First of all, an anisotropic conductor, zPDMS, was tested as an interface material between AgPDMS and flex PCB's containing rigid components. zPDMS conducts only along the direction of a magnetic field applied to it during the curing procedure. In this way, if one patterns an AgPDMS circuit with contact pads matching contact pads on a Flexible Printed Circuit Board (Flex PCB) containing a rigid module, this module can be integrated by placing the flex PCB over the AgPDMS contact pads with a zPDMS layer in between, as shown in Figure 2.18a. To further improve electrical contact, liquid metal droplets are alloyed to the contact pads on the flex PCB. This procedure is schematically illustrated in Figure 2.18b The placing of the flex PCB over the zPDMS layer is done before the curing procedure. Curing is normally done at 100°C for 30 minutes with the sample placed over a flat magnet. Alternatively, directly connecting copper traces on a flex PCB was tried as a simpler interfacing method, This was done by trapping a flex PCB between a PDMS layer and a stencil, in correct alignment, applying AgPDMS conductive paste and trapping the circuit layer and the flex pcb by applying another PDMS layer. This can be seen in Figures 2.19a and 2.19b.

Yet another method tested as a solution for interfacing rigid and soft components was crimping metal 'claws' with AgPDMS, followed by application of an additional PDMS layer to mechanically strengthen the interface region, which was fragilized upon crimping. The metal claws were then inserted in an adaptor with output pins that could, in turn, be soldered and connected to any other module (e.g. a

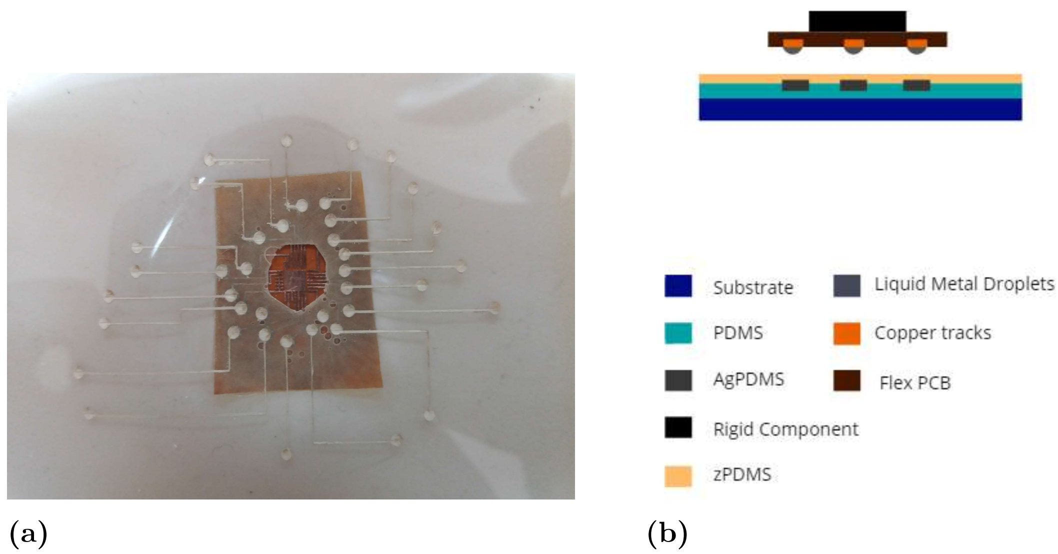

Figure 2.18: a) Flex PCB integration with zPDMS layer. b)Schematic representation of flex PCB integration procedure with zPDMS.

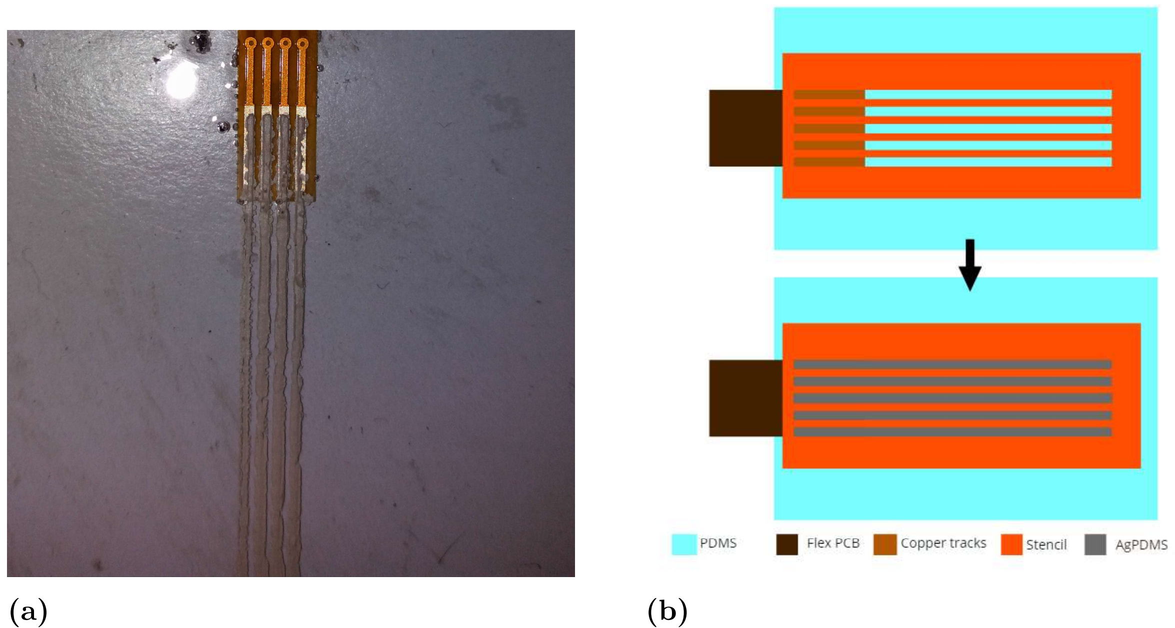

Figure 2.19: a) Direct flex PCB integration. b) Schematic representation of direct flex PCB integration procedure.

development board. Figures 2.20a and 2.20b illustrate this method. Figure 2.20b in particular shows this solution working with 1.27 millimeters pitch.

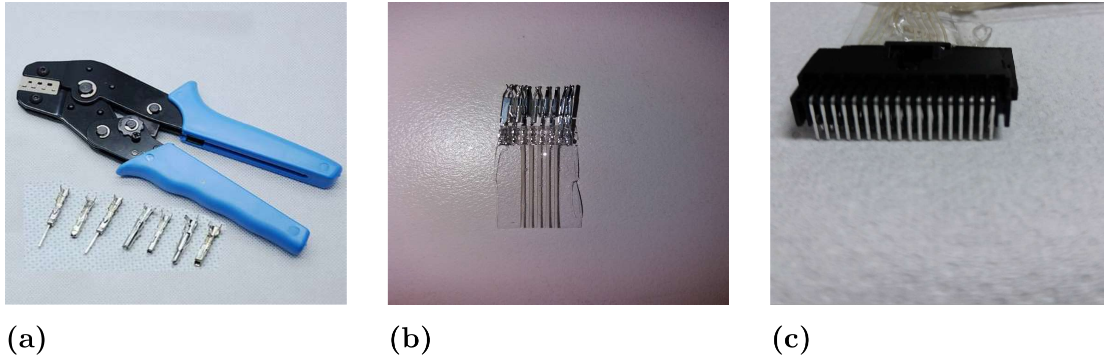

(a) **(b)** **(c)**

Figure 2.20: a) Crimping tool. b) Metal 'claws' crimped with AgPDMS lines. c) Crimp connector.

2.3 Conclusion

While this chapter presented the materials and methods used throughout this work, dwelving into the results - choice of composite, choice of patterning method, etc.- was avoided. This will be done in the following chapter, where, at first, the electrical characterisation of the different composites tested willbe presented. Then, results concerning the characterisation of different fabrication methods and rigid/soft interfacing methods will be presented, and arguments will be given to support the choice of specific procedures over others based on what the final goal is (e.g. rapid prototyping or scalable fabrication). Finally, electromechanical characterisation of samples built with the chosen materials and methods will be presented.

3

Results

In this chapter, results will be presented regarding the choice of conductive filler particles to be used in our AgPDMS-based stretchable electronics system, more specifically percolation tests for all tested particles and electrical stability over time for the selected particle type. Then, the results of tests meant to select/characterise the curing procedure, patterning methods, multilayer fabrication methods and soft-rigit interfacing methods will be discussed. Finally, the results of electromechanical characterisation tests of samples fabricated using the chosen materials and methods will be given.

3.1 Choice of conductive composite

3.1.1 Percolation Behavior

To begin with, a comparison of the percolation behavior of several conductive filler particles (the ones mentioned in table 2.1) was carried out. To this end, the weight percentage of conductive filler particles dispersed in PDMS was gradually increased starting at 60% weight, with the goal of finding the percolation threshold for each particle type, that is, the minimum percentage of filler particles at which the composite becomes conductive. For each conductive filler particle type and for each filler particle weight percentage, an average of the conductivities of five AgPDMS lines [W x L x T: 1 x 30 x 0.2 mm], deposited on top of a 500 μm PDMS layer, on top of a tempered glass substrate (as shown in Figure 3.1a) was taken (Figure 3.2). All samples were cured at 150°C for 1h.

.

A four-point resistance measurement technique was used, with liquid metal droplets placed at the contact points of the measurement probes to further reduce the contact

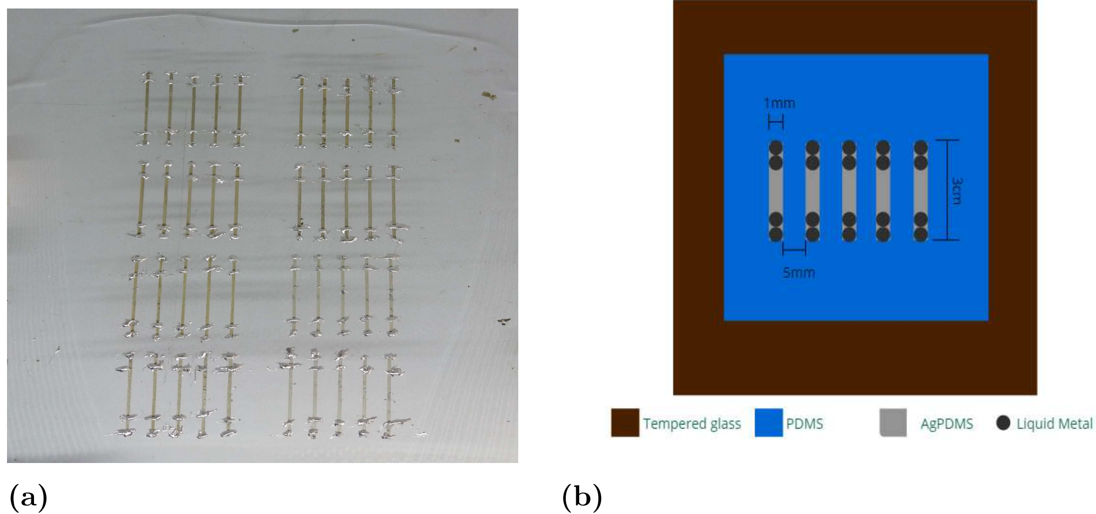

(a) **(b)**

Figure 3.1: a) Setup for measurement of resistances in percolation tests. b) Scheme of the setup for resistance measurements in percolation tests.

resistance. Furhtermore, this was done to avoid direct contact of the measurement probes with the AgPDMS lines, since this could cause mechanical damage to them. The setup for measurement can be seen in Figure 3.1b.

The results, illustrated in Figure 3.2, clearly show the onset of conductivity for filler particle weight percentages between 70% and 80%, with the exception of particles type III and IV. The superior conductivity of particles of types I, II, V and VIII (see Table 2.1) is apparent, specially particles types I and V (silver flakes and silver microparticles, respectively). At percentages of 84% by weight and higher, however, conductive composite made of particles type V is very hard to process due to its viscosity. This is evidenced by the sharp decrease of conductivity which can be seen in Figure 3.2.

Figure 3.2 can be compared with Figure 1.12a back in chapter 1, which shows the theoretical percolation curve for conductive composites.

In light of the information gathered from the percolation tests, silver flakes (type I, see Table 2.1) were chosen as the focus of more in-depth study and as the conductive particles to be used in the applications presented in the next chapter, which was expected if one takes in account geometrical arguments - on one hand, the smaller the particles are, the better they should fill the PDMS matrix, and on the other hand, the flake geometry leads to bigger contact area between adjacent particles when compared to the microparticle round geometry.

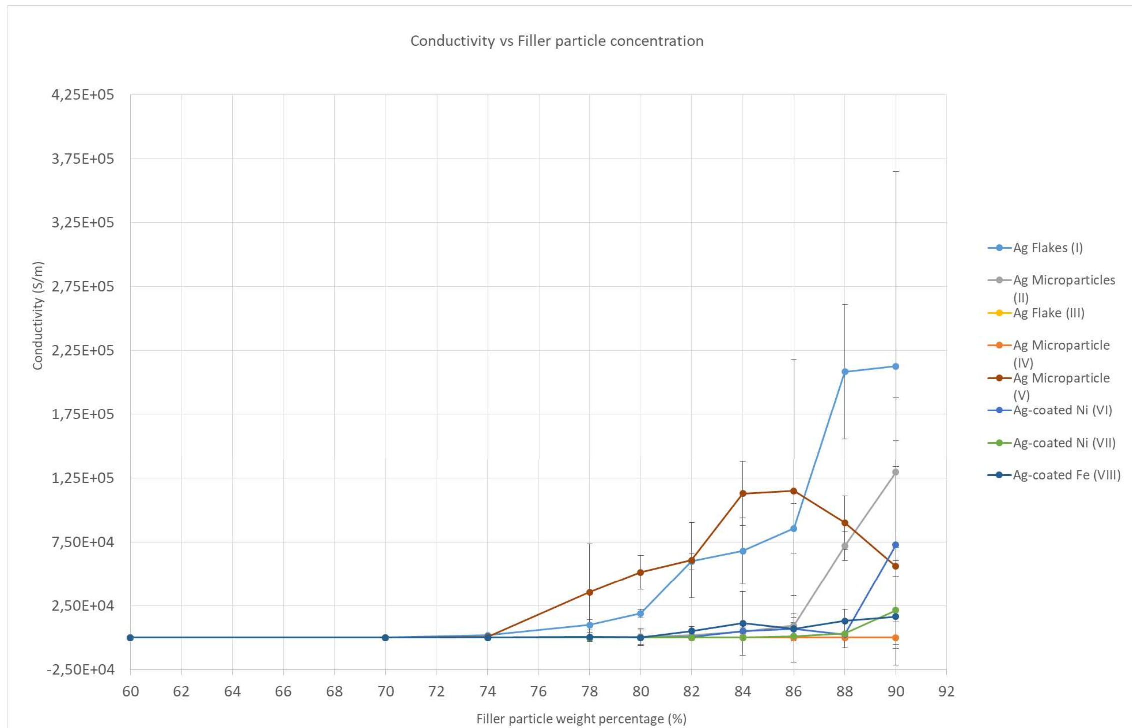

Figure 3.2: Average conductivity as a function of particle type and weight percentage of silver particles in PDMS matrix.

3.1.2 Electrical stability of AgPDMS over time

Tests of the variation in conductivity over time for the selected type of conductive filler particle (silver flakes type I, see 2.1) were conducted for over two months. To do so, a PDMS layer was first cured on top of a tempered glass substrate, followed by application of AgPDMS paste to form ten lines [W x L x T: 1 x 30 x 0.2 mm], which were then cured at 150°C for 1 hour. In this process, AgPDMS paste at a weight concentration of silver particles of 85% was used. To measure the resistance of the lines, a two point resistance measurement method was used, as the interest was in measuring changes in resistance, which should be due to the lines themselves. Figure 3.3 shows the obtained results. As one can verify, the conductivity values proved to be stable for at least over 1800 hours (two months). After a conductivity increase over the first few days after the sample was fabricated, one can only notice a slight tendency for conductivity to decrease over time.

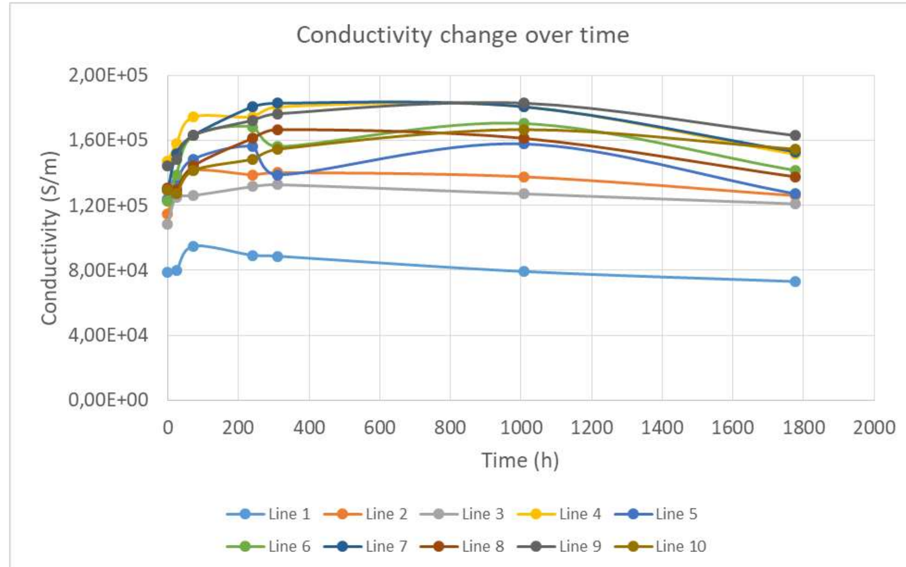

Figure 3.3: Conductivity as a function of time elapsed since fabrication of the test sample.

3.2 Fabrication procedure

3.2.1 Curing procedure

Taking the particle type which showed the most promise in the percolation tests (silver flakes type I, 2.1), tests were conducted to define the minimum temperature and curing time necessary for the particles to sinter and conduct properly. To this end, samples of eight lines [W x L x T: 1 x 30 x 0.2 mm] at 85% weight percentage were baked at progressively higher temperatures for progressively longer periods of time. The specific temperatures and times used can be seen in the table below, table 3.1. The values in this table are averages taken over each set of 8 lines.

Conductivity (S/m)				
	Time (h)	1	2	3
Temperature (°C)	-	-	-	-
50	-	0	$6{,}33 \times 10^2$	0
80	-	$2{,}90 \times 10^3$	$2{,}81 \times 10^3$	$8{,}90 \times 10^2$
100	-	$1{,}62 \times 10^4$	$1{,}34 \times 10^4$	$2{,}28 \times 10^3$
120	-	$3{,}02 \times 10^4$	$5{,}16 \times 10^4$	$3{,}61 \times 10^4$
150	-	$1{,}10 \times 10^5$	$1{,}59 \times 10^5$	$1{,}35 \times 10^5$
180	-	$1{,}53 \times 10^5$	$2{,}26 \times 10^5$	$2{,}80 \times 10^5$

Table 3.1: Conductivity of AgPDMS as function of curing temperature and curing time.

While AgPDMS with silver flakes begins exhibiting conductivity at low temperatures (80°C), sintering is still imperfect and the lines can easily be mechanically damaged, as can be seen in Figure 3.4. Up until temperatures of 100°C, the lines keep a glossy, pasty look and are easily damaged when the measuring probes come in contact with them. On the contrary, particles cured at a 150°C conduct one order of magnitude better than those cured at 100°C, and exhibit a more solid, dry texture. This can be seen in Figures 3.4a and 3.4b, which were taken after measuring the resistance of the lines, and is indicative that the AgPDMS paste fully sintered.

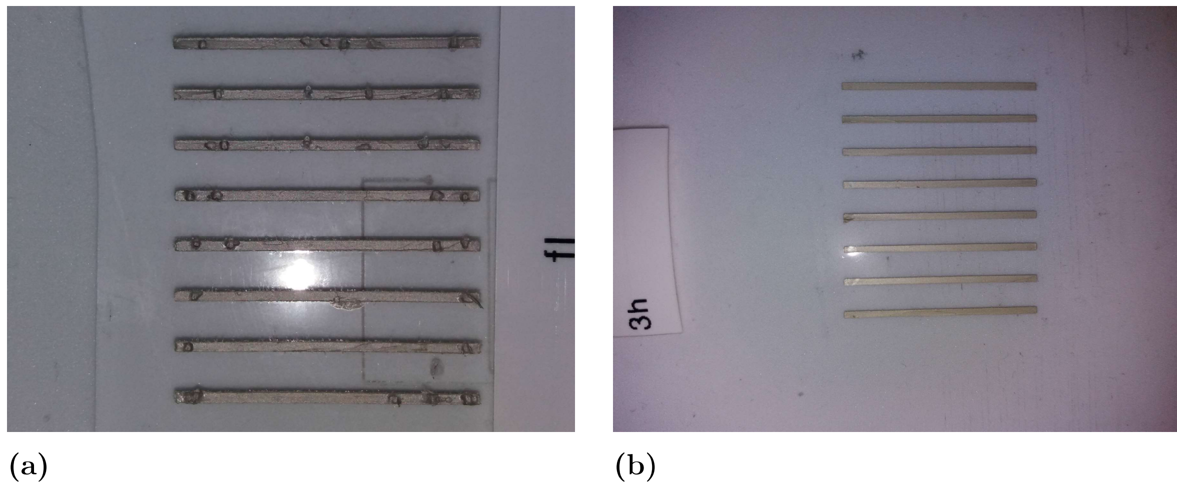

(a) (b)

Figure 3.4: AgPDMS with particles type I cured at a) 50°C, b) 150°C for 3h.

By looking at Table 3.1, one can see that while the conductivity of the samples still increases somewhat in going from 150°C to 180°C, this is not as pronounced as the increases from 100°C to 120°C or 120°C to 150°C. In light of this information, temperatures of 150°C or higher are advisable, and the exact temperature to be used should be selected taking also into account energy costs and behavior of the substrate material and other integrated components.

3.2.2 Patterning Methods

Different methods were tested as possible ways of patterning AgPDMS soft circuits, namely moulding, stencil printing and screen printing.

3.2.2.1 Moulding

As mentioned before, one of the possible ways of patterning soft AgPDMS circuits was moulding. To this end, AgPDMS paste was spread with a spatula on an acrylic

mould which had previously been patterned in the laser cutter. After this, the moulds would be covered with PDMS and subsequently taken to the oven to cure. However, this approach rapidly proved ineffective, as the moulds would begin to melt at the temperature needed to cure AgPDMS with filler particles of type I (roughly 150°C). Furthermore, lifting the soft circuit from the mould would often irretrievably damage the AgPDMS lines, due to the mechanical irregularities inherently present in the mould. Aluminum and Teflon were tested as alternative mould materials, given that their melting temperatures are considerably higher than the required 180°C, but the problem of damages inflicted upon the AgPDMS lines during the lifting step persisted. Lastly, moulding wasn't very suitable for multilayer device fabrication. This patterning method was dropped early on. Figure 3.5b shows a mould for AgPDMS electrodes which began melting while the electrodes were curing at 150°C. Furthermore, a considerable amount of cured AgPDMS can be seen to have not adhered to the PDMS substrate and to have been left behind in the mould cavities.

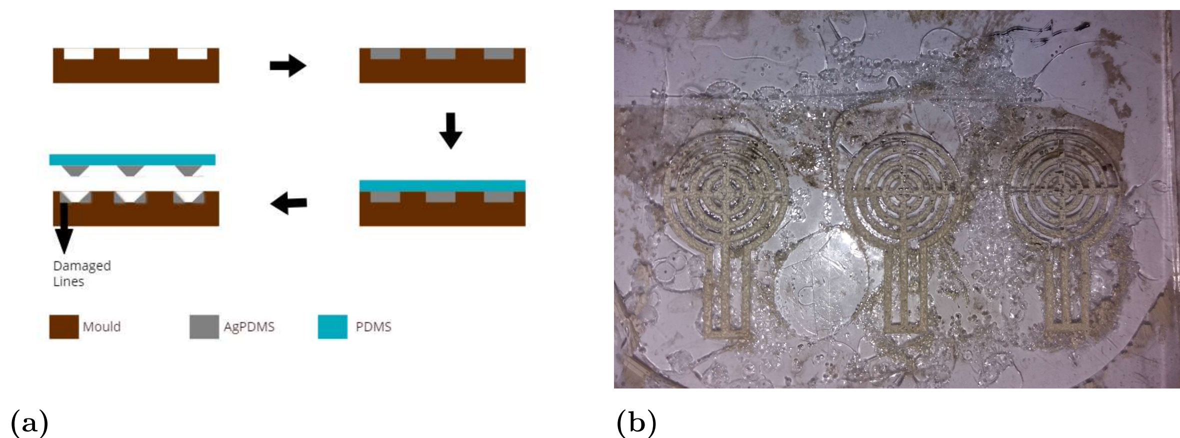

(a) **(b)**

Figure 3.5: a) Scheme of imperfect moulding process, with AgPDMS paste leftover in mould. b) Damaged electrodes mould, with AgPDMS leftover paste.

3.2.2.2 Stencil Printing

Alternatively, stencil printing was tested as a patterning method. The stencil printing process has already been explained in the Materials and Methods section. To make this procedure work appropriately, the optimal laser cutter parameters had to be found which effectively transferred the desired pattern to the adhesive paper stencil without burning it. 40% laser power was the minimum power which allowed perfect pattern transfer to the stencil, as at lower power values some burnt stencil material would be left attached to the stencil, interrupting the pattern lines. On the

other hand, 80% laser speed represented a good trade-off between rapid stencil fabrication and perfect pattern transfer. Using this procedure, defining submillimeter features down to roughly 500μm was possible. On the other hand, this procedure becomes problematic when the feature density increases, as the stencil might break down into two or more pieces, which complicates the lifting step. This problem can be easily circumvented by dividing the circuit into several layers, reducing the feature density while maintaining the overall circuit area. Overall, the stencil fabrication process is simple, rapid, and inexpensive. A typical circuit could be patterned in, at most, half an hour (ignoring curing times). For these reasons, stencil printing was the preferred patterning method during this work. Figure 3.6 shows how the stencil method can be used to pattern multilayer, fine-detail, AgPDMS circuits.

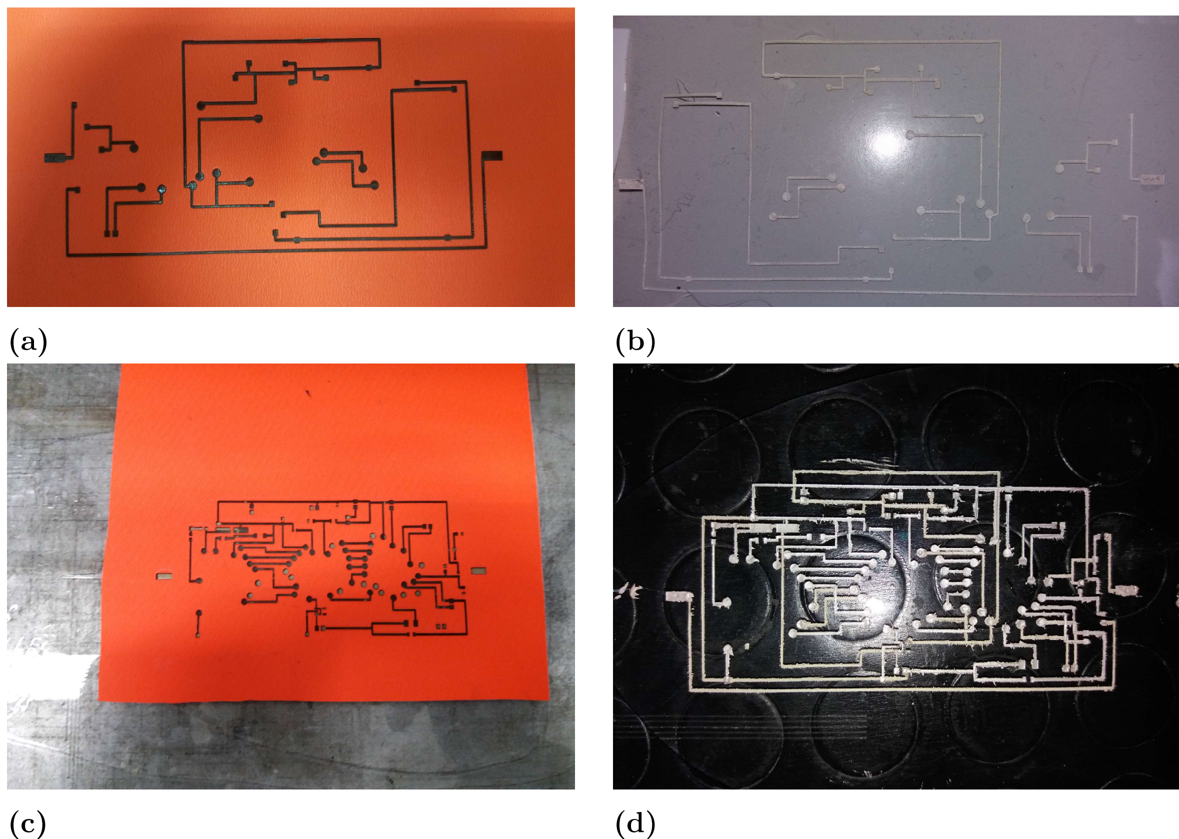

Figure 3.6: a) Stencil for 1st layer of circuit. b) Patterned 1st layer of AgPDMS circuit. c) Stencil for 2nd layer of circuit. d) Patterned 2nd layer of AgPDMS circuit.

To better understand the minimum feature size that could be patterned using adhesive paper stencil and a laser cutter, a resolution test was performed. A design with ten 3cm long lines, with widths ranging from 1mm to 100μm in steps of 100μm, was fed into the laser cutter, and lines down to 200μm were successfully patterned on the adhesive paper, as shown in Figure 3.7a. The 100μm line was not successfully

patterned on the stencil, setting a bottom limit on the width of the lines the laser cutter can print on this material.

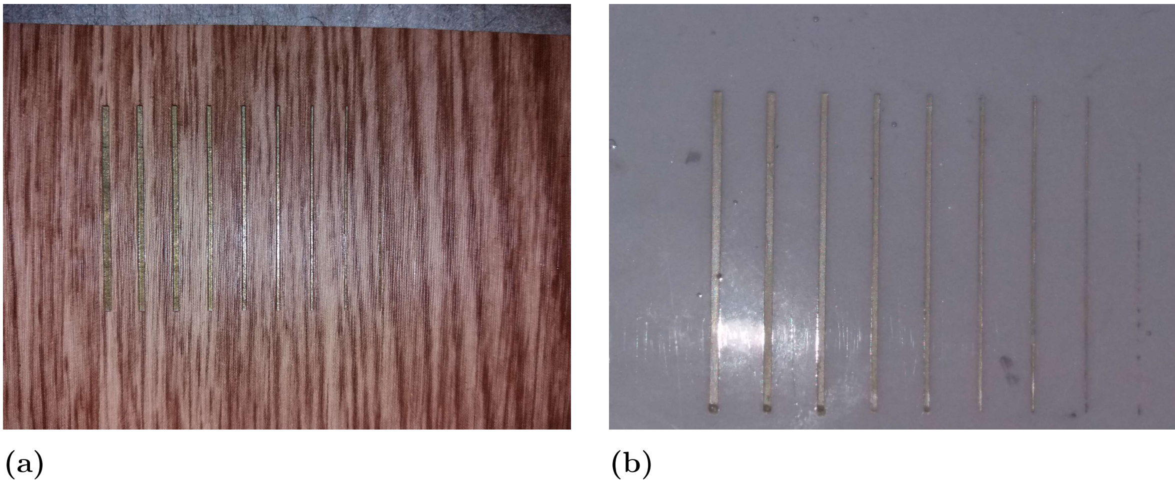

(a) **(b)**

Figure 3.7: a) Adhesive stencil paper with lines from 1 millimeter down to 200 micrometers. b) AgPDMS lines from 1 millimeter width down to 200 μm width.

After patterning, AgPDMS paste with silver particles type I at 85% weight percentage was applied to the stencil, to test how well features of each size would transfer from the stencil to the substrate. The results can be seen in Figure 3.7b. AgPDMS lines as narrow as 300 μm fully formed on the PDMS substrate, whereas the 200μm line which the laser was able to pattern on the stencil was poorly transferred to the circuit, with several interruptions occurring along the line.

To further test the quality of the lines, these were observed under an optical microscope. The main goals were to find whether the dimensions of the lines were consistent with the drawings fed into the laser cutter, and whether the lines had cracks or not. The images obtained for the 1mm, 500μm, 400μm and 300μm lines can be seen in Figure 3.8.

As can be seen, while the stencil printing method allows patterning 400μm and 300μm AgPDMS lines, these already start forming cracks which harm, or even prevent, conductivity. Indeed, while resistances for lines down to and including 600μm were measured to be consistently between 1 and 2 Ω, and 5 Ω for the 500μm line, for 400μm width and below lines either did not conduct or showed resistances of MΩ. Furthermore, microscopic measurements showed that the lines were generally narrower than the expected width according to the drawing fed to the laser cutter. To verify these conclusions, success rate tests were performed for 500μm, 400μm and 300μm wide lines. For each width value, ten lines were printed, patterned and cured with the methods mentioned above and the resistance of each one was measured, as

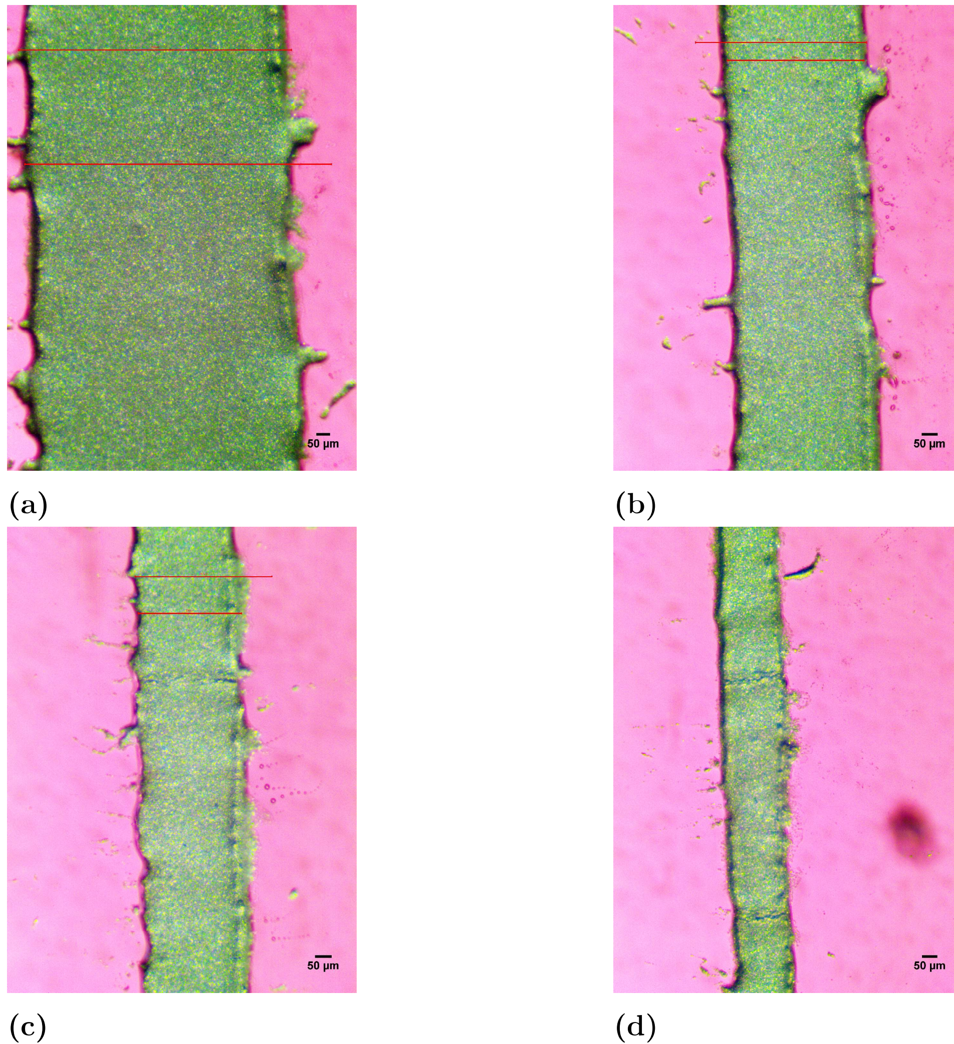

(a) (b) (c) (d)

Figure 3.8: a) 900 μm wide line. b) 500 μm wide line. c) 400μm wide line. d) 300μm wide line. All images were obtained under the same optical microscope with a 4x magnification lens. Cracks are already visibly forming in the 400μm and 300μm wide lines

.

well as the real width of each line. The success rates for each linewidth can be seen in Table 3.2. A sample was deemed unsuccessful if it had an electrical resistance of more than 5 times the lowest resistance value of the set of 30 sample lines.

Width (μm)	300	400	500
Success Rate (%)	70	90	100

Table 3.2: Success rate of line patterning as function of line width.

For the 500μm wide lines, which were fabricated with 100% success rate, observation under an optical microscope (Figures 2.11a and 2.11b) was carried out. A sample

line can be seen below in Figure 3.9. The laser-patterned stencil used to pattern these lines was also observed under the microscope before and after applying the AgPDMS paste and lifting the stencil, as can be seen in Figure 3.10.

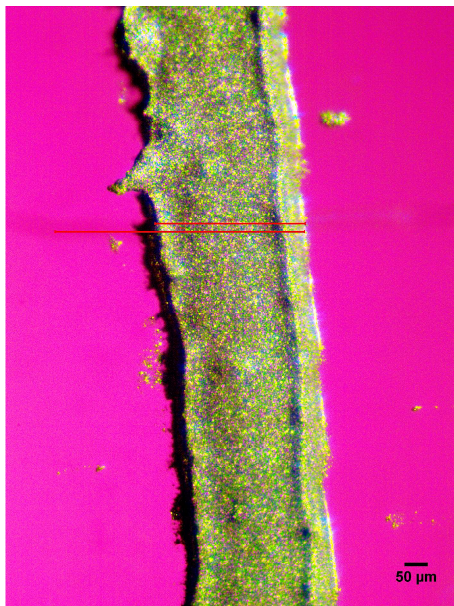

Figure 3.9: Stencil-patterned AgPDMS line with expected width of 500μm and real width of 300μm.

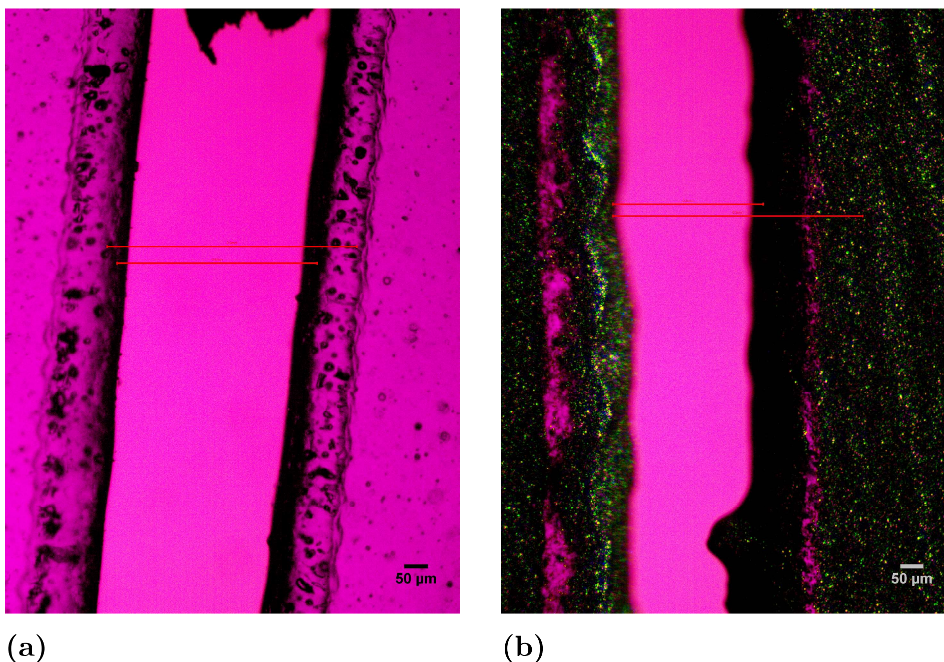

(a) **(b)**

Figure 3.10: a) Stencil line after laser patterning. b) Stencil line after application of AgPDMS paste and lifting from the substrate.

From these figures and the ones shown before, it's clear that real AgPDMS linewidths will be smaller than the widths specified in the drawing fed into the laser cutter by

about 100-200μm, both because of the process of laser-patterning the stencil and the process of lifting the stencil after application of the AgPDMS paste, which takes out AgPDMS paste from both sides of the lines.

Afterwards, a test to check the minimum spacing between features achievable with this technique was also performed. In this setup, a drawing with several 3cm long, 300μm wide lines with separations between them ranging from 1 mm down to 100μm in steps of 100μm, was fed to the laser cutter. Spacings down to 500μm were successfully preserved in the paper stencil, whereas lines separated by less than that merged together, as shown in Figure 3.12a by the much larger line on the right of the image compared to the one on the left.

Figure 3.11: Stencil used for minimum feature separation test.

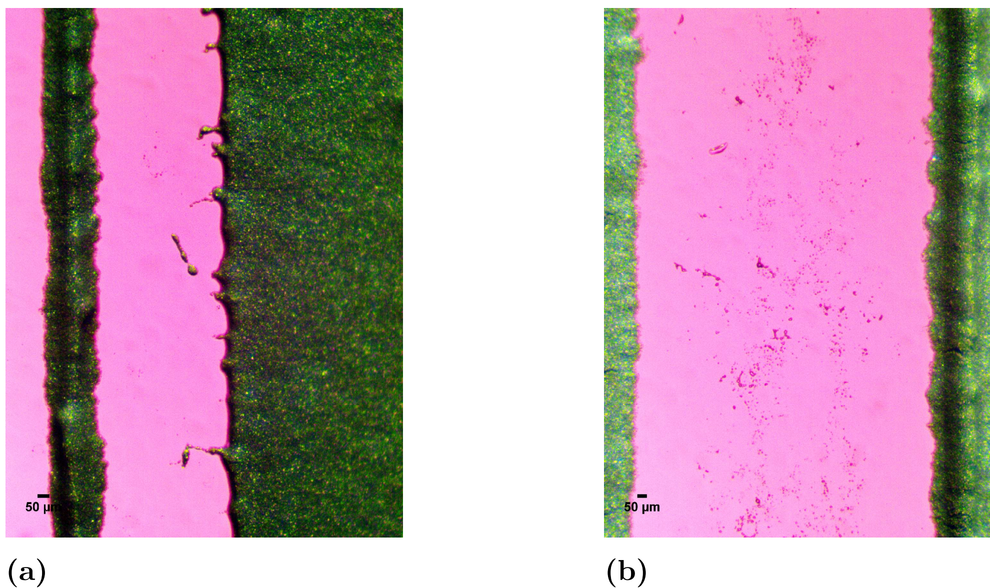

Figure 3.12: a) 500μm spacing between lines; on the right there are several lines blended together, as can be seen by the much bigger thickness compared to the line on the left. b) 900 μm spacing between lines.

In conclusion, after performing these tests it became clear that printing 500μm features, separated by at least 500μm, was the limit imposed by both the laser cutter and the stencil material.

3.2.2.3 Screen Printing

Screen printing was also tested as a known method for rapidly patterning AgPDMS circuit layers. The fine mesh used in the screen, this method constitutes an alternantive to stencil printing which could allow smaller feature size and greater feature density. The general procedure has already been explained in the 'Materials and Methods' section. For the screen printing procedure to work successfully, some process parameters had to be defined, such as emulsion drying time and screen exposure. In my experiments, I found that letting the emulsion (Figure 2.16) dry on the screen for thirty minutes would suffice, and exposing the screen to normally incident UV light with a 25W bulb for 1h was enough to lock the desired pattern onto the screen. After these steps, the unexposed emulsion could simply be removed with a water hose, leaving the screen ready for application of AgPDMS conductive paste. After application, soaking the screen in 10:1 diluted emulsion remover (Figure 2.16) for 2 minutes proved sufficient to unlock the emulsion from the screen, and by blasting the screen with water from a water hose, the emulsion would come off seamlessly. The AgPDMS paste was removed by simply applying propanol and scrubbing the paste off the screen. Figure 3.13 shows the screen with applied and dried emulsion and the photomasks. It also shows the screen exposure setup. Figure 3.14, on the other hand, shows the AgPDMS paste application step and the same circuit shown in Figure 3.6d, but fabricated in one layer with the screen printing method, illustrating the potential of the technique to increase feature density. Nonetheless, while screen printing would probably be the better choice for batch fabrication, it involves lengthy and somewhat complex steps, and stencil printing still proved to be the simplest and most rapid fabrication method for prototyping multilayer circuits.

3.2.3 Curing substrate

Having chosen stencil printing as the preferred patterning method for prototyping, choosing the substrate material on which to fabricate samples was necessary. The substrate on which one lets samples cure is of great importance, mostly because of its mechanical behavior when heated (thermal expansion) and the ease of lifting PDMS layers off of it. Given that the conductive composite being used - AgPDMS with silver flakes 2μm (type I, see Table 2.1) - requires curing at, at least, 150ºC, this imposes a tight restriction on the choice of substrate material. Indeed, acrylic, aluminum, tempered glass and Teflon were tested as possible substrate materials, in this order. Acrylic was rapidly disqualified since at 150ºC it already begins melting,

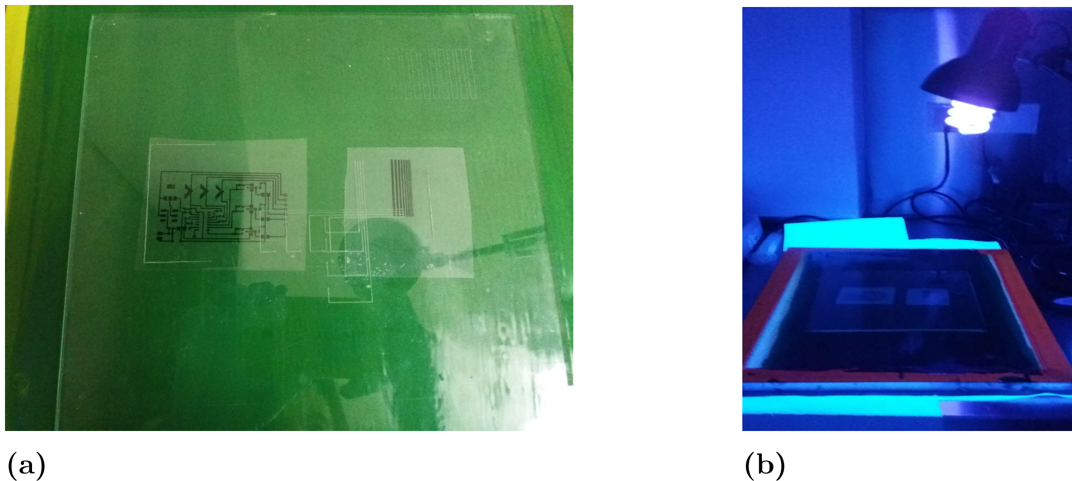

(a) (b)

Figure 3.13: a)Screen with emulsion applied and photomasks on top. b) Screen exposure setup.

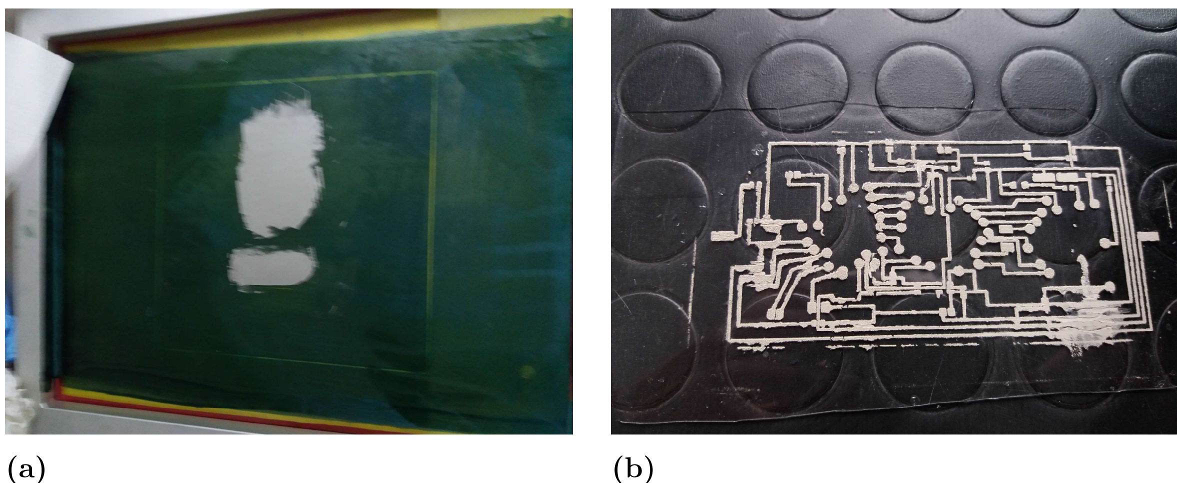

(a) (b)

Figure 3.14: a) AgPDMS paste application after exposure. b) Circuit produced with screen printing procedure.

which damages the sample and prevents precise overlay of multiple circuit layers. Given this outcome, a substrate which could endure high curing temperatures was necessary, and hence aluminum was tested. However, lifting thin PDMS layers from aluminum soon proved a taunting task, even using an ease release agent (see Figure 2.10) as the PDMS layers would easily be shattered in many pieces. After this, tempered glass was tested as the substrate material, and the results were very satisfactory. Indeed, tempered glass easily endures 150°C without expanding or bending significantly, and though lifting thin PDMS layers can be very difficult if PDMS is applied directly on the tempered glass surface, application of ease release agent (Figure 2.10) prior to application of PDMS layers solves this problem. One issue with using tempered glass is that depositing an AgPDMS layer in direct contact

with it can lead to damaged lines and leftover AgPDMS on the glass surface, which is why, when using tempered glass, starting with a protective PDMS layer is always advisable. Finally, so that the first protective PDMS layer could be avoided, Teflon was also tested as a possible substrate material, in the hope that the lifting step would be seamless even if the first layer (the one in contact with the Teflon substrate) were AgPDMS. While this proved to be the case, it quickly became apparent that Teflon expanded and bent at 150°C, making it unsuitable for fabrication of multilayer systems. In the end, it became clear that tempered glass was the best choice of substrate material on which to cure PDMS /AgPDMS soft systems. These results are summarised in Table 3.3

Substrate material	Bends (150°C)	Melts (150°C)	Lifting
Tempered glass	No	No	Easy
Acrylic	Yes	Yes	Easy
Teflon	Yes	No	Easy
Aluminum	No	No	Hard

Table 3.3: Properties of different materials tested as substrate.

3.2.4 Vias Characterisation

The next step was to study the process of creating vias between circuit layers and characterising them. This was done by laser ablating the PDMS layer covering interlayer contact points. For this purpose, the laser parameters of power and speed had to be tweaked to allow opening vias with the smaller amount of laser runs possible, while at the same time creating a small amount of debris. Furthermore, the success rate of the procedure for opening vias should be as close as possible to 100% to make the procedure reliable. Lastly, the vias should represent no bottleneck on the conductivity of the overall system. Figure 3.15 shows magnified pictures of vias under an optical microscope.

The setup for performing characterisation of the vias is as shown in Figure 3.16. Eight AgPDMS lines [W x L x T: 1 x 30 x 0.2 mm], were applied to a Teflon substrate using an adhesive paper stencil, patterned in the laser cutter, and then covered with a PDMS layer of varying thickness. The thickness of this layer is also the thickness of the vias, which is one of the parameters of interest. It was varied from 1mm to 750μm, and then further down to 500μm. The samples were then cured at 150°C for 40 minutes. After this, the samples were taken back to the laser cutter to open vias of variable diameter (the other parameter of interest regarding

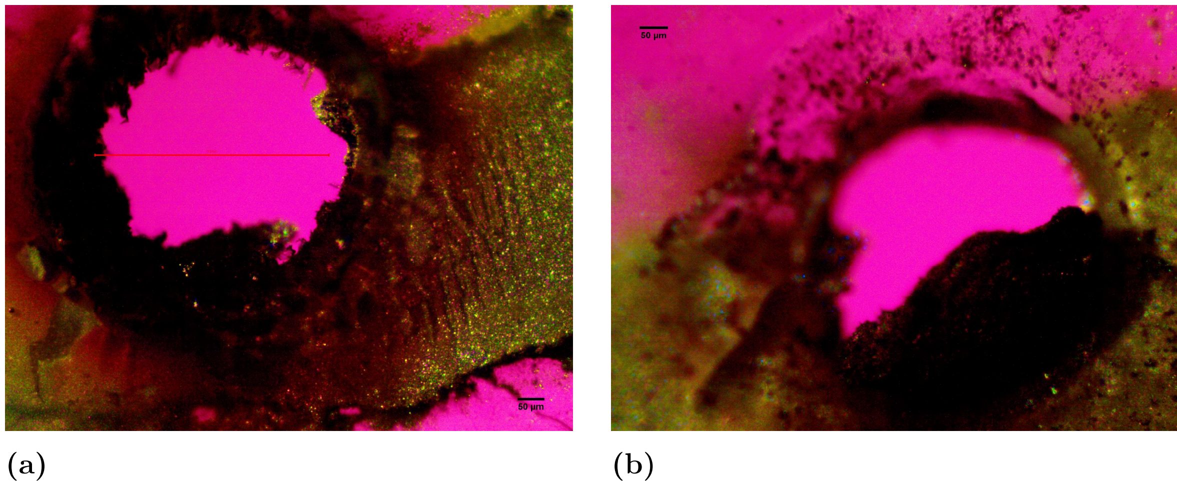

Figure 3.15: a) 500μm diameter, 500μm thick via after removal of burnt debris. b) 500μm diameter, 500μm thick via with burnt debris.

the vias) - 1mm, 750μm and 500μm - from the top of the insulating PDMS layer to the AgPDMS lines. Then, another laser patterned adhesive paper stencil was placed on top of the samples, with correct alignment, and eight more AgPDMS lines, of the same length and width, were applied to the top layer, connected to the lines in the bottom layer through the vias. Finally, the samples were taken to the oven to cure at 150ºC for another 40 minutes. One line was added to this test setup in which there was no via, to make sure that the AgPDMS lines were not thicker than the PDMS insulating layer.

Resistance measurements were performed with a two-probe method. More specifically, the resistance of the top and bottom lines were measured individually, and then the resistance of the overall lines were measured. The results, in terms of average resistance, standard deviation and total yield, for vias with diameter of 1mm are shown in Figure 3.17a. As can be seen, via resistance increases practically linearly with via thickness for the 1mm vias case, which is consistent with the direct proportionality between resistance and length. Furthermore, the success rate of the via-opening process, for vias with 1mm diameter, was 100%, with one laser passage at 40% power and 80% speed being required per 250μm of via thickness. For the 750μm and 500μm diameter vias, on the other hand, the behavior of conductivity with via thickness is not so linear. This is probably due to other factors which take on a larger role, such as the cleanliness of the via and its alignment with the underlying line. Nonetheless, the success rate of the process was 100% with great resistance values for all via thickness values in the 750μm diameter case, and for all but the 1mm thick vias in the 500μm diameter case. In this case, the success rate of the process was 80%. This happens because the vias are very narrow and, as the

Figure 3.16: Experimental setup for characterisation of the vias, with eight 3cm long, 1mm wide lines per layer and two control lines (one in each layer) which are not connected.

laser ablates consecutive PDMS layers, the next layer will be slightly more out of focus compared to the previous layer, calling for a readjustment of the laser table height.

3.2.5 Interface Characterisation

To enable collection and processing of signal from our soft electronics modules, these need to be interfaced to rigid components in some way. This can be achieved by direct interfacing, connecting a rigid component directly to the soft module, although this leads to accumulated stress in the interface region, where failure will happen first. Alternatively, interfacing can be done gradually, by first connecting a flexible, but not stretchable, connector to the soft module, and then connecting this flexible connector to a rigid component. In this work, the second approach was taken, and two alternatives were defined, as mentioned in the methods chapter. The first approach consisted in connecting 2-layer flexible pcb's directly to AgPDMS tracks and then connecting these flexible pcb's to rigid components through crimping. To check the reliability of this method, both in terms of yield and conductivity values, 5 AgPDMS lines at 85% weight concentration with filler particles of type I (2.1) were connected to a flex pcb with 5 copper tracks, as schematically illustrated in Figure 2.19b from the previous chapter.

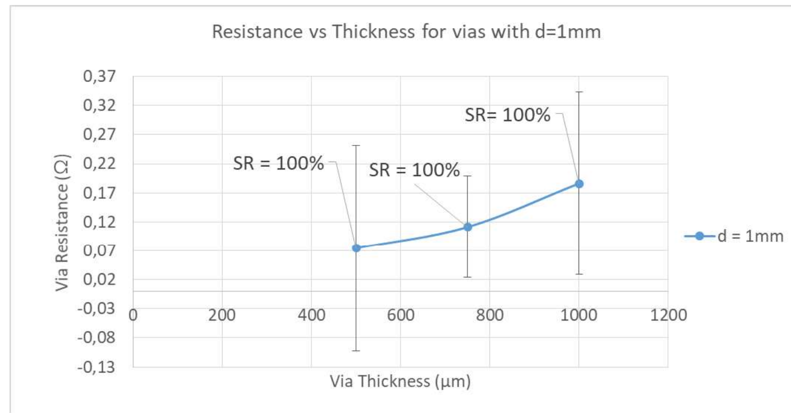

(a)

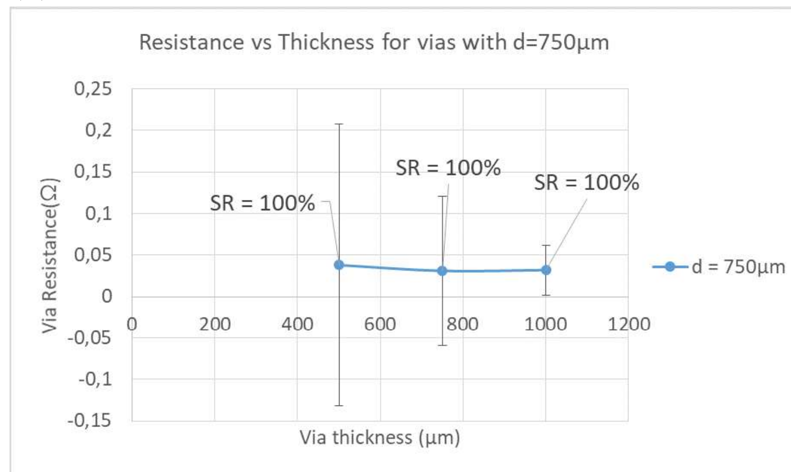

(b)

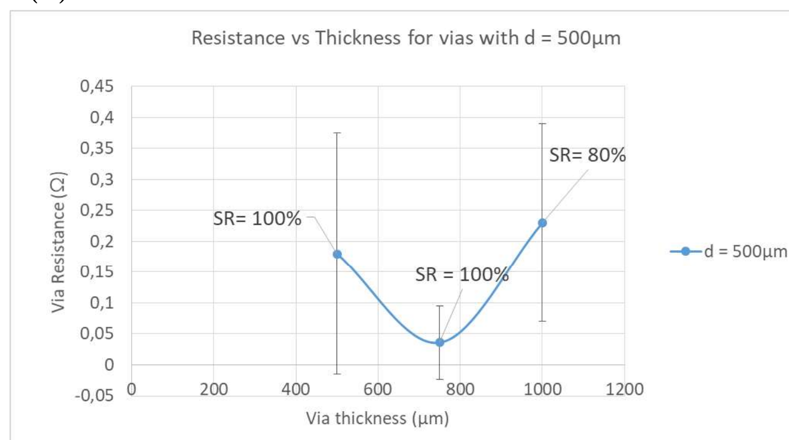

(c)

Figure 3.17: a)Average conductivity of 1mm diameter vias with 1mm, 750μm and 500μm thickness, and success rate of the via fabrication process. b) Average conductivity of 750μm vias with 1mm, 750μm and 500μm thickness, and success rate of the process. c) Average conductivity of 750μm vias with 1mm, 750μm and 500μm thickness, and success rate of the process.

Figure 3.18: Flex pcb connected to AgPDMS lines.

The resistances of all 5 flex pcb copper tracks were measured with a two probe method before connecting them to AgPDMS tracks, and all showed 0,29Ω resistance. Afterward, the flex PCB was connected to AgPDMS tracks 5cm long, 700μm wide, according to Figure 2.19b, after which a protective 500μm PDMS layer was applied on top of the junction. The sample was then taken to the oven at 150ºC for 40 minutes. After this, the resistance from one end of each AgPDMS line to the opposite end of its corresponding copper track was measured. All lines were successfully connected and resistance measurements varied between 1,35Ω and 1,70Ω, as shown in Figure 3.19.

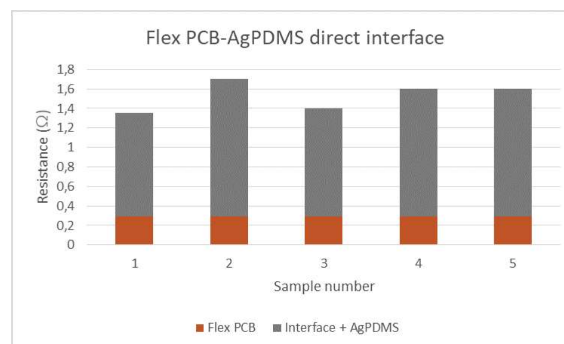

Figure 3.19: Outcome of resistance measurements for flex PCB interfaced with AgPDMS tracks

The contact between the AgPDMS lines and the copper tracks was further observed under an optical microscope, to check the quality of the connections. This can be seen in Figure 3.20.

A second approach, consisting of interfacing flex PCB's to AgPDMS circuits using an intermediate zPDMS layer, was also studied. For this purpose, 5 AgPDMS lines were patterned and cured at 150ºC for 1 hour on top of a 500μm PDMS layer,

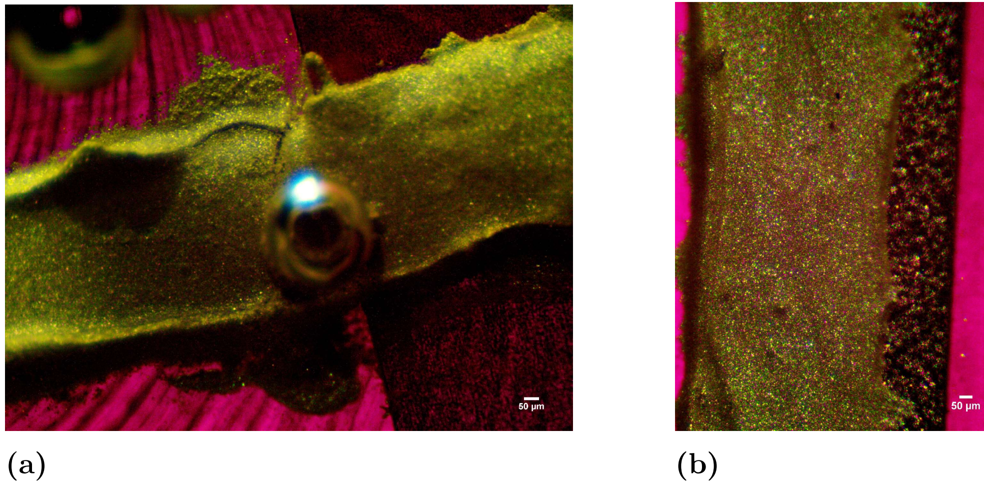

(a) (b)

Figure 3.20: a) Interface between AgPDMS lines and flex PCB copper tracks. b) AgPDMS line on top of copper track.

after which a 300μm zPDMS layer was applied on top the lines. The zPDMS was fabricated by dispersing conductive particles of tive VI (see Table 2.1) in PDMS at a weight concentration of 40%. A flex pcb was placed on top of each AgPDMS line in alignment, and the whole system was taken to the oven on top of a flat magnet at 150°C for 1 hour. Figure 3.21a shows the sample, while Figure 3.21b shows a scheme of the setup.

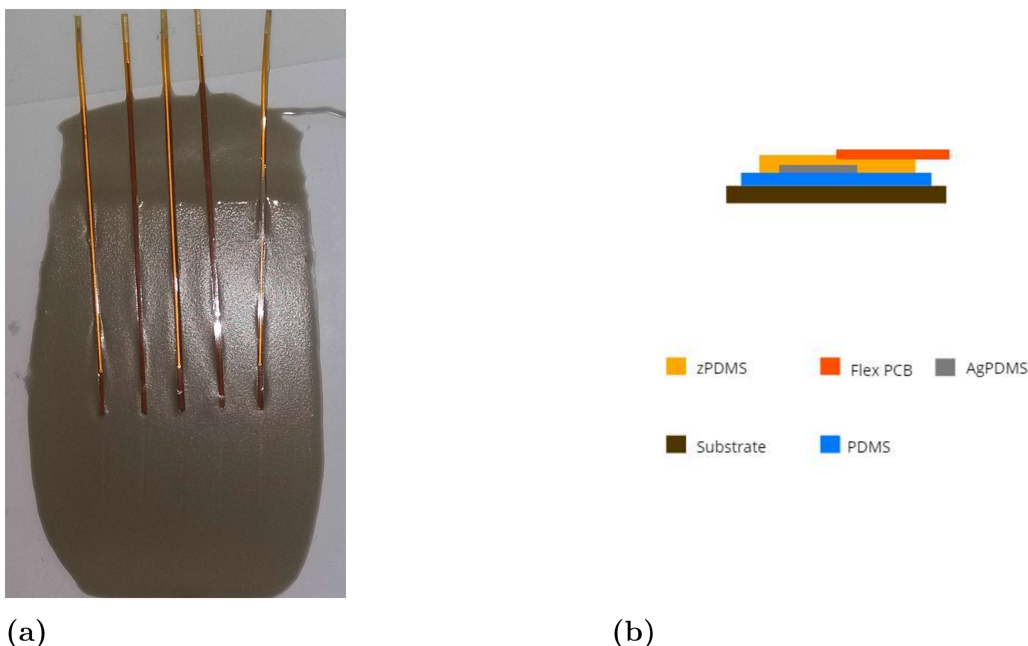

(a) (b)

Figure 3.21: a) Flex PCB's interfaced with AgPDMS lines through a zPDMS layer. b) Scheme of zPDMS interface between flex PCB and AgPDMS lines.

While one flex PCB had a slighly electrical contact with its corresponding AgPDMS

lines due to misalignment, the other four interfaces showed very satisfactory and consistent resistance values, as shown in Figure 3.22.

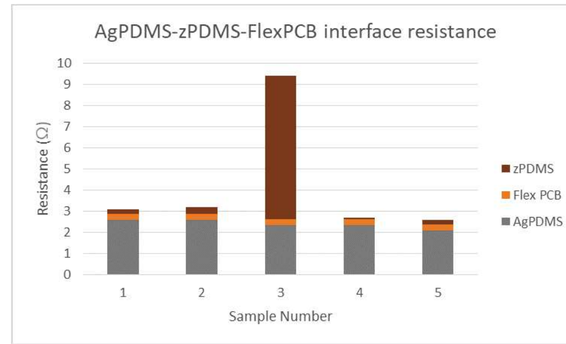

Figure 3.22: Resistance values of AgPDMS-zPDMS interface-flex PCB system.

3.2.6 Electromechanical characterisation

As the goal of this work was to enable the use of AgPDMS in stretchable electronics systems, it was necessary to perform electromechanical characterisation of these circuits under an applied tension. To do so, tests were preformed where the resistance of AgPDMS lines was measured as strain was increased until rupture or until resistance crossed a threshold value. Furthermore, tests were performed in which the resistance of AgPDMS lines was measured with a cyclic applied strain, for hundreds of cycles. First, the behavior of conductivity with strain up to the strain at break was tested at three different filler particle weight percentages, namely 83%, 85% and 90%, in an effort to understand how big the trade-off between conductivity and stretchability was. For this purpose, four 9 cm long AgPDMS lines sealed between two 500μm thick PDMS layers with a dogbone shape meant to concentrate stress at the middle of the line, each with two connections to the exterior at each end through two-layer flex PCB's, were individually put in the tensile testing machine. The setup used for tensile testing can be seen in Figures 3.23a and 3.23b below. Resistance measurements were performed with a four-point method, as can be seen in Figure 3.23b. The setup for measuring the resistance of the sample had a dynamic range from 0 to 500 ohms, which in this case was sufficient given the low resistance values of the samples when unstrained (initial resistance). The test was constructed in a way such that it stopped if this dynamic range was exceeded. Figures 3.24, 3.25 and 3.26 show both the resistance variation with strain (on the left) and strain values for selected values of normalised resistance, R/R_0 = 2, 5 and 10.

While samples with 83% filler particle concentration showed considerable stretcha-

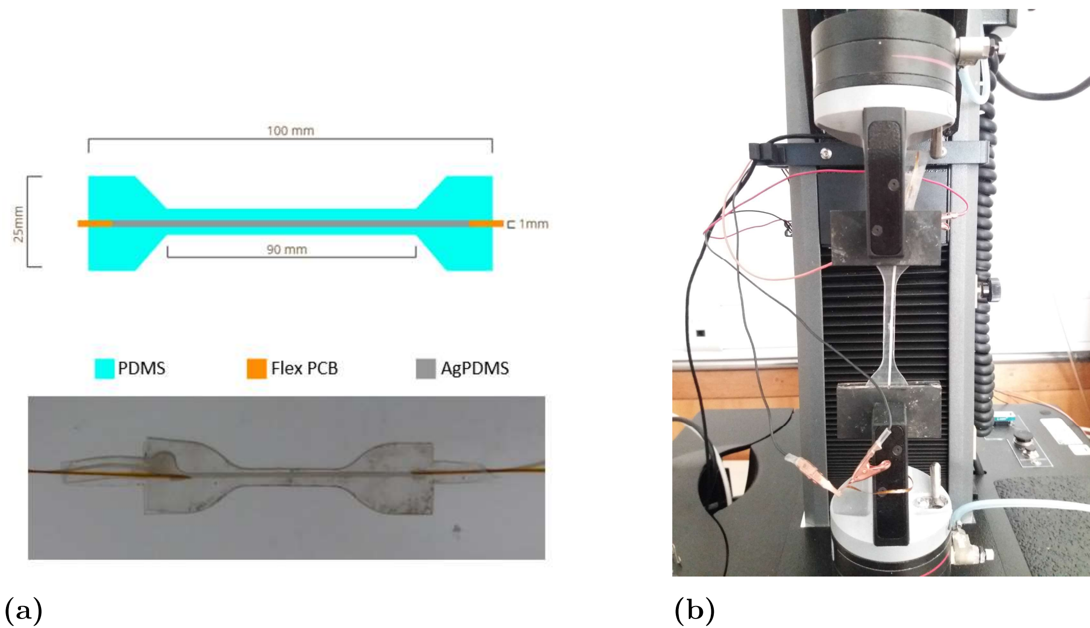

(a) **(b)**

Figure 3.23: a) AgPDMS sample line used for electromechanical characterisation b) Experimental setup for electromechanical characterisation.

bility - samples broke or crossed the 500Ω barrier between 60% and 112%strain - conductivity values are considerably lower when compared to those for 85% filler particle concentration. What is more, strain tests for 85% filler particle concentration showed equivalent (even better) results in terms of stretchability, making this a better choice than 83% concentration. Conversely, at 90% filler particle concentration, the AgPDMS lines become very brittle, as evidenced by the very low strain values at which resistances spike - this happens at strain values ranging from 0.1% to 1%. The low stretchability values were also the reason why a graph of the normalised resistance was not presented in this case. This evidences the trade-off between conductivity and stretchability. In light of this, 85% concentration of filler particles by weight was the chosen working point for developing AgPDMS-based soft electronics applications. It is worthwhile mentioning that for the majority of the samples, rupture did not happen during the tests, but rather the resistance of the lines under testing peaked above the dynamic range limit of the measurement setup.

After this, dogbone-shaped samples consisting of two 4.5cm, 85%wt AgPDMS lines, one in each layer, connected at their middle through a 500μm thick, 1mm wide via, were put through the same tensile test, in an attempt to better understand how much the presence of vias limited the stretchability of the circuit. The overall thickness of the samples was 1mm. The results are shown in Figure 3.27.

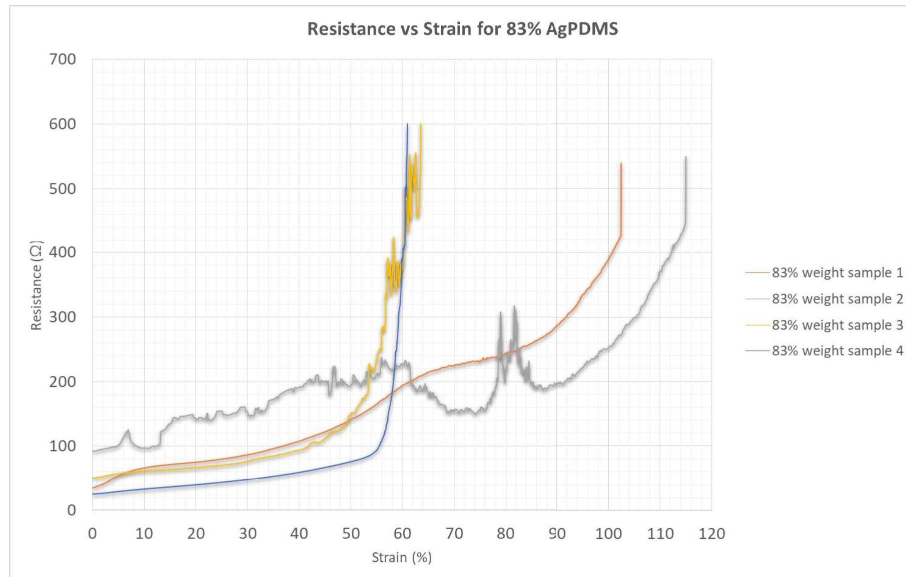

(a)

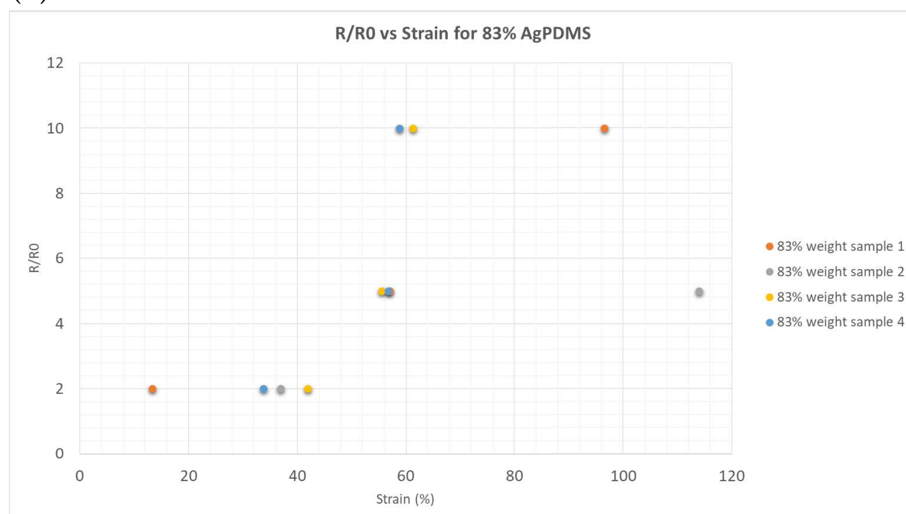

(b)

Figure 3.24: a) Resistance as function of uniaxial strain for sample lines with 83% filler particle concentration by weight. b) Uniaxial strain as function of normalised resistance ($R/R_0 = 2$, 5 and 10) for sample lines with 83% filler particle concentration by weight.

In light of these results, the strain at rupture seems to have fallen considerably as a consequence of drilling the vias, with most samples mechanically breaking at the center between 30% and 40% strain. However, a dogbone shape was being used for the samples, which is the standard shape in use for tensile tests in the field. This shape is unlikely to occur in actual applications and, while for single layer samples this didn't represent a problem, for the case of a two-layer line in the middle the dogbone shape could have significantly hindered the results. For this reason, similar

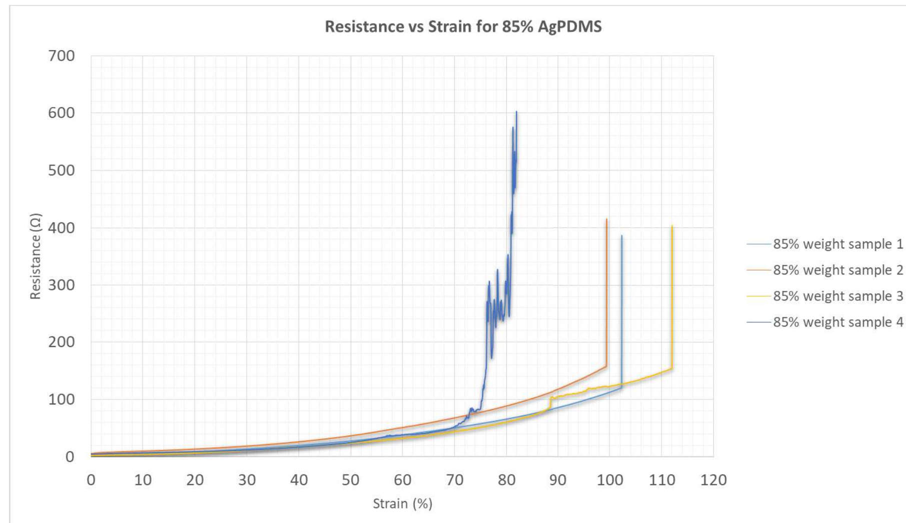

(a)

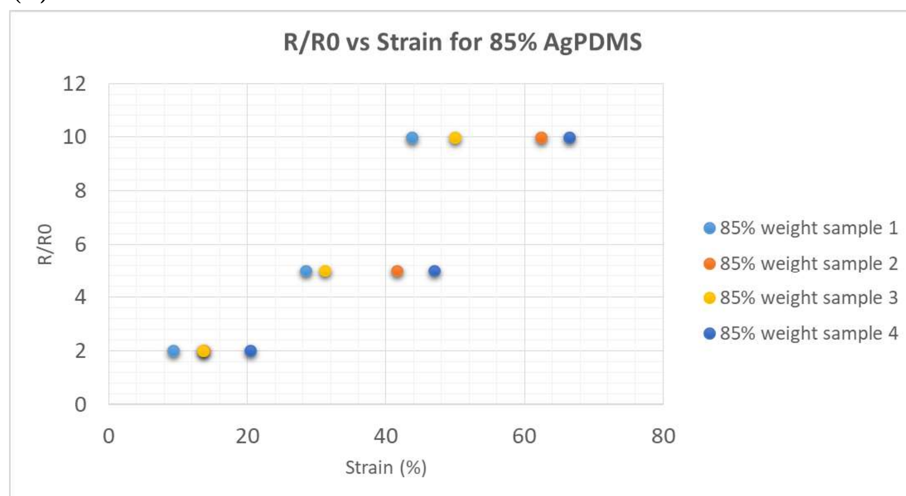

(b)

Figure 3.25: a) Resistance as function of uniaxial strain for sample lines with 85% filler particle concentration by weight. b) Uniaxial strain as function of normalised resistance ($R/R_0 = 2$, 5 and 10) for sample lines with 85% filler particle concentration by weight.

tests were performed with rectangular shaped samples of two 4.5cm lines connecting at the middle through a via. The results can be seen in Figure 3.28.

While the spread in the rupture strain values of the rectangular samples is big compared to that of dogbone-shaped samples, ranging from just over 60% to just over 100%, the former are much closer to the rupture strain values of single layer 85%wt AgPDMS lines on a 1mm thick PDMS slab, indicating that the presence of laser ablated vias should not significantly compromise the stretchability of typical soft systems. What is more, failure seldom occurred at the vias, and more often

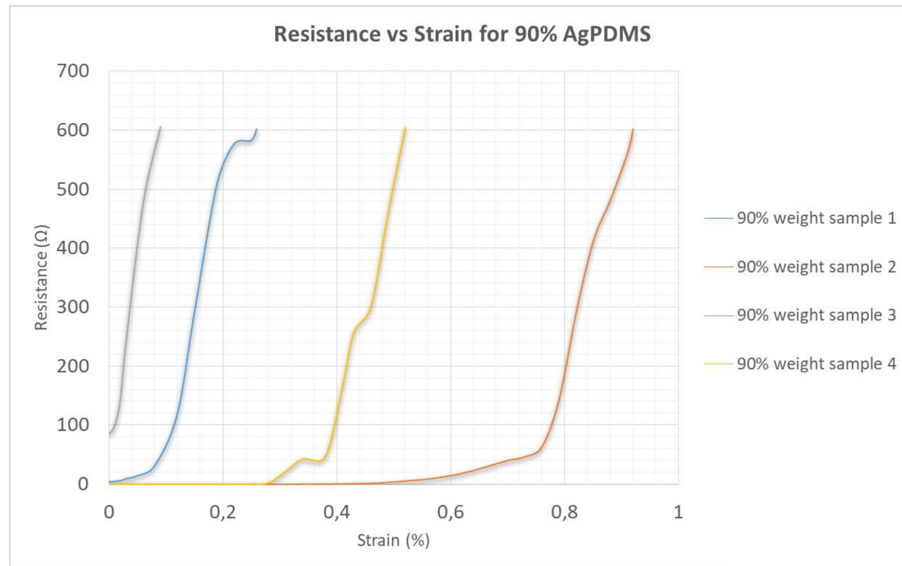

Figure 3.26: a) Resistance as function of uniaxial strain for sample lines with 90% filler particle concentration by weight.

occurred at the ends of the sample, which were grabbed by the machine grippers.

To finalise the electromechanical characterisation of our AgPDMS-based stretchable systems, cyclic strain tests were performed with four one-layer samples consisting of 9cm, 85%wt AgPDMS lines enclosed in a 1mm thick, 10cm long dogbone-shaped PDMS slab, to check for hysteresis in the curve of conductivity vs strain and to get a rough estimate for the life expectancy of soft systems based on these materials. For this purpose, each sample was put through 1000 cycles of straining up to 20% strain at a rate of 100 mm/minute, followed by relaxation back to the initial length. The tensile testing machine shown back in chapter 2 (see Figure 2.12a) was used for these tests. Figure 3.29 shows the results of these tests for the four tested samples.

As can be seen, resistance values oscillate between maxima and minima during each iteration of the test, but there is a clear overall tendency for these maxima and minima to increase from cycle to cycle. All samples exceeded the dynamical range of our measurement setup (500Ω) after roughly 600 strain cycles. Figure 3.30 shows the cyclic test of an individual sample, with a closeup showing only a few strain cycles.

The zoomed graph shows that the resistance of a sample increases when straining begins, decreases when the direction of straining is about to be inverted, increases again at the beginning of relaxation and, finally, has a peak minimum when the sample is back to its normal length.

Despite these results, after sufficient time, the resistance of the tested samples would

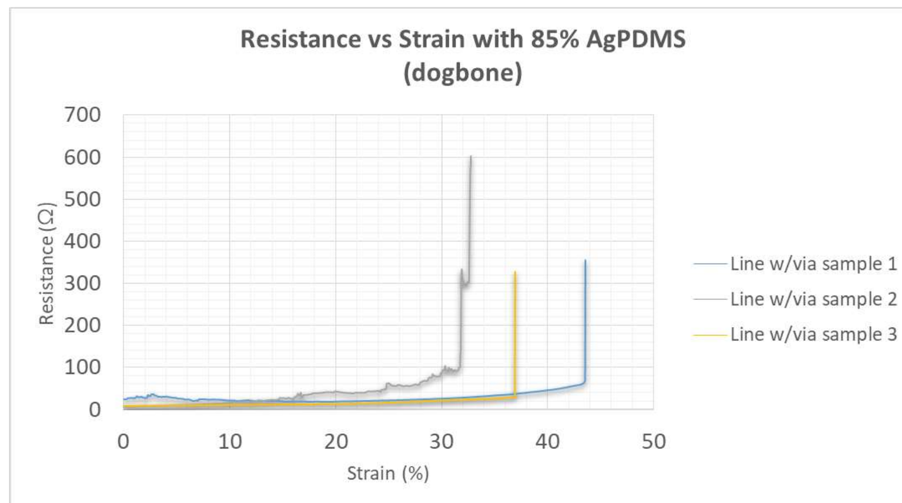

(a)

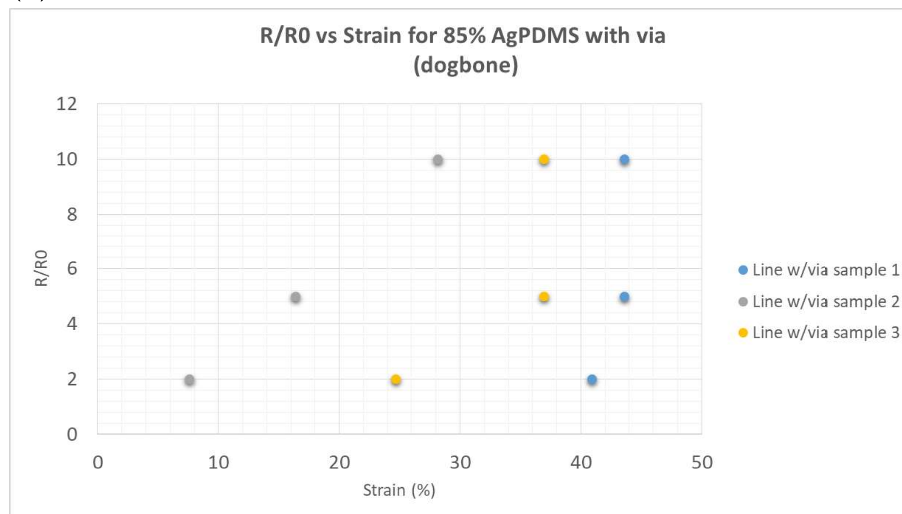

(b)

Figure 3.27: a) Resistance as function of strain for 85%wt concentration lines with vias at the middle. b) Uniaxial strain as function of normalised resistance for R/R_0 = 2, 5 and 10.

return to values only slightly higher than the initial values before the tests were performed. In light of this, two new cyclic tests were performed. In one of them, the samples were strained at a rate of 100mm/minute up to 20% strain and then relaxed back to 0% strain, resting for 10 seconds before the beginning of the following cycle. The second test was similar to this, but applied twice to the same sample, letting the sample rest for 5h between both iterations of the test. The results can be seen in Figures 3.31a and 3.31b.

The first test shows that electrical fatigue is considerably reduced if the rate at which strain cycles are applied is reduced. The resistance of the sample in Figure

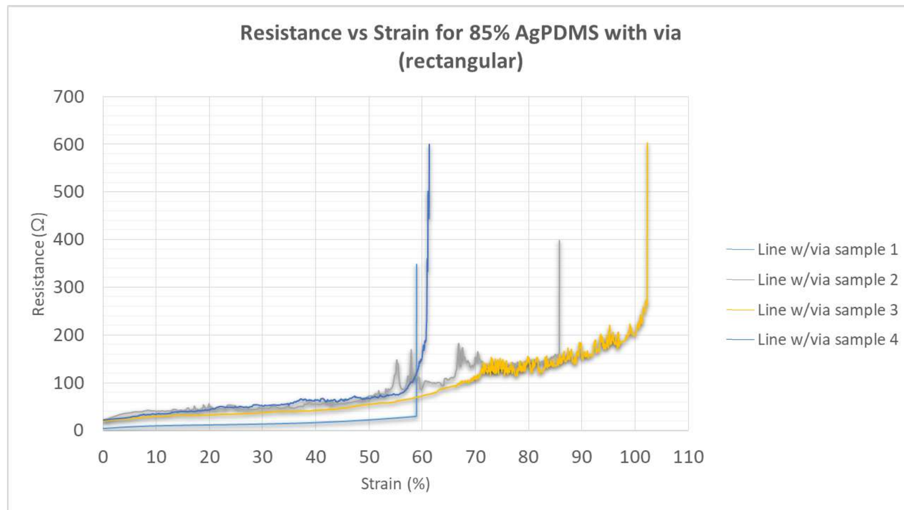

(a)

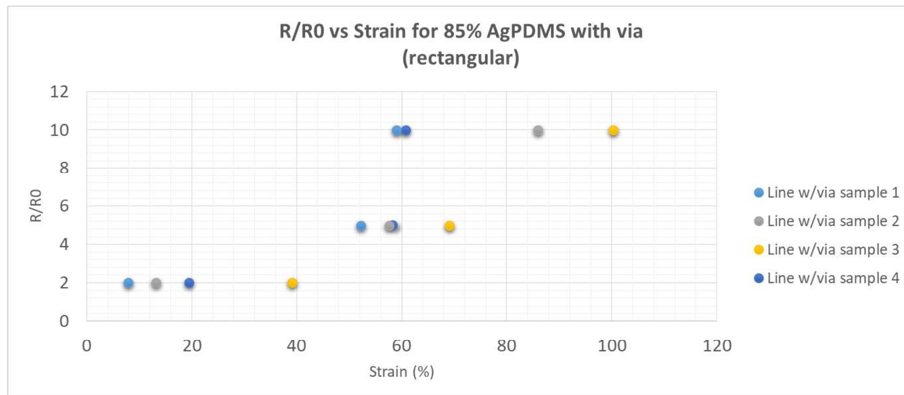

(b)

Figure 3.28: a) Resistance as function of uniaxial strain for rectangular two-layer samples. b) Uniaxial strain as function of normalised resistance for R/R_0 = 2, 5 and 10.

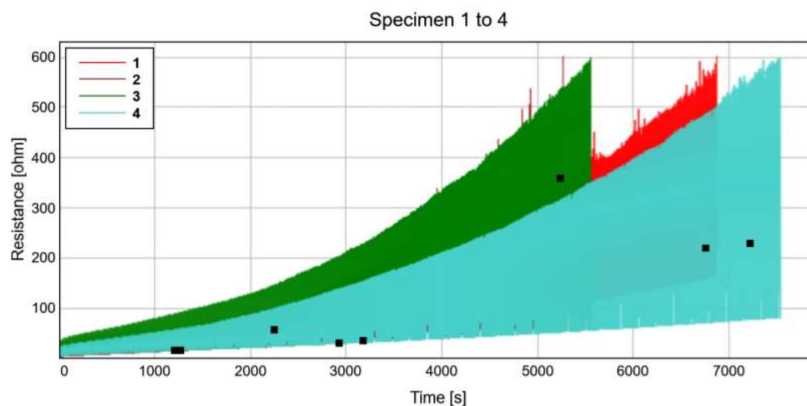

Figure 3.29: Resistance vs Time for 600 cycles of 20% applied strain.

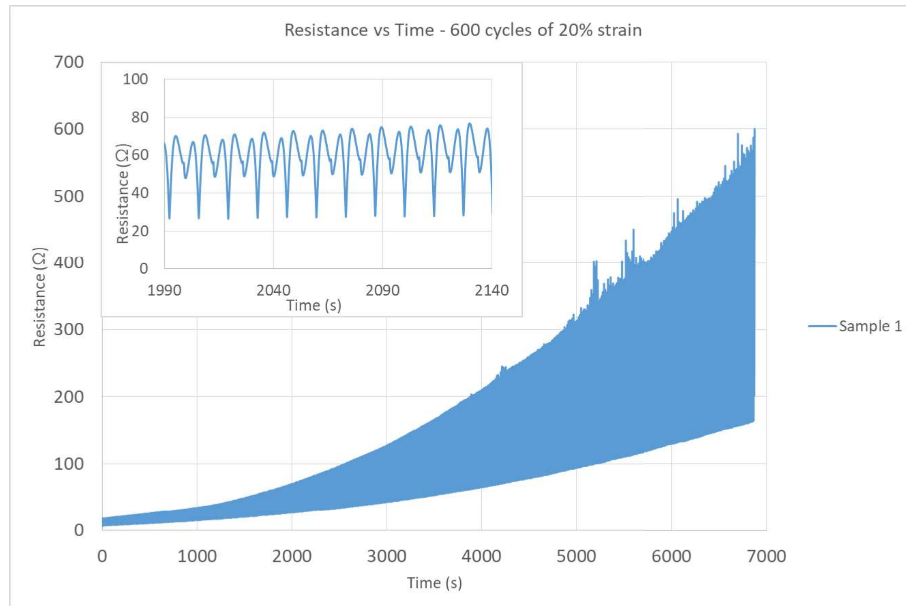

Figure 3.30: Resistance vs Time for 600 cycles of 20% applied strain of a single sample.

3.31a increased only approximately 10 times after 1000 strain cycles, considerably better than the 100-fold increase verified in the samples shown in Figure 3.29, where samples were not allowed to rest between cycles.

The second test, on the other hand, evidences hysteresis in the electrical properties of a single sample. After being submitted to a test of 500 cycles of 20% applied strain with 10 second intervals between consecutive cycles, the sample was stored for 5 hours and again submitted to the same test, and while its initial resistance dropped down to values close to those before the first test, the increase in resistance over time was more pronounced than in the first test.

3.2.7 Conclusion

Here, a summary of the results obtained is given:

1) Of all the tested silver particle types, silver flakes type I (Table 2.1) showed to have the best electrical properties at filler particle percentages low enough for processing to be easy. (Figure 3.2) These particles also showed stability in their electrical behavior for over 2 months.

2) Curing temperatures of 150°C or higher, and curing times of 1 hour or longer, were shown to be sufficient for sintering and satisfactory conductivity to be achieved (Table 3.1) using conductive composite made with silver flakes (type I, Table 2.1).

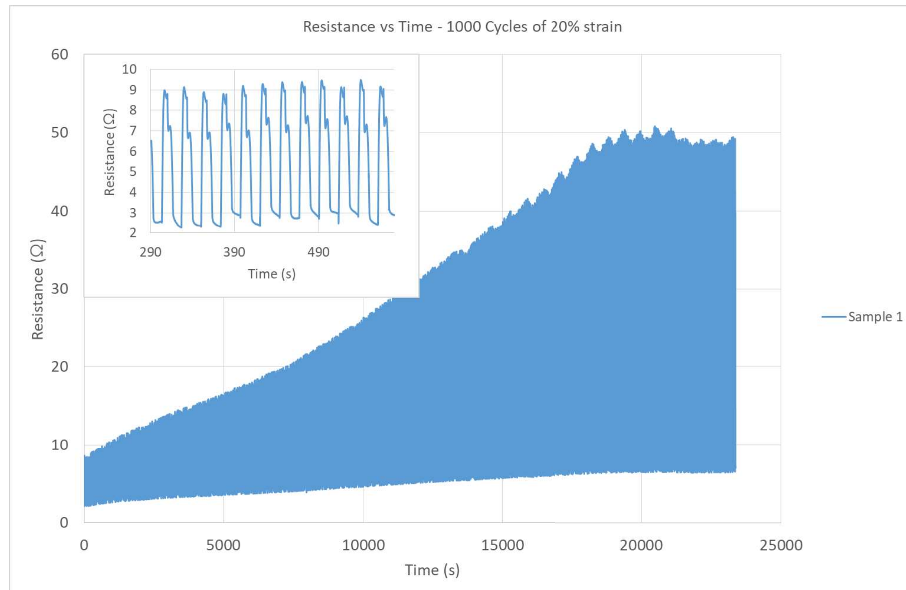

(a)

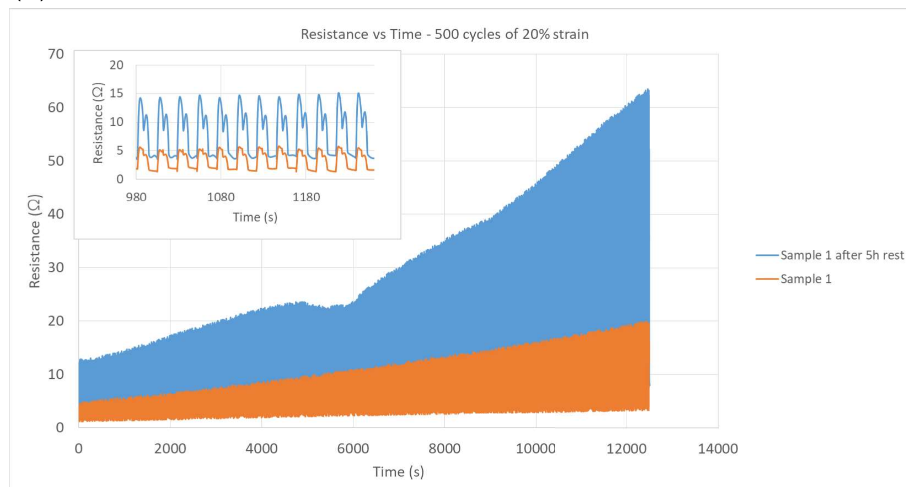

(b)

Figure 3.31: a) Resistance vs Time for 1000 cycles of 20% applied strain with 10 seconds pause between cycles. b) Resistance vs Time for 500 cycles of 20% applied strain with 10 seconds pause between cycles, repeated on the same sample with an interval of 5 hours.

3) Stencil printing using a laser-patterned adhesive stencil was chosen over moulding and screen printing as the best method for rapid prototyping of stretchable electronics systems, allowing for feature dimensions down to 500μm and being easily integrated into a multilayer fabrication method.

4) Fabrication of multilayer AgPDMS circuits by laser-drilling vias was shown to be feasible for vias down to 500μm diameter with success rates of 100% (Figure 3.17).

5) Two methods of interfacing flexible and rigid components to stretchable elec-

tronics systems were proposed. They were shown to be reliable and to impose no bottleneck on the conductivity of the overall system (Figures 3.19 and 3.22).

6) Samples fabricated with the selected materials and methods were shown to endure strains of just above 100% for the case of single layer samples at 85% filler particle concentration by weight and between 60% and 100% for the case of two-layer samples at the same concentration (Figures 3.25 and 3.28). Furthermore, these samples were shown to endure at least 1000 cycles of 20% strain whithout considerably compromising their electrical properties.

To close this chapter, two flowcharts of procedures for fabricating AgPDMS stretchable electronics systems are presented. The first describes the procedure for rapid prototyping of AgPDMS multilayer stretchable electronics systems using the stencil prining patterning technique, and is presented in Figure 3.32.

Alternatively, if scalable batch fabrication is desired, screen printing could be a better option, as patterning the screen has to be done only once, after which it can be successively applied to multiple samples in series. Only after patterning every sample would the screen require cleaning. The main disadvanage of this method is that if multilayer systems are required, alignment would be necessary both at the laser cutter table, where vias are opened, and between screens corresponding to different layers. On the other hand, screen printing allows greater feature density since it does not break into separate pieces as might happen with stencils. This attenuates the need for making multilayer systems. The flowchart of Figure 3.33 describes the necessary steps for fabrication of AgPDMS stretchable electronics systems using the screen printing patterning technique.

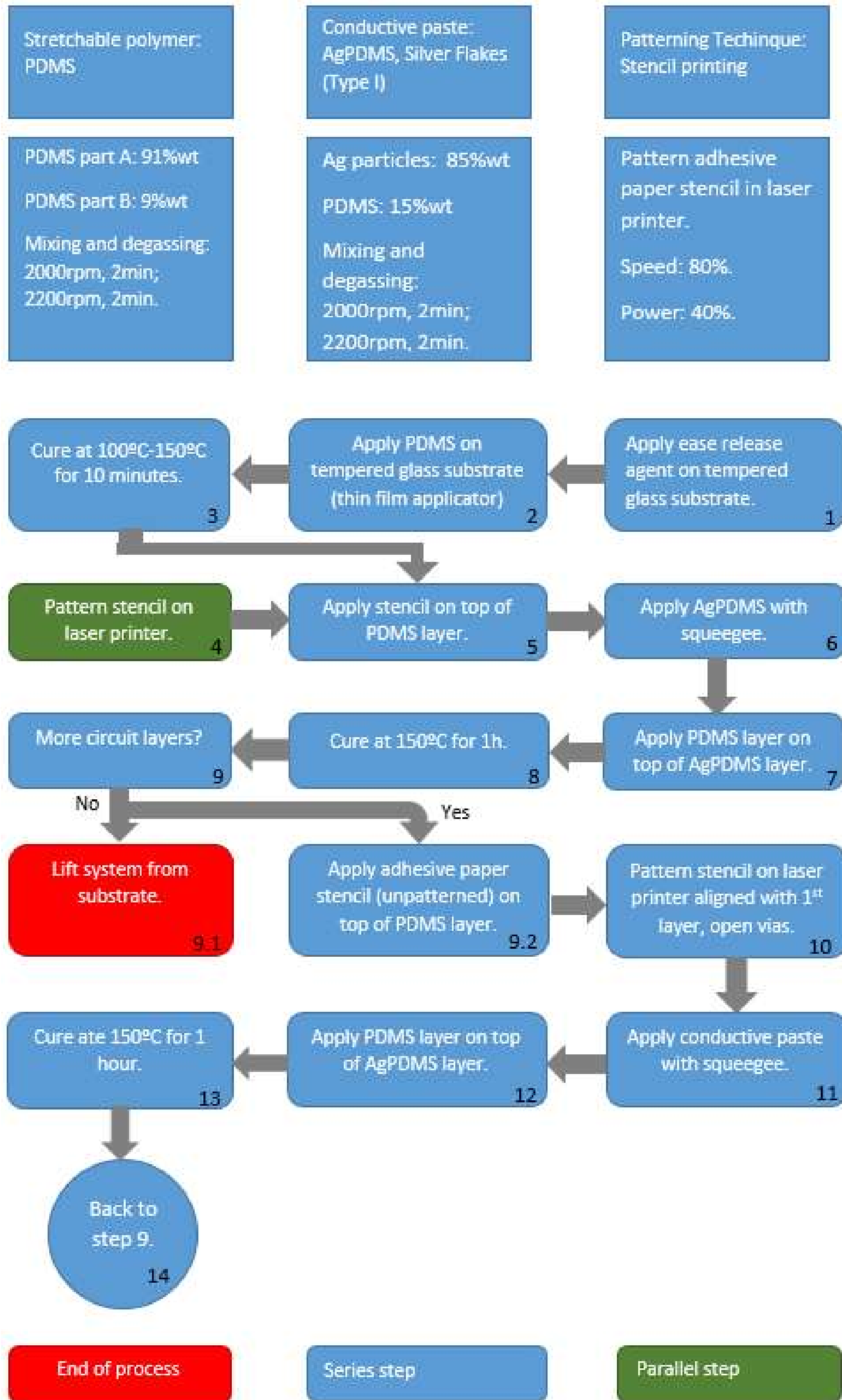

Figure 3.32: Flowchart for rapid, inexpensive prototyping of soft single/multilayer systems using stencil printing.

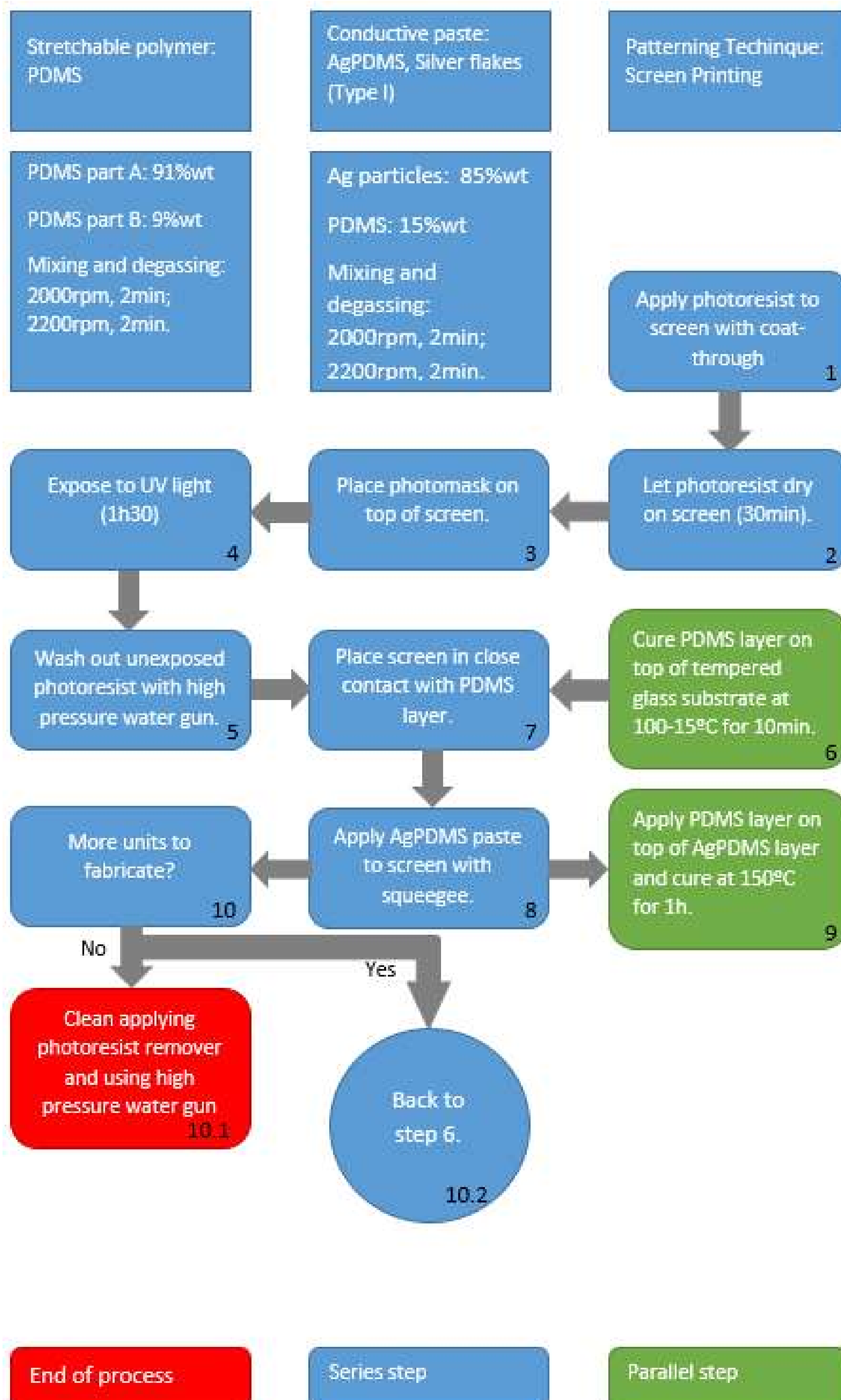

Figure 3.33: Flowchart for batch fabrication of soft systems using screen printing.

4

Case Studies

The applications of a technology as disruptive as soft electronics will be manifold. Not only new product concepts can emerge, but also old rigid electronics concepts can be adapted to take advantage of the inherent stretchability and bendability of soft electronics devices.

As an example of the potential applications the technology of soft electronics might have, two soft electronics systems were constructed based on the materials and methods studied throughout this dissertation, a capacitance-based stretchable touchpad and a wireless ECG module.

4.1 Stretchable Touchpad

As the first case study, an architecture similar to a capacitive touchpad was developed, consisting of a grid of 5 rows and 4 columns, an adaptation from ISR project "Soft Insole", a soft shoe sole intended for use in walking disorder therapy. Each crossing of a row and a column can be considered as a set of two parallel plate capacitors with a dielectric in between (a PDMS layer). By measuring the mutual capacitance between a certain row and column, one can detect the presence and determine the location of a finger, for instance.

This device was fabricated using only simple, inexpensive procedures, namely thin film application, stencil printing, laser ablation and heat treatment in an oven. Each half of this sensor contains two AgPDMS circuit layers, the bottom one being encapsulated between two PDMS layers and the top layer being exposed on the top side. These two circuit layers are in turn connected through conductive vias. In total, this device is a 4 layer system. Figure 4.1a shows a scheme of the structure of the sensor viewed from the top, while Figure 4.1b shows a side view scheme. Silver flakes (particles type I, see 2.1) were used as the conductive composite, mixed at

85% by weight with PDMS. The stretchable touchpad can be seen in Figure 4.2b with both halves separated, and in Figure 4.2a put together.

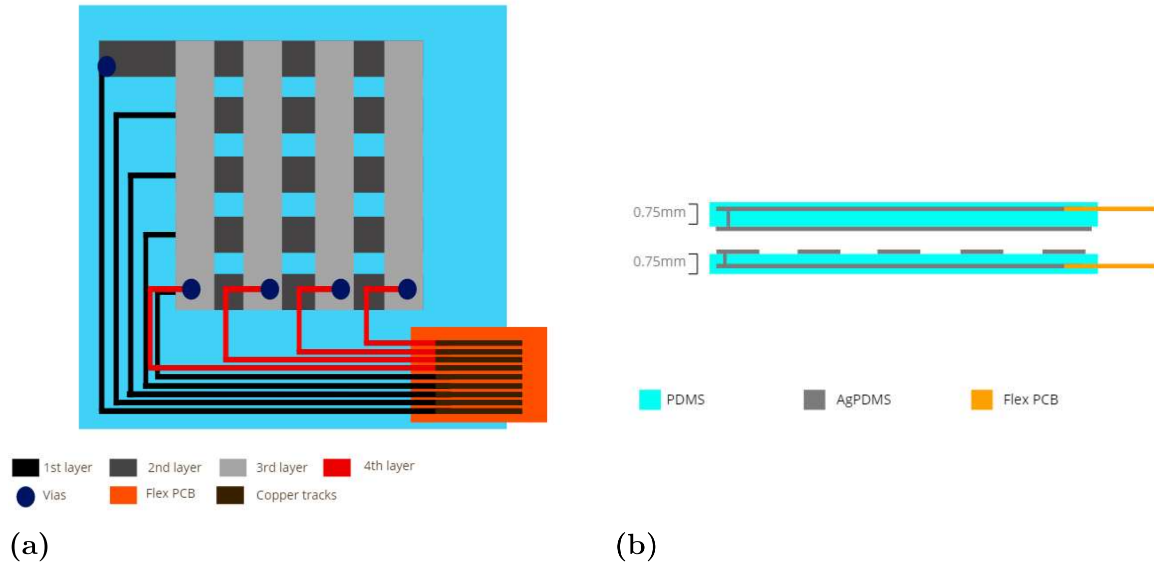

(a) **(b)**

Figure 4.1: a) Top view scheme of the structure of the stretchable touchpad. b) Side view scheme of the structure of the stretchable touchpad.

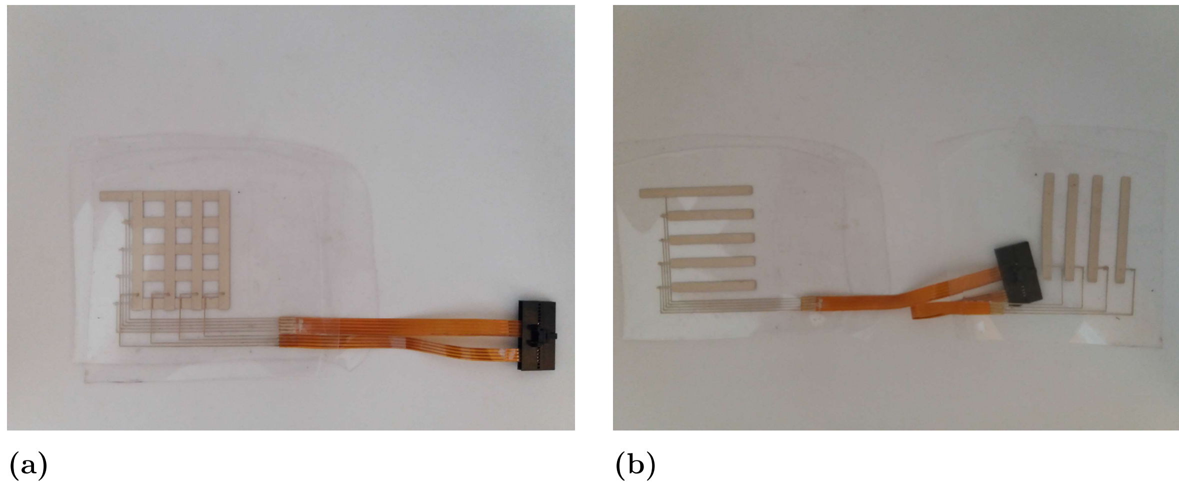

(a) **(b)**

Figure 4.2: a) Assembled stretchable touchpad. b) Stretchable touchpad with two halves separated.

Direct interfacing of the AgPDMS connection lines to copper tracks of a flex PCB was the chosen interfacing method, as illustrated in Figure 4.3a. The flex PCB was further interfaced to a rigid connector through crimping, as shown in Figures 4.3b and 4.3c. It is worthwhile mentioning that the pitch of the lines in Figure 4.3a, patterned with an inexpensive paper stencil method, is 1.27 mm.

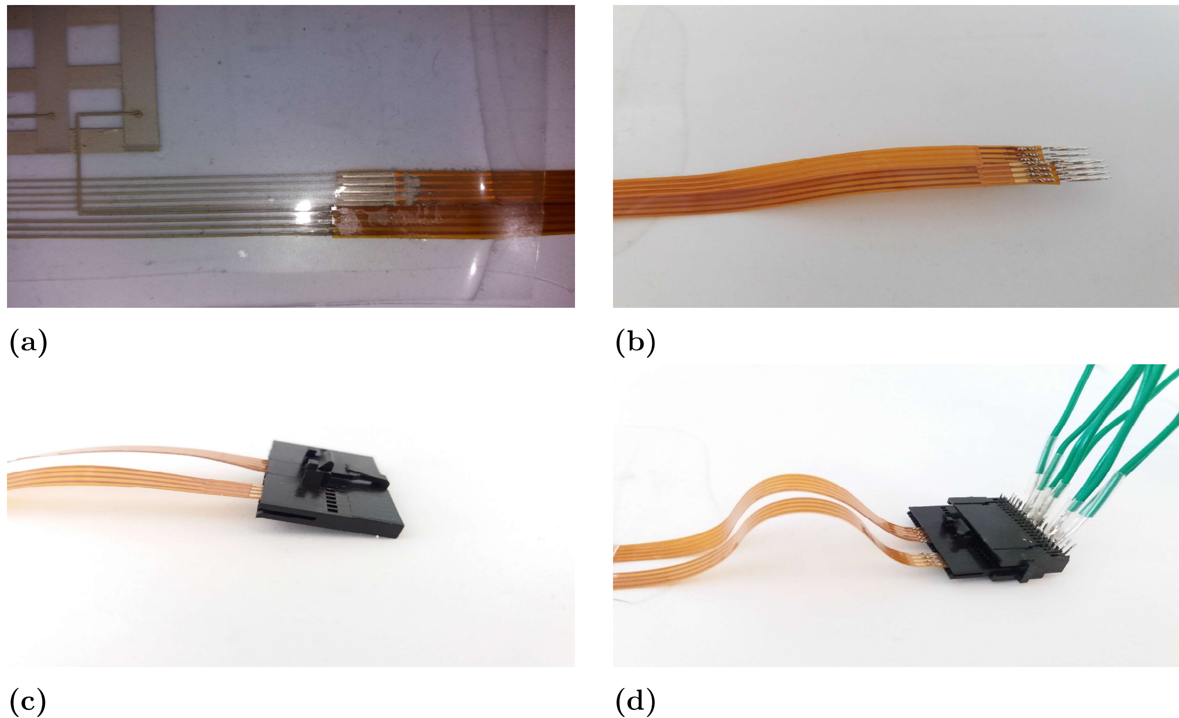

(a) (b) (c) (d)

Figure 4.3: a) Direct AgPDMS to flex PCB interfacing method. b) Metal crimps used to interface flex PCB and rigid connector. c) Flex PCB inserted into rigid connector. d) Wires soldered to connector pins.

After this, the touchpad was connected to a connector, shown in Figure 4.3d, with metal pins which could be wired to the inputs of Cypress development board 'CY8CKIT-041-40XX', which in turn was used to read the mutual capacitance values of each combination of one row and one column. The development board is shown in Figure 4.4a. The full setup for use of the stretchable touchpad is shown in Figure 4.4b.

Figures 4.5a, 4.5b, 4.5c and 4.5d show the stretchable touchpad working together with the software developed using PSoC Creator 4.2 and the aforementioned development board.

4.2 Wireless ECG module

The second application of AgPDMS stretchable systems which was developed in the context of this dissertation was a wireless ECG module. This module consists of a two-layer AgPDMS circuit fabricated with the simple, rapid methods previously mentioned. Figure 4.6 shows both the soft part of the ECG circuit and its design, made with EAGLE CAD software. Silver flakes (particles type I, see 2.1) were used

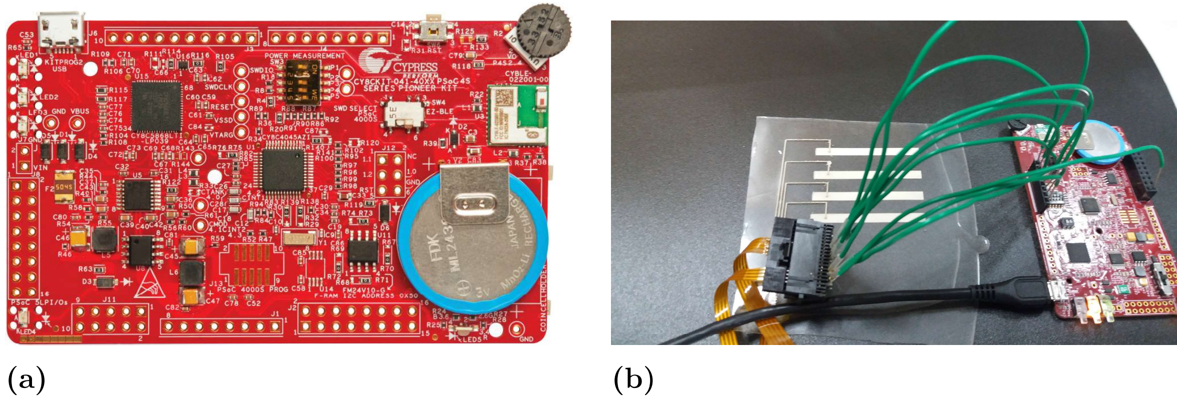

(a) (b)

Figure 4.4: a)Cypress' development board used for stretchable touchpad application. b) Stretchable touchpad connected to development board. The black layer under the sensor columns serves as the dielectric between columns and rows, the latter being under the black layer.

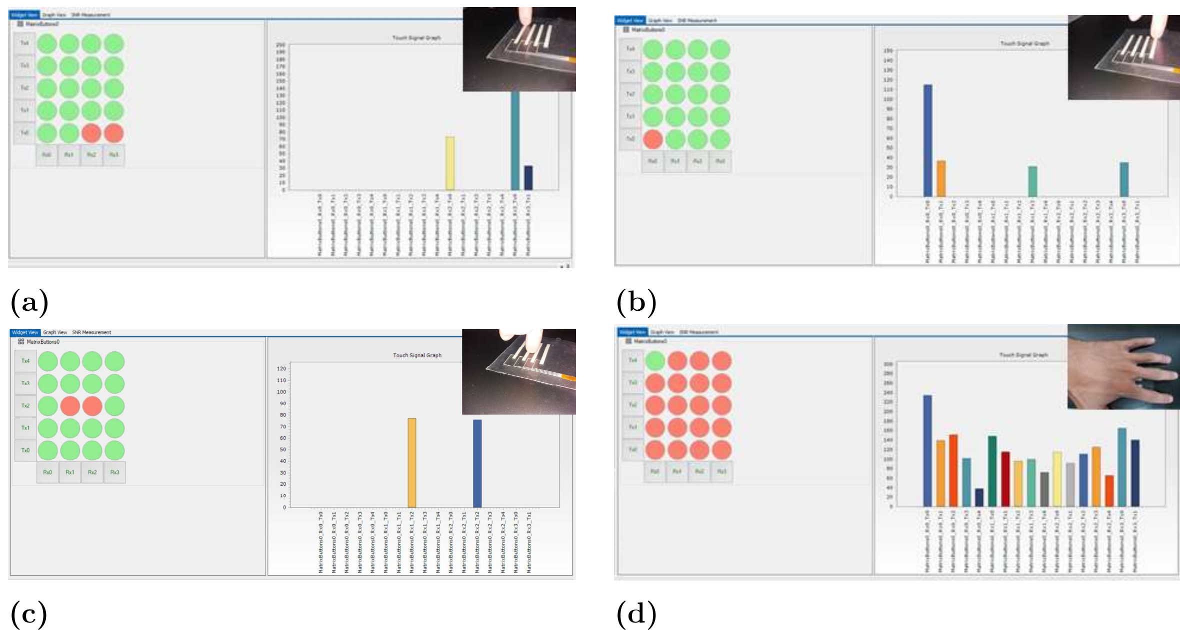

(a) (b) (c) (d)

Figure 4.5: Software response to finger pressing sensor at the a) top left corner, b)top right corner, c) center. d) Software response to full hand on top of sensor.

as the conductive composite, mixed at 85% by weight with PDMS.

Three main rigid islands (each one composed of a rigid component on top of a two-layer flex PCB) were connected to this circuit, by placing the contact pads of the flex PCB's in alignment over the corresponding contact pads of the soft circuit. Of these three rigid islands, one was the 'MAX30003CTI+ biopotential AFE' signal processor, the second one a Bluetooth communicator 'CYBLE 0220010', and the third the power converter 'TXB0108PWR'. Other smaller rigid components (e.g. capacitors and resistors) were placed in alignment on top of the circuit. Two

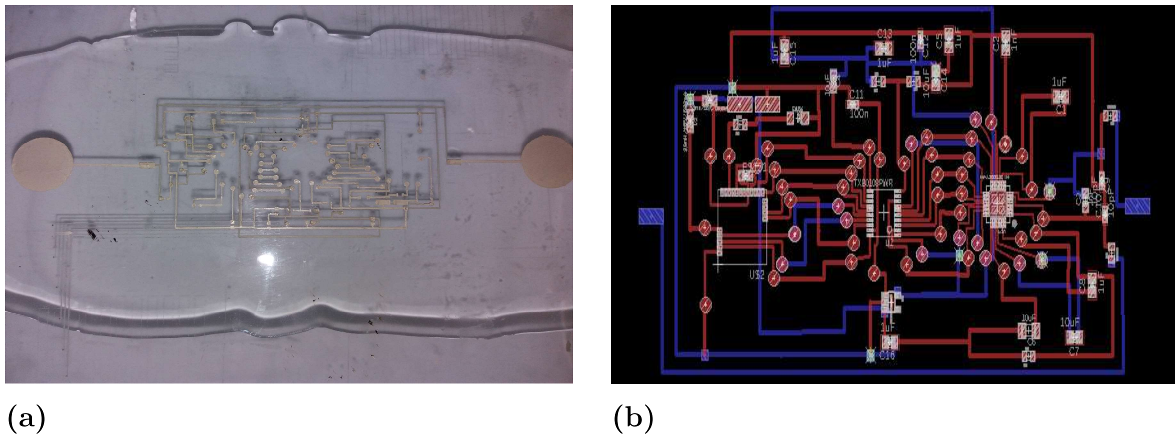

(a) (b)

Figure 4.6: a) Sample ECG circuit with two layers. b) Scheme of ECG module with top layer in red and bottom layer in blue.

alternative connection methods were tried, namely direct contact of the flex PCB's and components with the AgPDMS circuit and contact through an intermediate zPDMS layer. In the latter method, to enhance electrical contact, the contact pads of the flex PCB's were alloyed with liquid metal. The three rigid islands utilised are shown in Figure 4.7. The procedure for interfacing the rigid islands to the soft circuit with liquid metal and zPDMS is illustrated in Figure 4.8

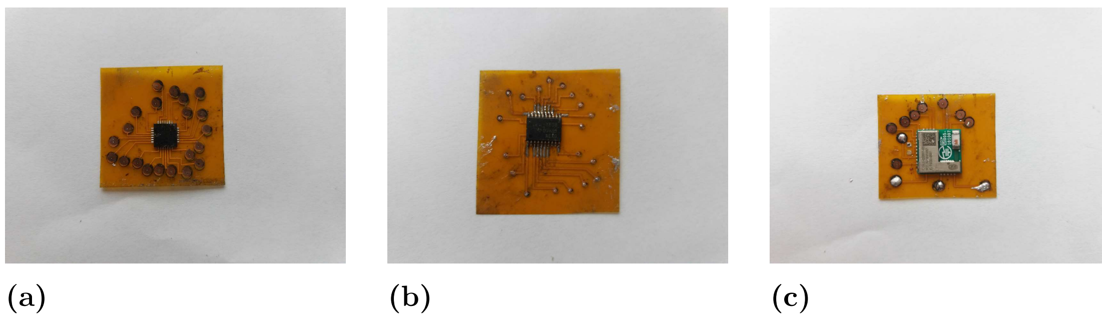

(a) (b) (c)

Figure 4.7: a) MAX30003CTI+ biopotential Analog Front End used for cardiac signal processing. b) TXB0108PWR Voltage Level Translator. c) CYBLE 022001-00 Bluetooth Low Energy communication module.

The full circuit, consisting of two AgPDMS circuit layers seperated by 500μm PDMS layers and connected through laser-ablated vias, both with and without a zPDMS layer electrically connecting rigid islands and components to the soft circuit, can be seen in Figures 4.9a below.

To the date of delivery of this disseration, this application hasn't been made functional due to a few technical issues. Regarding the samples fabricated using the zPDMS approach, while the two-layer AgPDMS circuit was fabricated without flaws, the step of bonding rigid components to it was undermined because these compo-

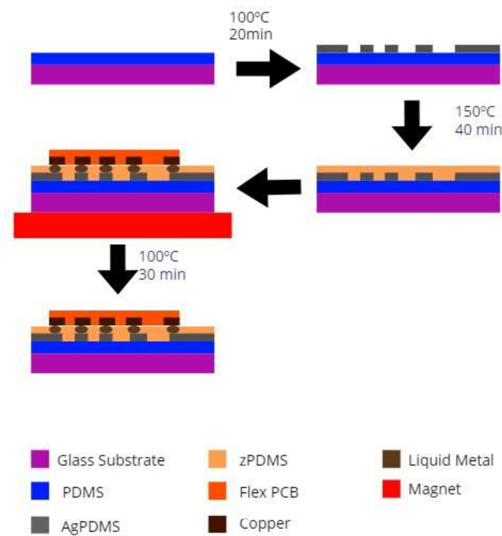

Figure 4.8: Procedure for interfacing rigid islands with soft circuit.

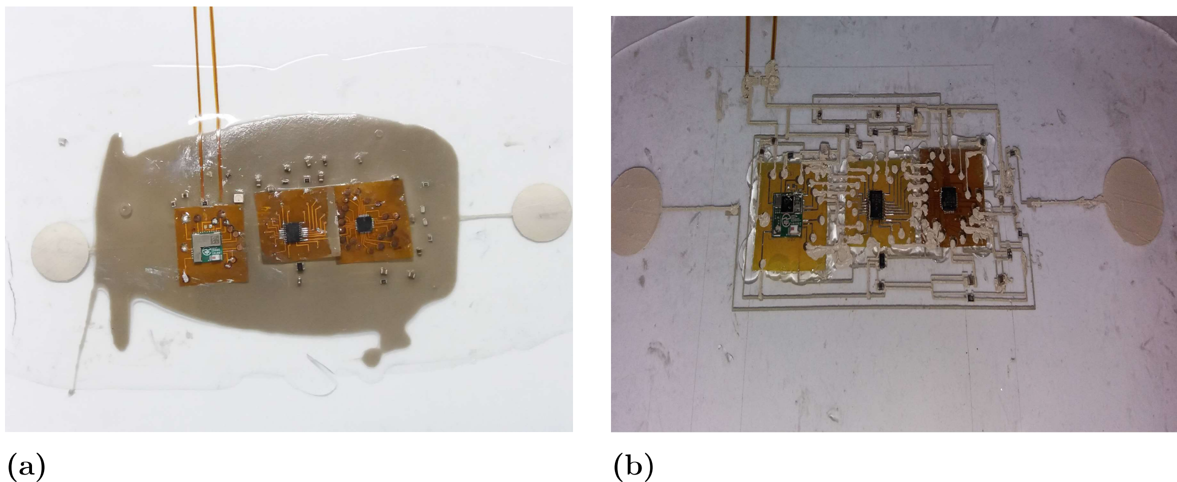

(a) **(b)**

Figure 4.9: a) Full ECG circuit fabricated with zPDMS interface method. b) Full ECG circuit fabricated direct contact method.

nents would move by action of the magnetic field which is required during zPDMS' curing procedure for vertically conductive columns to form. In turn, the issue with the samples fabricated by direct interfacing of the Flex PCB's and rigid components with the AgPDMS circuit was that the Flex PCB's had to be placed in alignment on top of the first circuit layer prior to application of the stencil for the second layer. This, however, led to the stencil removing the flex PCB's from their place. To circumvent this problem, the Flex PCB's were 'glued' to the first circuit layer by placing small amounts of PDMS on their edges and curing the PDMS, prior to

application of the second-layer stencil. The stencil for the second circuit layer, however, did not adhere well to these irregular PDMS surfaces covering the edges of the Flex PCB's, leading to a few short circuits, which can be seen in Figure 4.9b.

5

Conclusions

Stretchable electronics is a very broad field of research, and a multitude of stretchable polymers, conductive materials and fabrication methods have been explored for fabrication of stretchable circuits. While this work started out from the premise that only AgPDMS-based conductive composites would be the focus of study, the range of options available is still quite broad, as is visible from the number of conductive filler particle types, patterning methods and interfacing methods which were discussed and/or tested.

In light of this, one of the main contributions of this work was to narrow down in several dimensions (conductive composites, patterning methods, interfacing methods) the range of options available until a stepwise procedure for fabrication of AgPDMS stretchable systems could be prescribed.

An equally important contribution given was defining a reliable procedure for making interlayer electrical connections, thus enabling fabrication of AgPDMS multilayer stretchable systems and allowing reduction of feature density.

Finally, this work led to an improvement regarding the silver particle type used for AgPDMS stretchable circuit fabrication in our lab. Indeed, the type of particle which was previously in use in our lab was silver microparticles type V (see Table 2.1), which have less satisfactory properties and are considerably more costly ([37]) compared to silver flakes type I ([38]).

Despite these improvements and those of other groups in advancing fabrication methods, and although we are now capable of rapidly prototyping stretchable electronics systems, there are still challenges and difficulties. There are important fabrication steps which difficult the rapid prototyping process, such as manually placing small, rigid components which might have dimensions smaller than one millimeter. Solutions to this issue could come from automating this step or, alternatively, isolating as much as possible the processing electronics from the stretchable module. Applied

to the second case study in this work (Stretchable ECG patch), for example, this would mean having a stretchable patch with only two AgPDMS electrodes, and replacing all the rigid components by externally connecting the patch to a single rigid circuit and to an external battery, using only a few connecting wires. Furthermore, interfacing rigid components to stretchable modules without limiting stretchability is another challenge which still needs to be addressed. Under tension, stress accumulates at these interfaces, where failure often happens first. Solving these problems is essential for stretchable electronics technology to fulfill its commercial potential and will require a prolongued, intensive, multidisciplinary research effort.

Bibliography

[1] W. Dang, V. Vinciguerra, L. Lorenzelli, and R. Dahiya, "Printable stretchable interconnects," *Flexible and Printed Electronics*, vol. 2, no. 1, p. 13003, 2017.

[2] K. Ghaffarzadeh, J. Hayward, and X. He, "Stretchable and Conformal Electronics 2018-2028," 2018.

[3] S. Choi, J. Park, W. Hyun, J. Kim, J. Kim, Y. B. Lee, C. Song, H. J. Hwang, J. H. Kim, T. Hyeon, and D.-H. Kim, "Stretchable Heater Using Ligand-Exchanged Silver Nanowire Nanocomposite for Wearable Articular Thermotherapy," *ACS Nano*, vol. 9, no. 6, pp. 6626–6633, 2015.

[4] L. Song, A. C. Myers, J. J. Adams, and Y. Zhu, "Stretchable and Reversibly Deformable Radio Frequency Antennas Based on Silver Nanowires," *ACS Applied Materials & Interfaces*, vol. 6, no. 6, pp. 4248–4253, 2014.

[5] K. Tybrandt, F. Stauffer, and J. Vörös, "Multilayer patterning of high resolution intrinsically stretchable electronics," *Scientific Reports*, 2016.

[6] S. I. Park, Y. Xiong, R. H. Kim, P. Elvikis, M. Meitl, D. H. Kim, J. Wu, J. Yoon, Y. Chang-Jae, Z. Liu, Y. Huang, K. C. Hwang, P. Ferreira, L. Xiuling, K. Choquette, and J. A. Rogers, "Printed assemblies of inorganic light-emitting diodes for deformable and semitransparent displays," *Science*, 2009.

[7] Y. Mengüç, Y. L. Park, H. Pei, D. Vogt, P. M. Aubin, E. Winchell, L. Fluke, L. Stirling, R. J. Wood, and C. J. Walsh, "Wearable soft sensing suit for human gait measurement," *International Journal of Robotics Research*, 2014.

[8] M. Tavakoli, R. Rocha, L. Osorio, M. Almeida, A. De Almeida, V. Ramachandran, A. Tabatabai, T. Lu, and C. Majidi, "Carbon doped PDMS: Conductance stability over time and implications for additive manufacturing of stretchable electronics," *Journal of Micromechanics and Microengineering*, 2017.

[9] M. D. Bartlett, E. J. Markvicka, and C. Majidi, “Rapid Fabrication of Soft, Multilayered Electronics for Wearable Biomonitoring,” *Advanced Functional Materials*, 2016.

[10] A. Chortos, G. I. Koleilat, R. Pfattner, D. Kong, P. Lin, R. Nur, T. Lei, H. Wang, N. Liu, Y. C. Lai, M. G. Kim, J. W. Chung, S. Lee, and Z. Bao, “Mechanically Durable and Highly Stretchable Transistors Employing Carbon Nanotube Semiconductor and Electrodes,” *Advanced Materials*, 2016.

[11] H. J. Koo, J. H. So, M. D. Dickey, and O. D. Velev, “Towards all-soft matter circuits: Prototypes of quasi-liquid devices with memristor characteristics,” *Advanced Materials*, 2011.

[12] F. Bossuyt, T. Vervust, and J. Vanfleteren, “Stretchable electronics technology for large area applications: Fabrication and mechanical characterization,” *IEEE Transactions on Components, Packaging and Manufacturing Technology*, 2013.

[13] D.-H. Kim, J. Song, W. M. Choi, H.-S. Kim, R.-H. Kim, Z. Liu, Y. Y. Huang, K.-C. Hwang, Y.-w. Zhang, and J. A. Rogers, “Materials and noncoplanar mesh designs for integrated circuits with linear elastic responses to extreme mechanical deformations,” *Proceedings of the National Academy of Sciences*, 2008.

[14] M. D. Dickey, “Stretchable and Soft Electronics using Liquid Metals,” 2017.

[15] R. K. Kramer, C. Majidi, and R. J. Wood, “Masked deposition of gallium-indium alloys for liquid-embedded elastomer conductors,” *Advanced Functional Materials*, 2013.

[16] A. Larmagnac, S. Eggenberger, H. Janossy, and J. Vörös, “Stretchable electronics based on Ag-PDMS composites,” *Scientific Reports*, 2014.

[17] T. Lu, J. Wissman, Ruthika, and C. Majidi, “Soft anisotropic conductors as electric vias for Ga-based liquid metal circuits,” *ACS Applied Materials and Interfaces*, 2015.

[18] J. Liang, K. Tong, and Q. Pei, “A Water-Based Silver-Nanowire Screen-Print Ink for the Fabrication of Stretchable Conductors and Wearable Thin-Film Transistors,” *Advanced Materials*, 2016.

[19] J. Suikkola, T. Björninen, M. Mosallaei, T. Kankkunen, P. Iso-Ketola, L. Ukkonen, J. Vanhala, and M. Mäntysalo, “Screen-Printing Fabrication and Characterization of Stretchable Electronics,” *Scientific Reports*, 2016.

[20] V. Martinez, F. Stauffer, M. O. Adagunodo, C. Forro, J. Vörös, and A. Larmagnac, "Stretchable Silver Nanowire-Elastomer Composite Microelectrodes with Tailored Electrical Properties," *ACS Applied Materials and Interfaces*, 2015.

[21] B. W. An, E. J. Gwak, K. Kim, Y. C. Kim, J. Jang, J. Y. Kim, and J. U. Park, "Stretchable, Transparent Electrodes as Wearable Heaters Using Nanotrough Networks of Metallic Glasses with Superior Mechanical Properties and Thermal Stability," *Nano Letters*, 2016.

[22] F. Xu and Y. Zhu, "Highly conductive and stretchable silver nanowire conductors," *Advanced Materials*, 2012.

[23] J. Lee, P. Lee, H. B. Lee, S. Hong, I. Lee, J. Yeo, S. S. Lee, T. S. Kim, D. Lee, and S. H. Ko, "Room-temperature nanosoldering of a very long metal nanowire network by conducting-polymer-assisted joining for a flexible touch-panel application," *Advanced Functional Materials*, 2013.

[24] K. K. Kim, S. Hong, H. M. Cho, J. Lee, Y. D. Suh, J. Ham, and S. H. Ko, "Highly Sensitive and Stretchable Multidimensional Strain Sensor with Prestrained Anisotropic Metal Nanowire Percolation Networks," *Nano Letters*, 2015.

[25] W. Hu, X. Niu, L. Li, S. Yun, Z. Yu, and Q. Pei, "Intrinsically stretchable transparent electrodes based on silver-nanowire-crosslinked-polyacrylate composites," *Nanotechnology*, 2012.

[26] S. Yun, X. Niu, Z. Yu, W. Hu, P. Brochu, and Q. Pei, "Compliant silver nanowire-polymer composite electrodes for bistable large strain actuation," *Advanced Materials*, 2012.

[27] H. C. Jung, J. H. Moon, D. H. Baek, J. H. Lee, Y. Y. Choi, J. S. Hong, and S. H. Lee, "CNT/PDMS composite flexible dry electrodesfor long-term ECG monitoring," *IEEE Transactions on Biomedical Engineering*, 2012.

[28] A. R. Madaria, A. Kumar, F. N. Ishikawa, and C. Zhou, "Uniform, highly conductive, and patterned transparent films of a percolating silver nanowire network on rigid and flexible substrates using a dry transfer technique," *Nano Research*, 2010.

[29] J. W. Boley, E. L. White, and R. K. Kramer, "Mechanically sintered gallium-indium nanoparticles," *Advanced Materials*, 2015.

[30] L. Guo and S. P. DeWeerth, "High-density stretchable electronics: Toward an integrated multilayer composite," *Advanced Materials*, 2010.

[31] S. P. Lacour, S. Wagner, R. J. Narayan, T. Li, and Z. I. Suo, "Stiff subcircuit islands of diamondlike carbon for stretchable electronics," *Journal of Applied Physics*, 2006.

[32] T. Sekitani, Y. Noguchi, K. Hata, T. Fukushima, T. Aida, and T. Someya, "A rubberlike stretchable active matrix using elastic conductors," *Science*, 2008.

[33] S. Xu, Y. Zhang, L. Jia, K. E. Mathewson, K. I. Jang, J. Kim, H. Fu, X. Huang, P. Chava, R. Wang, S. Bhole, L. Wang, Y. J. Na, Y. Guan, M. Flavin, Z. Han, Y. Huang, and J. A. Rogers, "Soft microfluidic assemblies of sensors, circuits, and radios for the skin," *Science*, 2014.

[34] T. Lu, "Laser-based rapid prototyping techniques for liquid metal circuits," 2016.

[35] K. P. Mineart, Y. Lin, S. C. Desai, A. S. Krishnan, R. J. Spontak, and M. D. Dickey, "Ultrastretchable, cyclable and recyclable 1- and 2-dimensional conductors based on physically cross-linked thermoplastic elastomer gels," *Soft Matter*, 2013.

[36] I. D. Johnston, D. K. McCluskey, C. K. L. Tan, and M. C. Tracey, "Mechanical characterization of bulk sylgard 184 for microfluidics and microengineering," *Journal of Micromechanics and Microengineering*, vol. 24, no. 3, p. 035017, 2014.

[37] "Sigma aldrich, https://www.sigmaaldrich.com/catalog/product/aldrich/327085, accessed: 2018-09-13,"

[38] "Technic inc.,
https://www.technic.com/sites/default/files/resources/
silver%20flake%20material%20071%2c%2041-071.pdf,
accessed: 2018-09-13,"